

**Forschungszentrum Karlsruhe**

in der Helmholtz-Gemeinschaft

Wissenschaftliche Berichte

FZKA 6755

Behavior of oxyanions forming heavy metals in  
municipal solid waste incineration

Francesca Paoletti

Institut für Technische Chemie

Von der Fakultät Energietechnik der Universität Stuttgart genehmigte Dissertation

Forschungszentrum Karlsruhe GmbH, Karlsruhe  
2002

**Impressum der Print-Ausgabe:**

**Als Manuskript gedruckt  
Für diesen Bericht behalten wir uns alle Rechte vor**

**Forschungszentrum Karlsruhe GmbH  
Postfach 3640, 76021 Karlsruhe**

**Mitglied der Hermann von Helmholtz-Gemeinschaft  
Deutscher Forschungszentren (HGF)**

**ISSN 0947-8620**

# Behavior of oxyanions forming heavy metals in municipal solid waste incineration

Von der Fakultät Energietechnik der Universität Stuttgart  
zur Erlangung der Würde eines Doktors-Ingenieur (Dr.-Ing.)  
genehmigte Abhandlung

Vorgelegt von

Francesca Paoletti

aus Perugia, Italien

Hauptberichter: Prof. Dr.-Ing. H. Seifert  
Mitberichter: Prof. Dr.-Ing. K.R.G. Hein

Tag der mündlichen Prüfung: 10. Mai 2002

Institut für Technische Chemie  
Bereich Thermische Abfallbehandlung  
Forschungszentrum Karlsruhe

2002

## **Abstract**

A number of metals respectively half-metals of high environmental concern have the capability to form oxyanionic compounds. The purpose of the present work is to investigate the behavior of selected elements out of this group, namely arsenic, antimony, chromium and molybdenum, during the waste combustion process and the environmental properties of the solid combustion residues.

As a first investigation step, the concentration and the chemical speciation of the investigated metals in municipal solid waste are assessed on the base of literature review. The thermal behavior of the prevailing input species of the elements in question is successively estimated by the minimization of the thermodynamic function Gibbs' free enthalpy.

Thermogravimetric and calorimetric measurements in a thermobalance as well as X-ray diffractometric analyses of mixtures of metal salts and calcium oxide provide evidence that oxyanionic salts are formed in the temperature range around 500-900°C.

The results of spiking tests in the TAMARA pilot plant for waste incineration show that the primary air number has a distinct effect on the transfer of the elements out of the fuel bed into the flue gas and on their partitioning among the solid residues. The effect is particularly strong for the two volatile metals arsenic and antimony.

Sampling and analysis of fly ash samples at different locations along the flue gas path allow the characterization of the ashes as a function of the deposition temperature. The analysis of samples of filtered gas show the insignificance of gaseous metallic species at temperatures below 200°C and hence the low stack emission potential for the investigated metals.

The last part of this work is concerned with the characterization of the TAMARA grate and fly ashes and with the assessment of the leaching potential of the selected metals from the residues. Different regulatory tests have been performed, the results are compared and interpreted in view of the speciation of the elements in question in these residues. All elements showed clearly an oxyanionic pattern in their elution from the grate and boiler ashes. The elution from filter ashes instead showed a cationic pattern, especially for arsenic and antimony.

The leachate pH appears to be the dominant factor controlling the mobilization of the metals. Molybdenum shows a very high potential for leaching over the entire pH range as a consequence of the formation of highly soluble molybdates. Chromium exhibits a leaching behavior which is strongly dependant on the combustion conditions. For low air number values the amounts released by means of leaching processes from the grate ashes are nearly two orders of magnitude lower than for the reference air number value. Thus, the oxygen concentration in the furnace seems to play an important role in the formation of highly toxic and highly soluble hexavalent chromates.

## **Verhalten Oxianionen bildender Schwermetalle in der Abfallverbrennung**

### **Zusammenfassung**

Einige umweltrelevante Schwermetalle bzw. Halbmetalle besitzen die Eigenschaft, oxyanionische Verbindungen zu bilden. Ziel dieser Arbeit ist die Untersuchung des Verhaltens ausgewählter Elemente aus dieser Gruppe, und zwar Arsen, Antimon, Chrom und Molybdän, bei der Abfallverbrennung und in Hinsicht auf das Elutionspotential aus den Verbrennungsrückständen.

Erster Schritt dieser Untersuchung ist die Abschätzung der Konzentration und chemischen Speziation der untersuchten Elemente im Hausmüll. Somit können die in die Verbrennungsanlage eingebrachten Verbindungen (Eingangsspezies) definiert werden. Auf dem chemischen Gleichgewicht basierende thermodynamische Berechnungen (Minimierung der Gibbsschen Energie) ermöglichen eine Abschätzung der Reaktionen, die während des Verbrennungsprozesses mit der höchsten Wahrscheinlichkeit auftreten.

Zum Nachweis der Bildung oxianionischer Verbindungen während der Verbrennung wurden thermogravimetrische und kalorimetrische Messungen in der Thermowaage (TG-DSC) sowie röntgendiffraktometrische Analysen (XRD) der Rückstände dieser Messungen durchgeführt. Diese Versuche zeigen, dass sich oxianionische Salze im Temperaturbereich zwischen 500°C und 900°C bilden.

Die durchgeführten Spiking-Versuche in der Testanlage für Abfallverbrennung TAMARA zeigen, dass die Änderung der Luftzahl sich stark auf die Verflüchtigung von Arsen und Antimon aus dem Gutbett auswirkt, während bei Molybdän und Chrom die Auswirkung sehr gering ist.

Die Entnahme von Flugstaubproben an verschiedenen Stellen der Abkühlstrecke der Rauchgase (von 800°C bis 190°C) erlaubt Rückschlüsse auf die Kondensationsmechanismen der Schwermetalle. Bei der Analyse von abfiltrierten Rauchgasproben konnten keine gasförmigen Verbindungen bei Temperaturen unter 200°C nachgewiesen werden.

Der letzte Teil dieser Arbeit befasst sich mit der Charakterisierung der Rost- und Flugaschen aus der durchgeführten Verbrennungskampagne mit dem Ziel der Beurteilung des Elutionsverhaltens der Schwermetalle und ihres Mobilisierungspotentials aus den Rückständen.

Es wurden verschiedene standardisierte Laugungstests durchgeführt und deren Ergebnisse verglichen in Hinsicht auf die chemische Speziation der Elemente in den Rückständen. Das Elutionsverhalten aus den Rost- und Kesselaschen weist bei allen untersuchten Elemente deutlich auf deren oxianionische Speziation. Die Eluate aus den Filteraschen zeigen dagegen eine kationische Auslaugtendenz, insbesondere bei Arsen und Antimon.

Die Elution der Metalle ist in erster Linie durch den pH-Wert beeinflusst. Molybdän zeigt ein sehr hohes Elutionspotential über den gesamten pH-Bereich in Folge der Bildung von hochlöslichen Molybdate.

Das Elutionsverhalten von Chrom hängt stark von den Verbrennungsparametern ab. So ist die aus den Rückständen eluierte Fracht dieses Metalls bei geringer Luftzahl fast zwei Größenordnungen geringer als bei der Referenzluftzahl. Die Sauerstoffkonzentration in der Brennkammer ist offensichtlich von großer Bedeutung bei der Bildung hochtoxischer und hochlöslicher sechswertiger Chromaten während der Verbrennung.

## Zusammenfassung

### **Zielsetzung**

Ziel dieser Arbeit ist die Untersuchung des Verhaltens ausgewählter Schwermetalle bei der Abfallverbrennung insbesondere in Hinsicht auf die Auswirkungen von chemischen Reaktionen, die während des Verbrennungsprozesses stattfinden und die zur Bildung von oxianionischen Spezies führen. Die vier untersuchten Metalle (bzw. Halbmetalle) sind: Arsen, Antimon, Chrom und Molybdän (analoge Betrachtungen gelten für andere Metalle mit ähnlichem chemischem Verhalten, wie zum Beispiel Vanadin und Wolfram).

Unter Oxianionen versteht man sauerstoffhaltige Anionen. In einer wässrigen Umgebung sind sie im ionischen Zustand aufzufinden, während sie in der Festphase an metallische Kationen gebunden als oxianionische Salze (Oxi-Salze) auftreten. Die Bildung oxianionischer Verbindungen ist eine Folge des schwach metallischen Charakters der ausgewählten Elemente und findet normalerweise in einer alkalischen wässrigen Phase oder bei hohen Temperaturen auch in der Festphase statt, sofern alkalische Reaktionspartner zur Verfügung stehen. Letzteres ist im Gutbett einer Müllverbrennungsanlage zu erwarten.

### **1. Einleitung**

Die Auswirkungen der Bildung von oxianionischen Spezies sind bei den vier untersuchten Metallen unterschiedlich.

Bei **Arsen** und **Antimon**, zwei Halbmetallen, die für die Flüchtigkeit vieler ihrer Verbindungen bekannt sind, hat die Bildung thermisch stabiler Arsenate und Antimonate eine Reduzierung des Transferkoeffizienten aus dem Gutbett zur Folge, das heißt, des Anteils des Gesamtinventars des jeweiligen Elementes, welcher während der Verbrennung aus dem Gutbett in das Rauchgas ausgetragen wird. Eine reduzierte Freisetzung aus dem Gutbett ist nicht unbedingt als positiv zu betrachten, da einerseits auch bei hohen Transferkoeffizienten keine Luftemissionen dieser Elemente erwartet werden - vorausgesetzt, dass ein effizientes Partikelrückhaltesystem in der Rauchgasreinigungsstufe vorhanden ist - und andererseits ein erhöhter Verbleib dieser Elemente in den Rostaschen nicht wünschenswert ist, weil diese Rückstände als Baumaterial wiederverwendet werden und daher möglichst geringe Konzentrationen an toxischen Metallen enthalten sollten.

Für **Chrom** ist die mögliche Bildung sechswertiger Chromate während der Verbrennung von großer Bedeutung, da die Toxizität von Chrom in starkem Maße von seiner Oxidationsstufe abhängig ist. Sechswertige Verbindungen sind aufgrund ihres hohen Oxidationspotentials erheblich schädlicher für die Organismen als dreiwertige. In der Regel wird davon ausgegangen, dass bei den in einer Müllverbrennungsanlage herrschenden relativ niedrigen Gutbetttemperaturen keine Oxidation zu

sechswertigen Chromverbindungen stattfinden kann. Andererseits deuten die in dieser Arbeit durchgeführten Untersuchungen in Hinsicht auf das Laugungsverhalten dieses Elementes aus den Verbrennungsrückständen darauf hin, dass zumindest ein Teil des Inventars in sechswertiger Form vorliegt. Chromatbildung als Folge der chemischen Reaktion mit alkalischen Brennstoffkomponenten ist eine wahrscheinliche Erklärung. Verbrennungsparameter wie die Primärluftzufuhr bzw. -verteilung sind für die chemische Speziation von Chrom in den Verbrennungsrückständen von großer Bedeutung, da sechswertige Chromate nur gebildet werden können, wenn der Sauerstoffpartialdruck in der Brennkammer ausreichend ist.

Das vierte untersuchte Element **Molybdän** verhält sich, ähnlich wie Chrom, während der Verbrennung lithophil und nicht-flüchtig und ist zum größten Teil in den Rostaschen wiederzufinden. Die Bildung hochlöslicher Molybdate hat eine erhöhte Auslaugbarkeit aus den Verbrennungsrückständen zur Folge. Diese Verbindungen werden für gewöhnlich (außer in den Niederlanden) nicht zu den Umweltschadstoffen gezählt, können jedoch im Falle einer Bodenkontamination aufgrund ihrer Toxizität für Wiederkäuer ökologisch relevant sein.

## 2. Vorkommen der Elemente im Hausmüll

Erster Schritt dieser Untersuchung war die Abschätzung der Konzentration und chemischen Speziation (Input-Inventar) der untersuchten Schwermetalle im Hausmüll. Somit konnten die in die Verbrennungsanlage eingebrachten Verbindungen (Eingangsspezies) definiert werden.

Untersuchungen der Hausmüllzusammensetzung, wie sie in der Literatur vorhanden sind, ermöglichen eine Abschätzung der Herkunft und Menge dieser Metalle in den häuslichen Abfällen und erlauben Rückschlüsse auf die chemische Speziation.

**Arsen** wurde in der Vergangenheit als Insektizid und Pestizid in der Landwirtschaft verwendet. Diese Anwendung ist allerdings mittlerweile in den meisten Ländern stark eingeschränkt. Heutzutage wird Arsen noch als Legierungselement (Blei- oder Kupferlegierungen), als Holzschutzmittel und in der Elektronikindustrie als Halbleiter (intermetallische Verbindungen mit Gallium oder Indium) eingesetzt. Die wichtigsten Arsenanteile im Hausmüll entstammen der organischen und der metallischen Fraktion. Insgesamt kann die Konzentration von Arsen im Hausmüll auf ungefähr 5-10 mg/kg abgeschätzt werden.

Metallisches **Antimon** wird gewöhnlich in metallischen Legierungen, wie z.B. Pewter (Schüsselzinn), Blei-Antimon und Zinn-Antimon verwendet. Als heutzutage wichtigste industrielle Anwendung wird Antimon als Zusatz in bromhaltigen Flammenschutzmitteln eingesetzt (insbesondere bei PVC). Der größte Teil des Antimons im Hausmüll stammt daher aus der Kunststofffraktion sowie aus Textilien und elektrischen Kleingeräten, d.h. aus den Fraktionen, bei

denen eine Flammschutzmittelbehandlung üblich ist. Die Konzentration von Antimon im Hausmüll liegt bei etwa 30-50 mg/kg.

**Chrom** hat zahlreiche industrielle Anwendungen, die grob in drei verschiedene Kategorien eingeordnet werden können: Eisen-/Nichteisenlegierungen (z.B. Edelstahl), Herstellung feuerfester Materialien sowie chemische Produkte. Chromate dienen als gelbe, rote und grüne Pigmente, Dichromate werden aufgrund ihrer Oxidationseigenschaften in der Textil- und Photoindustrie eingesetzt. Die Anwendungsgebiete der Chromoxide sind sehr umfangreich: dreiwertiges Chromoxid wird als grüner Farbstoff und Katalysator verwendet. Vierwertiges Chromoxid wird in der Herstellung von Audio- und Videomagnetbändern eingesetzt. Sechswertiges Chromoxid wird in der Verchromung verwendet und dient außerdem als Holzschutz- und Oxidationsmittel. Basische Chromsulfate spielen eine wichtige Rolle beim Gerben von Leder. Über die Hälfte der Gesamtkonzentration an Chrom im Hausmüll stammt aus der organischen Fraktion. Holz, Leder und Gummi sind wahrscheinlich die Hauptquellen. Andere Anteile stammen aus den Kunststoff- und Metallfraktionen. Der Chromgehalt des Hausmülls kann auf etwa 250-300 mg/kg eingeschätzt werden.

Metallurgische Anwendungen (als Legierungselement in Stahl, Gusseisen und Superlegierungen) machen über 90 % der gesamten **Molybdän**nutzung aus. Des Weiteren gibt es zahlreiche chemische Anwendungen von anderen Molybdänverbindungen: Molybdäntrioxid findet als Katalysator breite Anwendung, ebenso wird es in Flammschutzmitteln für PVC eingesetzt. Molybdändisulfid ist ein Hochtemperaturschmiermittel, das bei der Herstellung von Fetten bzw. Motor- und Industrieölen verwendet wird. Alkalimolybdate dienen als Korrosionsschutzmittel. Bleimolybdat findet breite Anwendung als gelbes oder orangefarbenes Pigment. Natriummolybdat wird als Bodenzusatz und Düngemittel eingesetzt, da Molybdän ein wichtiges Spurenelement ist. In der Literatur gibt es keine detaillierten Untersuchungen über die Herkunft von Molybdän im Hausmüll. Die Konzentration von Molybdän im Hausmüll liegt etwa bei 20 mg/kg.

Aufgrund der industriellen Anwendungen der vier untersuchten Metalle, kann die Eingangsspeziation hauptsächlich als metallisch oder oxidisch angenommen werden. Allerdings ist damit zu rechnen, dass mindestens ein Teil der Input-Menge bereits in oxianionischer Form vorliegen kann, insbesondere bei Arsen und Molybdän.

### 3. Physikalische und chemische Vorgänge bei der Verbrennung

Auf dem chemischen Gleichgewicht basierende thermodynamische Berechnungen ermöglichen eine Abschätzung der Reaktionen, die während des Verbrennungsprozesses mit der höchsten Wahrscheinlichkeit auftreten. Alle chemischen Systeme lassen sich durch die Variation der

Zustandsfunktion Gibbs'sche Energie  $\Delta G$  beschreiben. Erreicht das System das chemische Gleichgewicht, erreicht der Wert für  $\Delta G$  sein Minimum.

Der weitere Verbleib der Reaktionsprodukte, die sich während der Verbrennung bilden - Verflüchtigung mit dem Rauchgas oder Fixierung in den Rostaschen - lässt sich aufgrund ihrer Dampfdruckkurven abschätzen.

**Arsen** und **Antimon** weisen ein ähnliches chemisches Verhalten auf, allerdings liegen für Arsen mehr thermodynamische Daten vor als für Antimon. Beide Elemente haben schwachmetallische Eigenschaften und sind für die Flüchtigkeit einiger ihrer Verbindungen bekannt. Thermodynamische Berechnungen zeigen, dass flüchtige Arsen- und Antimonoxide mit großer Wahrscheinlichkeit im Gutbett gebildet werden. Auch die Bildung von Antimonchloriden ist sehr begünstigt. Bei Arsen scheint die Bildung von Chloriden weniger begünstigt zu sein, was möglicherweise auf den schwächer metallischen Charakter von Arsen und die entsprechend geringere Chloraffinität zurückzuführen ist. Experimentelle Ergebnisse aus der Literatur sowie aus dieser Arbeit über das Verhalten von Arsen und Antimon bei Verbrennungsprozessen widersprechen jedoch diesen theoretischen Betrachtungen und deuten auf eine geringere Flüchtigkeit dieser Elemente hin. Die Bildung thermisch stabiler oxianionischer Verbindungen im Gutbett, wie Arsenate und Antimonate, ist hierfür eine sehr wahrscheinliche Erklärung.

Die Abschätzung der Variation der freien Gibbs'schen Energie  $\Delta G$  für chemische Reaktionen des **Chroms** zeigt, dass die Bildung dreiwertiger Verbindungen im Vergleich zu jener sechswertiger Verbindungen begünstigt ist. Zudem scheint die Chlorierung der Oxide weniger begünstigt zu sein. Die Bildung stark flüchtigen (und toxischen) Chromylchlorids scheint aus theoretischer Sicht ziemlich unwahrscheinlich. Vor diesem Hintergrund ist kaum eine Chromverflüchtigung während der Verbrennung zu erwarten. Andererseits könnte trivalentes Chrom direkt mit Alkali- und Erdalkalimetallverbindungen im Gutbett reagieren und so sechswertige Chromate bilden. Diese Reaktionen würden zwar zu keiner erhöhten Chromflüchtigkeit führen, können aber, da Chromate sich durch eine sehr hohe Löslichkeit auszeichnen, ein ungewünscht hohes Auslaugpotential von Chrom aus den festen Verbrennungsrückständen zur Folge haben.

**Molybdän** zählt zu den Metallen mit dem höchsten Schmelzpunkt ( $2610^{\circ}\text{C}$ ). Man würde daher eine sehr geringe Flüchtigkeit bei der Verbrennung dieses Metalls erwarten. Dennoch weist Molybdän eine unerwartete (und relativ hohe) thermische Mobilität sowie eine Anreicherung in den Flugaschen auf, was auf die Bildung flüchtiger Verbindungen während der Verbrennung hinweist. Sechswertiges Molybdänoxid ist eine sehr flüchtige Verbindung mit einer hohen Bildungswahrscheinlichkeit. Auch Molybdänchloride besitzen eine außerordentlich hohe Flüchtigkeit und sind in ihrer Bildung thermodynamisch begünstigt.

#### 4. Bildung oxianionischer Spezies

Zum Nachweis der Bildung oxianionischer Verbindungen während der Verbrennung wurden thermogravimetrische und kalorimetrische Messungen in der Thermowaage durchgeführt (TG-DSC), sowie röntgendiffraktometrische Analysen (XRD) der Rückstände dieser Messungen. Das thermische Verhalten von Mischungen aus Metallsalzen und Kalziumoxid zeigte, dass sich oxianionische Salze im Temperaturbereich zwischen 500 und 900°C bilden. Kalziumoxid wurde als Reaktionspartner gewählt, da es im Hausmüll relativ häufig vorhanden ist (ungefähr 3%). Allerdings kann davon ausgegangen werden, dass ähnliche Reaktionen auch mit anderen Alkali- oder Erdalkalimetallen (Na, K, Mg, Sr, Ba) stattfinden können, die in geringeren Konzentrationen vorkommen.

Die Bildung thermisch stabiler Antimonate konnte mit Hilfe der thermogravimetrischen Analyse nachgewiesen werden. Während sich **Antimontrioxid** allein schnell und vollständig verflüchtigte, zeigte die Mischung mit Kalziumoxid kaum Gewichtsverluste bis zu 1400°C. Ähnliche Ergebnisse wurden für **Arsentrioxid** ermittelt, obwohl die Versuche aufgrund der hohen Flüchtigkeit (und Toxizität) dieser Verbindung gewissen Einschränkungen unterlagen.

Dreiwertiges **Chromoxid** ist eine sehr stabile Verbindung und weist bis 1400°C keine Anzeichen einer Oxidation oder einer thermischen Zersetzung auf. Die Mischung von Chromoxid und Kalziumoxid in oxidativer Atmosphäre (synthetische Luft) weist demgegenüber ein sehr interessantes thermisches Verhalten auf. Die Bildung sechswertigen Kalziumchromats führt zu einer schnellen Massenzunahme zwischen 500°C und 850°C. Bei 850°C wird das sechswertige zu dreiwertigem Chromat reduziert, was einen Massenverlust der Probe zwischen 850°C und 1000°C zur Folge hat. Diese Ergebnisse wurden durch die Röntgenstrukturanalyse der Rückstände bestätigt. Die Oxidation von vierwertigem zu sechswertigem **Molybdänoxid** beginnt bei etwa 300°C und ist bei 500°C abgeschlossen. Die kalorimetrische Analyse der Molybdänoxid- und Kalziumoxidsmischung ergab ab 450°C ein exothermes Signal, welches bei 575°C sein Maximum erreichte. Dieses Signal ist offensichtlich auf die Reaktionswärme zurückzuführen, die bei der Molybdätdatbildung entsteht. Mit Hilfe der diffraktometrischen Analyse konnte die Bildung von Kalziummolybdätdat eindeutig nachgewiesen werden.

#### 5. Verbrennungsversuche an der Testanlage TAMARA

Im Rahmen dieser Arbeit wurde eine Verbrennungskampagne in der Testanlage TAMARA durchgeführt. Die Testanlage zur Abfallverbrennung TAMARA ist eine Rostfeuerung mit einem Nominaldurchsatz von etwa 250 kg/h. Der Brennstoff besteht aus einer Mischung von ungefähr 75% vorbehandeltem Hausmüll (unterer Heizwert etwa 6 MJ/kg) und 25% Brennstoff aus Müll

(BRAM, unterer Heizwert etwa 16 MJ/kg). Der Vorschubrost hat eine Fläche von ungefähr 2,5 m<sup>2</sup> und ist in vier Zonen mit getrennter Primärluftzufuhr und Bewegungssteuerung unterteilt. Die Geometrie des Brennraums kann durch eine einsetzbare Decke zwischen Gegen-, Mittel- oder Gleichstrom variiert werden.

In dem Abhitzekessel wird das Rauchgas von ungefähr 800°C auf 200°C abgekühlt. Die Entstaubung erfolgt in einem Gewebefilter. Das Rauchgasreinigungssystem besteht aus einer zweistufigen Abgaswäsche mit einer vorgeschalteten Quenchstufe.

Die Testanlage TAMARA ermöglicht eine repräsentative Probenahme von allen festen Verbrennungsrückständen (Rostaschen, Rostdurchfall, Kesselaschen, Flugstäube). Die Rauchgasprobenahme zur Analyse filtergängiger metallischer Verbindungen wurde nach VDI-Methode Nr. 3868 durchgeführt.

Die Metallkonzentrationen der Proben wurden durch Totalreflexions-Röntgenfluoreszenzanalyse (TRFA) bestimmt. Die Elementaranalyse des TAMARA-Brennstoffes erfolgte in einem Leco-Ofen.

Ziel der Testkampagne war die Untersuchung des Einflusses der Luftzahl, die sich für die Primärluft errechnen lässt, auf das Verhalten der Oxidation bildenden Schwermetalle. Dabei wurde stufenweise, durch Reduzierung der Primärluftzufuhr, die Luftzahl vom üblichen Referenzwert von etwa 1,5 bis auf einen Wert von 0,6 abgesenkt. Es wurde dabei davon ausgegangen, dass die Luftzahl nicht nur das Temperaturprofil des Gutbettes, sondern auch die Verflüchtigung aus der Brennkammer sowie die Auslaugbarkeit aus den Verbrennungsrückständen der Schwermetalle beeinflusst.

Die Temperaturprofile über dem Gutbett zeigen, dass sich bei abnehmender Primärluftzufuhr der Zündpunkt des Brennstoffes zum Ende des Rostes hin verschiebt. Mit der Abnahme der Überschussluft verläuft die Kohlenstoffoxidationsreaktion langsamer. Das Temperaturprofil wird dadurch weniger steil und breiter. Mit zunehmender Profilfläche nimmt aber auch gleichzeitig die Verweilzeit des Brenngutes im Hochtemperaturbereich zu, so dass die verzögerte Zündung des Brennstoffes durch diesen vorteilhaften Effekt teilweise ausgeglichen wird. Für Luftzahlwerte unter 0,7 lässt sich kein bestimmter Zündpunkt im Temperaturprofil erkennen. Der Hochtemperaturbereich wird in der Nähe des Rostendes erreicht, die Kohlenstoffoxidation im Gutbett ist daher unvollständig.

Bei den sogenannten Spiking-Versuchen wird die Eingangskonzentration eines Elementes in der Feuerung künstlich erhöht. Dies ist insbesondere bei den Elementen sinnvoll, deren Konzentration üblicherweise im Hausmüll sehr gering ist, denn somit können sowohl die Verteilung auf den Verbrennungsrückständen als auch der Einfluss von Prozessparametern oder die Wechselwirkungen

mit anderen Elementen deutlicher erkannt werden. Bei den während der TAMARA-Verbrennungskampagne durchgeführten Spiking-Versuchen wurde dem Brennstoff eine Mischung der chemischen Verbindungen zugegeben, von denen angenommen wird, dass sie die Speziation der Elemente im Hausmüll am besten repräsentieren.

## 6. Verteilung der Elemente auf die Verbrennungsrückstände und Transferkoeffizient

Durch die Analyse der entnommenen Proben kann die Verteilung der Schwermetalle auf den Verbrennungsrückständen (Partitioning) sowie deren Transferkoeffizienten ermittelt werden. Der Transferkoeffizient wird definiert durch den Anteil des Gesamtinventars eines Elementes, der aus der Brennkammer gemeinsam mit dem Rauchgas verflüchtigt und in den Kessel- und Flugstäuben wiedergefunden wird. Er ist ein wichtiger Parameter für die Beurteilung des Verhaltens von Schwermetallen bei Verbrennungsprozessen.

Auf der Basis ihres Transfers aus der Brennkammer können die untersuchten Elemente in zwei Gruppen aufgeteilt werden, und zwar als Flüchtige (Arsen und Antimon, mit ein Transfer von 19% bzw. 24%) oder Lithophile (Chrom und Molybdän, 3% bzw. 10%). Überraschenderweise wurde für **Arsen** ein eher geringer Transferkoeffizient nachgewiesen, obwohl dieses Element für seine Flüchtigkeit sehr bekannt ist. Dies ist ein Hinweis auf die Speziation des Arsens im Gutbett in Form stabiler Arsenate.

Die Änderung der Luftzahl hat keine Auswirkung auf die Verflüchtigung von **Chrom** aus dem Gutbett und nur eine geringe Wirkung auf die Verflüchtigung des **Molybdäns**. Bei Arsen und **Antimon** wirkt sie sich dagegen sehr stark aus. Eine Reduzierung der Luftzahl vom Referenzwert 1,5 auf 0,7 führt zu einer Zunahme des Elementtransfers um einen Faktor von mehr als 2. Dafür gibt es zwei Erklärungen: einerseits begünstigt ein erhöhter Sauerstoffpartialdruck (Luftüberschuss) in der Brennkammer die Bildung von thermisch stabilen Oxiden und oxianionischen Salzen. Andererseits geht aus den Temperaturprofilen hervor, dass sich mit einem abflachenden Profil (Luftzahl kleiner als 1) die Verweilzeit des Gutbetts im Hochtemperaturbereich erhöht und damit auch die für die Verflüchtigungsreaktionen verfügbare Zeit zunimmt. Bei geringen Luftzahlen (unter 0,7) verringert sich der Metalltransfer wiederum wieder.

Die Entnahme von Flugstaubproben an verschiedenen Stellen der Abkühlstrecke der Rauchgase erlaubt Rückschlüsse auf die Kondensationsmechanismen der Schwermetalle. Die Flugstäube decken einen Temperaturbereich von etwa 800°C bis hinunter auf 190°C (Filteraschen) ab.

**Antimon** und **Arsen** zeigen eine starke Anreicherung in den Filteraschen, was darauf hindeutet, dass diese Elemente während der Verbrennung gasförmige Verbindungen bilden, die später bei der Rauchgasabkühlung heterogen an den Flugstauboberflächen kondensieren.

Unter den lithophilen Metallen zeichnet sich **Molybdän** durch seine Anreicherung in den Filteraschen aus. Dies ist möglicherweise auf die Bildung flüchtiger halogenierter Verbindungen zurückzuführen. **Chrom** zeigt dagegen nur eine sehr geringe Anreicherung. Dies bedeutet, dass eine Bildung flüchtiger (und toxischer) Verbindungen nur in sehr begrenztem Maße oder überhaupt nicht stattfindet.

Die Konzentrationen aller untersuchten Schwermetalle in den abfiltrierten Rauchgasproben (Gaskondensate, Absorptionslösungen) lagen in der Nähe, meistens sogar unter der analytischen Nachweisgrenze. Dies bedeutet, dass so gut wie keine gasförmigen Verbindungen bei Temperaturen unter 200°C nachgewiesen werden konnten. Daher sind auch keine Umweltrisiken als Folge einer Emission aus dem Kamin zu erwarten.

## 7. Charakterisierung der Rostaschen

Der letzte Teil dieser Arbeit befasst sich mit der Charakterisierung der Rost- und Flugaschen aus der durchgeführten Verbrennungskampagne mit dem Ziel der Beurteilung des Laugungsverhaltens der Schwermetalle und ihres Mobilisierungspotentials aus den Rückständen.

Zu diesem Zweck wurden verschiedene standardisierte Laugungstests an den Verbrennungsrückständen (Rostaschen, Kesselaschen und Filteraschen) durchgeführt. Bei einem Vergleich zeigt sich, dass die verschiedenen Laugungstests bei den gleichen Proben zum Teil zu unterschiedlichen Ergebnissen führen können. Dies ist hauptsächlich darauf zurückzuführen, dass diese Versuche bei unterschiedlichen pH-Werten und mit unterschiedlichen Laugungsmitteln durchgeführt wurden. So ergab das für Deutschland vorgeschriebene Laugungsverfahren DEV S4 sehr geringe Werte für Arsen und Antimon und somit eine mögliche Unterschätzung des tatsächlichen Mobilitätspotentials. Grund dafür ist die starke Abhängigkeit der Auslaugbarkeit dieser beiden Elemente vom pH-Wert.

Die Analyse der Eluate aus den Rostaschen zeigte, dass zumindest ein Teil des Chrominventars in Form hochlöslicher und toxischer sechswertiger Chromate vorliegt. Außerdem zeigte **Chrom** ein Laugungsverhalten, das stark von den Verbrennungsparametern abhing. So war die aus den Rückständen eluierte Fracht dieses Metalls bei geringer Luftzahl (0,6) fast zwei Größenordnungen geringer als bei der Referenzluftzahl (1,5). Dieses Ergebnis ist von großer praktischer Relevanz und muss noch im Großmaßstab bestätigt werden. Eine Kompromisslösung zwischen einem vollständigen Ausbrand der Rostaschen und einer reduzierten Chromauslaugung als Folge einer Reduzierung der primären Luftzahl sollte angestrebt werden. Die Verteilung und die Gesamtmenge an Primärluft (zum Beispiel bei der Luftstufung) könnten dabei eine wichtige Rolle spielen.

Das Laugungsverhalten in Abhängigkeit vom pH-Wert aller vier untersuchten Schwermetalle wies deutlich auf deren oxianionische Speziation in den Eluat aus den Rostaschen hin. Dies bedeutet, dass sich die Auslaugtendenz der meisten anderen Metalle, bei denen von einer kationischen Speziation ausgegangen werden kann, erheblich unterscheidet, so dass das Auslaugpotential dieser Elemente möglicherweise unter- bzw. fehlgeschätzt werden könnte.

**Arsen** und **Antimon** zeigten eine starke Abhängigkeit vom pH-Wert mit einer maximalen Löslichkeit im neutralen Bereich und einer schnellen Abnahme unter die Nachweisgrenze bei stark sauren und alkalischen pH-Werten. **Chrom** und **Molybdän** zeigten im Gegensatz dazu eine viel schwächere Abhängigkeit der Elution vom pH-Wert und eine hohe Löslichkeit über den gesamten pH-Bereich.

Zusätzlich fand die Mobilisierung dieser beider Elemente aus der Aschenmatrix durch Auswaschprozesse zu Beginn des Kontakts zwischen dem wässrigen Laugungsmittel und den festen Rückständen statt. Daher sollten relativ hohe Frachten dieser Metalle im Wasser des Rostasche-Quenchtanks zu finden sein. Dies setzt allerdings eine für einen Auswascheffekt ausreichende Verweilzeit der Rostaschen im Abkühlbehälter voraus. Somit würde eine erste Schlackenwäsche schon innerhalb der Verbrennungsanlage stattfinden und dadurch eine Reduzierung des Inventars dieser Metalle in den Rostaschen. Das Abkühlwasser könnte dann zurückgeführt und in den Rauchgaswäschern wiederverwendet werden, um anschließend einer Behandlung mittels Metallfällung unterzogen zu werden. Die Wirksamkeit dieser relativ einfachen und kostengünstigen Maßnahmen zur Verringerung des Auslaugpotentials von oxianionischen Verbindungen sowie weitere Behandlungsmöglichkeiten (Sorbentienzugabe, Alterung und Wäsche) sollten im Großmaßstab gezielt untersucht werden.

## 8. Charakterisierung der Kessel- und Flugaschen

Das Elutionspotential (*Availability*, Verfügbarkeit) von **Arsen** aus Kesselaschen im Hochtemperaturbereich entsprach von der Größenordnung her dem der Rostaschen (10 bis 20%) und schien unabhängig von der Änderung der Luftzahl zu sein. Ganz anders war dies bei abnehmender Temperatur der Kesselaschen, bei der die Verfügbarkeit auf Werte von 5 bis 10% abnahm. Bei Filteraschen lag das Elutionspotential unter 1%.

Das geringe Elutionspotential in Filteraschen lässt sich mit dem vergleichsweise geringen pH-Wert dieser Rückstände in Kontakt mit Wasser erklären. Die Filteraschen besaßen einen schwach alkalischen bis neutralen pH-Wert als Folge der relativ langen Kontaktzeit mit den sauren Rauchgasen. In ähnlicher Weise zeigten Kesselaschen verschiedene pH-Werte im Bereich von

alkalisch bis neutral und in einigen Fällen bis schwach sauer, was auf Sulfatablagerungen zurückzuführen ist.

**Antimon** zeigte ein geringeres Elutionspotential als Arsen in Rostaschen und Flugaschen. Außerdem schien das Elutionsverhalten aus den verschiedenen Flugaschefraktionen homogener als bei Arsen zu sein.

**Chrom** wies eine bemerkenswert hohe Verfügbarkeit in Kesselaschen aus dem Hochtemperaturbereich aus, insbesondere bei hohen Luftzahlen (bis zu 20%). Angesichts des geringen Elutionpotentials dieses Metalls aus den Rostaschen (unter 2%) ist dies überraschend.

**Molybdän** zeigte ein außerordentlich hohes Elutionspotential in Kesselaschen, das in einigen Fällen bis zu 80% des in den Rückständen gebundenen Molybdäns betrug. Filteraschen zeigten eine mittlere Verfügbarkeit, die mit reduzierter Luftzahl abnahm.

Die Änderung der Auslaugtendenz der untersuchten Metalle von anionisch zu kationisch bei Rückständen aus dem Kesselbereich, in dem niedrigere Temperaturen herrschen, sowie aus den Filterstäuben, insbesondere für Arsen und Antimon, deutet darauf hin, dass die Kondensation der flüchtigen kationischen Verbindungen hauptsächlich im Niedrigtemperaturbereich des Kessels stattfindet.

## 9. Ausblick

Die Ergebnisse aus dieser Arbeit zeigen insgesamt, dass die Bildung von oxianionischen Spezies bei der Abfallverbrennung eine erhebliche Auswirkung auf das Verhalten der vier untersuchten Schwermetalle hat. Wenn einerseits, bei einer effektiven Rauchgasreinigung, keine Gefährdung der Umwelt durch Kaminemission selbst der flüchtigeren Metalle zu erwarten ist, so darf andererseits das Risikopotential einer Grundwasserkontamination durch Auslaugung von hochlöslichen oxianionischen Verbindungen aus den Verbrennungsrückständen nicht unterschätzt werden.

In Hinsicht auf diesen letzten Aspekt sollten alle Möglichkeiten der Beeinflussung der chemischen Form der Schwermetalle in den Rückständen (insbesondere bei Chrom) durch eine Prozessoptimierung bezüglich Primärluftzufuhr (zum Beispiel durch gezielte Luftstufung) im Großmaßstab überprüft werden. Gleichzeitig sollte die Auswirkung von relativ einfachen und kostengünstigen Schlackenbehandlungsmaßnahmen, die schon innerhalb der Verbrennungsanlage durchgeführt werden können, wie zum Beispiel eine Waschstufe durch erhöhte Verweilzeit im Quenchbad, überprüft werden. Diese Maßnahmen würden zu einer verbesserten Umweltqualität der Rostaschen und somit gleichzeitig auch zu einem erhöhten Potential der Wiederverwertung führen.

## Acknowledgements

A very grateful acknowledgement goes to Prof. Dr.-Ing. Helmut Seifert (Institut für Technische Chemie-Bereich Thermische Abfallbehandlung, Forschungszentrum Karlsruhe) and to Prof. Dr.-Ing. Klaus R. G. Hein (Institut für Verfahrenstechnik und Dampfkesselwesen, University of Stuttgart) for accepting the part of director and co-director of this work and for their reviewing work.

A further special acknowledgement goes to Dr. Jürgen Vehlow (ITC-TAB) for his supervision and advice throughout all the phases of this work.

The present work has been made possible by the help and the contribution of many people, to all of whom goes the author's deepest gratitude:

*Institut für Technische Chemie- Bereich Thermische Abfallbehandlung:*

Hans Geisert: thermal analysis (TG-DSC)

Andreas Gerig, Gerd Häfele, Reinhold Siegel, Günther Zimmermann, TAMARA technical staff: residue sampling and sample treatment.

Petra Bosch, Rainer Härtel, Patrick Hammer, Julia Marquardt, Heide Mathieu, Monika Schleinkhofer, Juliane Wilhelm: sample analysis.

Christine Sack, Erich Schmidt: database and computer support.

Pia Bengert, Elisabeth Juerges, Stefanie Pressmann, Klaus Rieber, Fritz Riffel, Helmut Reis: general technical support.

Britta Bergfeldt, Hans Hunsinger, Daniela Merz, Bernd Zimmerlin: ideas, suggestions, helpful advice.

*Forschungszentrum Karlsruhe:*

Dr. Adelhelm (IMF-III), Ms. Ansbach, Mr. Bumiller, Ms. Winkler (BTI-LFU), Mr. Gramegna (ITC-CPV).

*Netzsch Gerätebau:*

Dr. Kaiser, Mr. Strobel.

*Institut für Mineralogie, Universität Karlsruhe:*

Dr. Karotke, Coco Fuhlberg (XRD Analysis).

The author also wishes to gratefully acknowledge the invaluable contribution of the following persons:

Daniela Ceremigna (University "La Sapienza", Rome),

Markus Hauser (University of Karlsruhe),

Davide Marino (University of Perugia) .

Finally, a personal thank you goes to my family and all my friends for their constant encouragement and support.



**Contents**

	Page
List of figures	iii
List of tables	v
List of abbreviations	vii
List of chemical compounds	ix
<b>Introduction and aims</b>	<b>1</b>
<b>1. About the elements</b>	<b>5</b>
1.1 Properties of the elements	5
1.1.1 Arsenic	5
1.1.2 Antimony	6
1.1.3 Chromium	7
1.1.4 Molybdenum	8
1.2 Concentration of the elements in municipal solid waste	10
1.3 Enrichment of the elements in municipal solid waste	11
1.4 Origin and speciation of the elements in municipal solid waste	12
<b>2. Physical and chemical transformations during combustion</b>	<b>15</b>
2.1 Pathways of metals through a combustion system	15
2.2 Modeling the chemical equilibrium	17
2.3 Behavior of arsenic and antimony	19
2.4 Behavior of chromium	23
2.5 Behavior of molybdenum	26
<b>3. Oxyanion formation</b>	<b>29</b>
3.1 Theoretical considerations	29
3.2 Thermal analysis	31
3.3 Experimental program	33
3.4 Results	34
3.4.1 Arsenic and antimony	34
3.4.2 Chromium	39
3.4.3 Molybdenum	42
<b>4. Experimental methods</b>	<b>45</b>
4.1 TAMARA test facility for waste incineration	45
4.2 Sampling strategies	47
4.3 Sample treatment	48

	Page
4.4 Analytical methods	50
4.5 Leaching procedures	51
<b>5. Incineration tests on pilot plant TAMARA</b>	<b>55</b>
5.1 Incineration campaign	55
5.2 Spiking experiments	58
5.3 Relevance of test results	60
5.4 Transfer factor of the elements	63
5.5 Condensation on fly ashes	67
5.6 Filter-passing species	72
<b>6. Characterization of grate ashes</b>	<b>73</b>
6.1 Characteristics of municipal solid waste incinerator grate ashes	73
6.2 Availability of the elements	76
6.3 Regulatory leaching tests	77
6.4 Effect of leachate pH on leaching behavior	79
6.5 Time resolution of leaching	83
<b>7. Characterization of fly ashes</b>	<b>85</b>
7.1 Characteristics of municipal solid waste incinerator fly ashes	85
7.2 Availability of the elements in the fly ashes	89
7.3 Effect of leachate pH on the leaching behavior of the elements	92
<b>Conclusions and outlook</b>	<b>97</b>
<b>References</b>	<b>103</b>

**List of figures**

	Page	
1.1	Distribution of As among MSW fractions	12
1.2	Distribution of Sb among MSW fractions	13
1.3	Distribution of Cr among MSW fractions	13
2.1	Vapor pressure of As compounds	19
2.2	Vapor pressure of Sb compounds	19
2.3	$\Delta G$ values for As reactions	20
2.4	$\Delta G$ values for Sb reactions	21
2.5	$\Delta G$ values for Cr reactions	24
2.6	$\Delta G$ values for Mo reactions	28
3.1	Netzsch Thermobalance STA 409	32
3.2	Scheme of the TG-DSC system	32
3.3	$Sb_2O_3$ in nitrogen atmosphere	35
3.4	$Sb_2O_3$ in synthetic air atmosphere	35
3.5	$Sb_2O_3 + CaO$ in nitrogen atmosphere	36
3.6	$Sb_2O_3 + CaO$ in synthetic air atmosphere	36
3.7	XRD spectrum of sample <i>Sb2</i>	37
3.8	$As_2O_3 + CaO$ in synthetic air atmosphere	38
3.9	XRD spectrum of sample <i>As2</i>	38
3.10	$Cr_2O_3 + CaO$ in synthetic air atmosphere	39
3.11	XRD spectrum of sample <i>Cr2</i> (1 hour @850°C)	40
3.12	XRD spectrum of sample <i>Cr2</i> (1 hour @1250°C)	40
3.13	$Cr_2O_3 + CaO$ in inert atmosphere	41
3.14	XRD spectrum of sample <i>Cr2</i> (1 hour @1000°C, inert atmosphere)	41
3.15	$MoO_2$ in synthetic air and in nitrogen atmosphere	42
3.16	$MoO_3 + CaO$ in synthetic air atmosphere	43
3.17	XRD spectrum of sample <i>Mo2</i>	44
4.1	TAMARA test facility	45
4.2	TAMARA combustion chamber	46
4.3	Plane filter chamber	48
4.4	Absorption system	48
4.5	Riffle for sample subdivision	49
4.6	Ball mills and sieves	49

	Page
4.7 Automatic titration unit (Metrohm Titrino 719 S)	53
4.8 Column leaching test equipment	54
4.9 Vacuum filtration equipment	54
5.1 Temperature profiles along the grate	57
5.2 Percent partitioning of the elements (campaign average)	63
5.3 Transfer factor (as % of the inventory)	65
5.4 Transfer factor standardized to calcium transfer	66
5.5 Enrichment of the elements on fly ashes (campaign average)	69
5.6 Enrichment on fly ashes of Sb	70
5.7 Enrichment on fly ashes of As	70
5.8 Enrichment on fly ashes of Mo	71
5.9 Enrichment on fly ashes of Cr	71
6.1 TAMARA grate ash	74
6.2 Availability of the elements in grate ashes	76
6.3 Regulatory leaching tests (averaged values)	77
6.4 Leaching of As as a function of pH	80
6.5 Leaching of Sb as a function of pH	80
6.6 Leaching of Cr as a function of pH	81
6.7 Leaching of Mo as a function of pH	82
6.8 Column leaching test	83
7.1 pH values of the fly ashes	88
7.2 Availability of As from boiler and filter ashes	89
7.3 Availability of Sb from boiler and filter ashes	90
7.4 Availability of Cr from boiler and filter ashes	91
7.5 Availability of Mo from boiler and filter ashes	91
7.6 As leaching from boiler and fly ashes	92
7.7 Sb leaching from boiler and fly ashes	93
7.8 Cr leaching from boiler and filter ashes	94
7.9 Mo leaching from boiler and filter ashes	95

**List of tables**

	Page
1.1 Concentration of the elements in municipal solid waste	11
1.2 Concentration and enrichment of the elements in MSW and coal	11
1.3 Industrial applications and speciation of the elements	14
2.1 Melting points of chromium compounds	23
2.2 Volatility of molybdenum and tungsten compounds	27
3.1 Electronegativities of the elements	30
3.2 Investigated model reactions	30
3.3 Calibration substances	33
3.4 Samples for thermal analysis	34
4.1 Leaching procedures carried out	51
4.2 Leaching parameters	52
5.1 Combustion air	57
5.2 Temperatures in the boiler	58
5.3 Input mass flows	59
5.4 Spiking experiments	59
5.5 Inventory of the metals (averaged values)	60
5.6 Output mass flows	60
5.7 Frequent error causes	62
5.8 Test performance (output/input ratio)	62
5.9 Partitioning data and transfer factor of the elements (campaign average)	64
5.10 Transfer factor of the elements (as % of the inventory, spiked runs)	65
5.11 Transfer factor of the elements (standardized to calcium transfer, spiked runs)	66
5.12 Accumulated enrichment factor of the elements (campaign average)	68
5.13 Filter-passing species	72
6.1 Characteristics of TAMARA grate ashes	75
6.2 Concentration of the investigated elements in grate ashes	75
6.3 Hexavalent chromium concentration in DEV S4 leachates	78
7.1 Chemical composition of boiler and filter ashes	86
7.2 Concentration of the investigated elements in boiler ashes	87
7.3 Concentration of the investigated elements in filter ashes	87
7.4 Total carbon content of boiler and filter ashes	88



**List of abbreviations**

AVA	availability leaching test
C	fuel carbon content
CLT	column leaching test
$c_p$	molar heat (at constant pressure)
$Cr_{tot}$	total chromium
Cr(VI)	hexavalent chromium
DEV	Deutscher Einheitsverfahren (German standard procedure)
DIN	Deutsches Institut für Normung (German standardization institute)
DSC	differential scanning calorimetry
$\Delta EN$	difference in electronegativity
$\Delta G$	variation of the state function Gibbs energy
E&E	electrical and electronic
EF	enrichment factor
G	Gibbs energy
H	molar enthalpy
	fuel hydrogen content
HSAB	Hard-Soft-Acid-base principle
IAWG	International Ash Working Group
IC	ionic chromatography
IR	infra-red
L/S	liquid-to-solid ratio
$I_{min}$	theoretical air demand
$\lambda$	air ratio
M	molarity
MSW	municipal solid waste
MSWI	municipal solid waste incineration
N	fuel nitrogen content
	normality
NEN	Netherlands Normalization Institute
O	fuel oxygen content
$O_{min}$	stoichiometric oxygen demand
PIC	products of incomplete combustion
ppm	parts per million
PTFE	polyethylenethereftalate
PVC	polyvinylchloride
RDF	refuse-derived fuel
S	molar entropy
	fuel sulphur content
T	temperature
TAMARA	Testanlage zur Müllverbrennung, Abgasreinigung, Rückstandsverwertung, Abwasserbehandlung (test facility for waste combustion, flue gas cleaning, residue treatment and wastewater purification)
TC	total carbon content
TG	thermogravimetry
TOC	total organic carbon content
TRFA	total reflection X-ray fluorescence analysis
TVA	Technische Verordnung über Abfälle (technical regulation on waste)

US EPA	United States of America Environmental Protection Agency
VDI	Verein Deutscher Ingenieure (German engineers' association)
VGB	Vereinigung Großkraftwerksbetreiber (German association of power plant operators)
WASTE	waste analysis, sampling, testing and evaluation program
XRD	X-ray diffractometry

**List of chemical compounds**

$\text{Al}_2(\text{SO}_4)_3 \cdot 18\text{H}_2\text{O}$	aluminium sulphate-18-hydrate
$\text{Al}_2\text{O}_3$	dialuminium trioxide (alumina)
As	arsenic
$\text{AsBr}_3$	arsenic tribromide
$\text{AsCl}_3$	arsenic trichloride
$\text{AsH}_3$	arsenic hydride
$\text{As}_2\text{O}_3$	arsenic trioxide
$\text{As}_2\text{S}_3$	arsenic trisulfide (auripigment)
$\text{As}_4\text{S}_4$	arsenic tetrasulfide (realgar)
Ba	barium
$\text{BaCrO}_4$	barium chromate
$\text{Br}^-$	bromide ion
C	carbon
Ca	calcium
$\text{Ca}_6\text{Al}_2(\text{SO}_4)_3(\text{OH})_{12} \cdot 26\text{H}_2\text{O}$	ettringite
$\text{Ca}_3(\text{AsO}_3)_2$	calcium arsenate (trivalent)
$\text{Ca}_3(\text{AsO}_4)_2$	calcium arsenate (pentavalent)
$\text{CaCl}_2$	calcium chloride
$\text{CaCO}_3$	calcium carbonate
$\text{Ca}(\text{CrO}_2)_2$	calcium chromate (trivalent)
$\text{CaCrO}_4$	calcium chromate (hexavalent)
CaO	calcium oxide
$\text{Ca}(\text{OH})_2$	calcium hydroxide (portlandite)
$\text{CaMoO}_3$	calcium molybdate (tetravalent)
$\text{CaMoO}_4$	calcium molybdate (hexavalent) (powellite)
$\text{Ca}_3(\text{SbO}_3)_2$	calcium antimonate (trivalent)
$\text{Ca}_3(\text{SbO}_4)_2$	calcium antimonate (pentavalent)
$\text{CaSO}_4$	calcium sulphate
$\text{CH}_3\text{COOH}$	acetic acid
Cl	chlorine
$\text{Cl}^-$	chloride ion
$\text{CO}_2$	carbon dioxide
Cr	chromium
$\text{CrCl}_2$	chromium dichloride
$\text{Cr}(\text{CO})_6$	chromium hexacarbonyl
$\text{CrF}_3$	chromium trifluoride
$\text{CrO}_2$	chromium dioxide
$\text{Cr}_2\text{O}_2\text{Cl}_2$	chromylchloride
$\text{CrO}_2\text{OH}$	pentavalent chromium oxyhydroxide
$\text{CrO}_2(\text{OH})_2$	hexavalent chromium oxyhydroxide
$\text{CrO}_3$	chromium trioxide
$\text{Cr}_2\text{O}_3$	dichromium trioxide
$\text{Cr}_2\text{S}_3$	dichromium trisulfide
F	fluoride ion
FeO	iron monoxide
$\text{Fe}_2\text{O}_3$	iron trioxide
$\text{H}_2$	hydrogen
$\text{H}_2\text{O}$	water
$\text{H}_2\text{O}_2$	hydrogen peroxide

H <sub>3</sub> PO <sub>4</sub>	orto-phosphoric acid
HBr	hydrobromic acid
HCl	hydrochloric acid
HF	hydrofluoric acid
HNO <sub>3</sub>	nitric acid
K	potassium
KCl	potassium chloride (sylvine)
K <sub>2</sub> HPO <sub>4</sub> *3H <sub>2</sub> O	phosphorous buffer
K <sub>2</sub> O	potassium oxide
Mg	magnesium
MgO	magnesium oxide
Mo	molybdenum
MoCl <sub>5</sub>	molybdenum pentachloride
MoF <sub>5</sub>	molybdenum pentafluoride
MoF <sub>6</sub>	molybdenum hexafluoride
MoO <sub>2</sub>	molybdenum dioxide
MoO <sub>2</sub> Cl <sub>2</sub>	molybdenum oxydichloride
MoO <sub>2</sub> F <sub>2</sub>	molybdenum oxydifluoride
MoO <sub>3</sub>	molybdenum trioxide
MoOCl <sub>3</sub>	molybdenum oxytrichloride
MoOF <sub>4</sub>	molybdenum oxytetrafluoride
MoS <sub>2</sub>	molybdenum disulfide (molybdenite)
N <sub>2</sub>	nitrogen
Na	sodium
NaCl	sodium chloride (halite)
Na <sub>2</sub> MoO <sub>4</sub>	sodium molybdate
NaOH	sodium hydroxide
Na <sub>2</sub> O	sodium oxide
NO	nitrogen monoxide
NO <sub>3</sub> <sup>-</sup>	nitrate ion
O <sub>2</sub>	oxygen
PbCrO <sub>4</sub>	lead chromate
PbMoO <sub>4</sub>	lead molybdate (wulfenite)
S	sulphur
Sb	antimony
SbBr <sub>3</sub>	antimony tribromide
SbCl <sub>3</sub>	antimony trichloride
SbCl <sub>5</sub>	antimony pentachloride
Sb <sub>2</sub> O <sub>3</sub>	antimony trioxide (valentinite)
Sb <sub>2</sub> O <sub>4</sub>	antimony tetraoxide
Sb <sub>2</sub> O <sub>5</sub>	antimony pentaoxide
Sb <sub>2</sub> S <sub>3</sub>	antimony trisulfide
SiC	silicium carbide
SiO <sub>2</sub>	silicium dioxide (quartz)
SO <sub>2</sub>	sulphur dioxide
SO <sub>4</sub> <sup>2-</sup>	sulphate ion
Sr	strontium
W	tungsten
WBr <sub>5</sub>	tungsten pentabromide
WBr <sub>6</sub>	tungsten hexabromide
WCl <sub>6</sub>	tungsten hexachloride

$\text{WCl}_5$	tungsten pentachloride
$\text{WF}_6$	tungsten hexafluoride
$\text{WO}_2\text{Cl}_2$	tungsten oxydichloride
$\text{WO}_3$	tungsten trioxide
$\text{WOB}_4$	tungsten oxytetrabromide
$\text{WOCl}_4$	tungsten oxytetrachloride
$\text{WOF}_4$	tungsten oxytetrafluoride

## **Introduction and aims**

For efficient environmental control of combustion processes and for the evaluation of the potential risk represented by trace metals emissions into the geosphere, it is essential to achieve detailed knowledge of chemical reactions which take place in the combustion system and which affect the successive fate of these elements. This is especially true in the case of municipal solid waste incineration, where the input fuel is a highly inhomogeneous material which might be considerably enriched in toxic metals, compared to other fossil fuels.

Metals cannot be destroyed during combustion, but they undergo changes in their chemical speciation which result in formation of different compounds. That means chemical reactions affect the fate of the metals present in municipal solid waste in several ways and the products of these reactions might differ greatly from the original input species.

The formation of volatile compounds implies a certain transfer of a metal out of the fuel bed and diverts part of the metal inventory to the combustion raw gas, where, depending on the temperature, it stays in the gas phase or it ends up in the boiler or filter ashes. The resulting partitioning process is described by the transfer factor, i.e. the fraction of the input inventory which leaves the combustion chamber along with the flue gas and ends finally up in the respective compartment.

While today the improvements in air pollution technologies for incinerators have reached such efficiency levels that even the strictest emission limits can be complied with easily, the mechanisms that control the partitioning of specific elements among the different residue streams are still not fully understood. The assessment of the main factors influencing the fate of heavy metals (such as chemical interactions with other fuel bed constituents, main combustion parameters, i.e. fuel bed temperature) is an essential issue for the evaluation of the emission potential of combustion processes.

Another fundamental aspect in assessing the potential environmental impact of an element is the knowledge of its speciation in the various solid combustion residues and its potential for release out of the solid matrix into an aqueous environment, or its leachability. The latter is a direct consequence of the chemical and geochemical transformations that take place in the fuel bed and determines the form in which the element is fixated in the ash matrix. The assessment of the main factors governing the mobilization mechanisms and of the leaching potential of toxic elements is

fundamental for the evaluation of the mid- and long-term consequences of residue utilization and/or disposal.

This work intends to focus on a special group of chemical reactions, the formation of oxygen-containing anions, or oxyanions. The metals involved in these reactions are mainly those the metallic character of which is not very marked, and some of them (for example arsenic) should more correctly be grouped among half-metals. These metals are prevalently found in the 5<sup>th</sup> main group and in the 4<sup>th</sup> to the 7<sup>th</sup> group of transition elements.

The elements chosen for this investigation on account of their environmental relevance are arsenic, antimony, chromium and molybdenum. However, it can be expected that many of the considerations that will result from experimental evidence will apply to other metals exhibiting a similar behavior, such as tungsten or vanadium, as well.

The two half-metals arsenic and antimony are well-known for the volatility of many of their compounds and are thus listed among the heavy metals with a high emission potential. However, several authors have pointed out the limited volatilization exhibited by arsenic in presence of high calcium amounts in the fuel bed. Interaction with calcium and subsequent formation of thermally stable arsenates is a very plausible hypothesis which needs more detailed investigation. For antimony, there is less information available in literature, but a similar reaction mechanism can be expected on behalf of the close chemical similarity between these two elements.

For chromium, the possible formation of hexavalent chromates during combustion is an issue of great importance. The toxicity of this element is strongly dependent on its oxidation state, as the hexavalent compounds are much more harmful than trivalent ones. Normally, in a municipal solid waste incinerator, no oxidation to hexavalent chromium should be expected to take place, because of the comparatively low fuel bed temperatures. On the other side, hexavalent chromate formation as a consequence of chemical reaction with alkaline fuel components is a reaction route which should not be underestimated.

Molybdenum is a heavy metal which is normally not associated with environmental concerns. However, the very high solubility of molybdates and most of all their toxicity to ruminants might become an environmental issue in case of groundwater contamination. For this reason, some countries (for example the Netherlands) have listed molybdenum among environmental polluting

substances. Mechanisms controlling the chemical speciation of molybdenum in solid combustion residues and its leaching potential deserve therefore an increased attention.

The starting point to understand the fate of an element in the waste incineration process is its concentration in municipal solid waste and – eventually even more important – its speciation. For this purpose a literature review has to be performed to get detailed information about the occurrence of the chosen elements in the major waste constituents and about the industrial applications of the most relevant chemical compounds.

The thermal behavior of the prevailing input species of the elements in question will be successively investigated from a theoretical point of view by calculating free formation enthalpies. This thermodynamic evaluation is helpful in pointing out which reactions are more likely to take place in the combustion chamber and in making first estimates on the volatility of the reaction products.

Formation of oxyanions is normally assumed to take place in an alkaline aquatic environment. However, there is evidence that the formation of oxyanionic salts can also occur in a solid-phase, high temperature environment.

Thermogravimetric and calorimetric investigations in a thermobalance can provide effective evidence for such reaction routes, since oxidation or decomposition of constituents of a sample cause distinct mass variations at specific temperatures. Furthermore, the reaction enthalpy can be measured in a differential scanning calorimeter and diffractometric analysis of sample residues allows the identification of reaction products. The combination of these experimental techniques is useful not only to assess the likelihood of the formation of oxyanionic species in the fuel bed during incineration, but it gives also an insight on the reaction kinetics and on the combustion parameters which are likely to control these processes. Furthermore, thermal analysis can supply thermodynamic data which are lacking in literature for specific elements.

Spiking incineration tests in the pilot plant TAMARA allow to point out the effect of the primary air ratio on the transfer factor of the investigated metals, as well as their partitioning in the different solid residue streams. The evaluation of the enrichment of metals on fly ashes collected at different temperatures and locations along the flue gas cooling path enables to speculate on temperature-dependant condensation mechanisms. Collection of dedusted raw gas samples by means of a condensation and absorption system allows the analysis of the gaseous or filter-passing metallic

species at temperatures below 200°C, thus giving a first estimate of the emission potential for these heavy metals.

The assessment of the leaching characteristic of the metals in question in the different incineration residues (grate ashes, boiler and filter ashes) provides evidence of their chemical speciation and hence helps understand the reactions that took place in the combustion chamber. Furthermore, the different leaching test procedures are an important instrument to evaluate the potential impact of the incineration residues on aqueous systems (for example groundwater) and their suitability for environmentally sound utilization.

The main objective of the present work is to provide a better understanding of some chemical reaction routes which are normally neglected and which might strongly influence the fate and hence the environmental impact of the selected heavy metals.

Once the most likely reaction routes are identified, they need to be verified on a laboratory-scale basis. Incineration experiments on pilot-scale will subsequently indicate which consequences can be extrapolated for incineration plants. The final goal is to point out the topics on which a further optimization of the combustion process is necessary and which need more detailed clarification on a full-scale basis.

## **Chapter 1**

### **About the Elements**

#### **1.1 Properties of the elements**

##### **1.1.1 Arsenic**

Arsenic (chemical symbol As) is a half-metal belonging to the fifth main group of the periodic table of elements. It occurs in two solid modifications: gray, or metallic (the ordinary stable form), and yellow. Three unstable amorphous forms are also known. Arsenic exhibits oxidation states  $-3$ ,  $0$ ,  $+3$ ,  $+5$ .

The name of the element comes from the ancient Greek *arsenikon*, “fearless, brave, masculine”. The origin of the name is based upon the reactivity of the sulfide with metals, derived from the custom prevailing at that time of classifying the metals as feminine or masculine [Hanusch et al., 1997].

Two arsenic sulfides, realgar ( $\text{As}_4\text{S}_4$ ) and auripigment ( $\text{As}_2\text{S}_3$ ) were in use in ancient times as pigments. The poisonous properties of some arsenic compounds (mainly  $\text{As}_2\text{O}_3$ ) were well known to the medieval alchemists and in the Renaissance. However, numerous medical applications are also reported by Theophrastus Bombastus von Hohenheim, also known as Paracelsus [Paracelsus, 1589].

The average arsenic content of the earth’s crust is approximately  $6 \cdot 10^{-4}\%$  [Hanusch et al., 1997]. Arsenic is comparatively widespread and can be detected in traces nearly everywhere. Although arsenic-bearing minerals are known, only a few occur in such quantities that they can be extracted economically. Usually arsenic is recovered as a by-product in the smelting of non-ferrous ores (gold, silver, nickel, cobalt or antimony). However, today it is rather regarded as an unwanted accompanying element in metallurgy.

Arsenic production reached high levels during the first decades of the 20<sup>th</sup> century, when the possibility of its application as insecticide and pesticide was discovered. This kind of application is strongly limited today and in many countries even prohibited. Another utilization in strong decline nowadays used to be as a green paint pigment (Scheele’s green, Paris green, Emerald green).

Apart from its agricultural utilization, arsenic is still employed as an alloying element (lead or copper alloys), in the electronical industry as a semiconductor (especially its intermetallic compounds with gallium or indium). Furthermore, organoarsenic compounds have a variety of medical uses (mainly in the cure of some tropical diseases).

Nearly all arsenic compounds are considerably toxic, especially the inorganic ones. Uptake in the body can take place by means of ingestion, inhalation or through skin contact. Trivalent compounds

show a higher toxicity than pentavalent ones. The most poisonous compounds are trivalent oxide ( $\text{As}_2\text{O}_3$ ) and the gaseous hydride ( $\text{AsH}_3$ , arsine). On the other hand, it must be remembered that, as for all trace elements, arsenic is essential for many life functions, and it plays a particular role in body growth. Thus, the necessary amount in the human body is estimated to be approximately 0,2 mg/kg body weight [Endriss, 1997]. Below this value, deficiency symptoms may occur, mainly in form of growth limitations.

An overview about arsenic cycles in the geosphere can be found in the work by Matschullat [Matschullat, 2000].

### 1.1.2 Antimony

Antimony (chemical symbol *Sb*) is located in the periodical table of elements just below arsenic in the fifth main group. Arsenic and antimony have many common properties and show very similar chemical behavior, except for the fact that in antimony the metallic character is more clearly pointed out. In fact, while arsenic is generally classified among half-metals, antimony is generally grouped among metals.

Antimony is stable in its metallic form, even if other unstable allotropes (the so-called yellow, black and explosive antimony) are known. Antimony shows the oxidation states  $-3, 0, +3, +5$ . Trivalent compounds are more stable than the pentavalent ones.

The origin of the name is not very clear. The Latin used to call it *stibium*, from the Egyptian *stim* "lead". Some indicate the origin of the name antimony in the Greek *anti + monos* (element not to be found alone) [Lide, 1994].

Antimony has been known since over 5000 years: it was used by the Chinese, the Egyptians and the Romans for cosmetic purposes and by the alchemists in the middle ages to separate gold from silver. Paracelsus reports medical uses [Paracelsus, 1589]. However, until the 16<sup>th</sup> century it was believed to be a variety of lead [Herbst et al., 1997].

The average antimony concentration in the lithosphere amounts to approximately  $3 \cdot 10^{-5}\%$ . It is usually found in volcanic areas in form of antimony glance ( $\text{Sb}_2\text{S}_3$ ) or valentinite ( $\text{Sb}_2\text{O}_3$ ). The main producers nowadays are Bolivia, Republic of South Africa, People's Republic of China and the states of the former Soviet Union. Frequently, it is a by-product of the extraction of other metals such as lead, silver and gold.

Today, different antimony compounds have a wide range of industrial uses. Metallic antimony is commonly used in metallic alloys, such as pewter, lead-antimony, tin-antimony: it improves alloy properties like hardness, durability and resistance to chemical corrosion. For these reasons, antimony alloys are used in the industrial production of batteries (until recently the main industrial

use for antimony), power transmission devices, solder, pumps, pipes and tanks for chemical products, antifriction bearings, type metal, ammunition. High purity antimony metal is used for inter-metallic compounds for electronic semiconductors and thermoelectric devices.

The decline in the use for batteries is being offset by increased consumption of antimony trioxide as an addition to bromine-containing flame retardants, now the dominant market for this element. Flame retarding treatment is required for all kind of materials which, because of their nature or of their use, are subject to fire risk, such as textiles, tapestries, heat insulating materials used in cars or in the building sector, and plastics, especially those applied in the electrical and electronic (E&E) sector.

Other secondary uses of antimony include paint, ceramic, glass and plastic production, matches and pyrotechnics manufacturing, white, yellow and orange pigments, rubber vulcanization. Gallium and indium antimonides are used in optical information memories working with laser signals, such as compact disks and digital optical recording. Some organic antimony compounds have medical uses [Herbst *et al.*, 1997].

It is difficult to estimate the degree of toxicity of antimony, since generally the exposure takes place in presence of other toxic elements, such as lead, arsenic and mercury. However, the toxicity of antimony can be considered to be very close to that of arsenic. Similarly to arsenic, the trivalent compounds are more toxic than the pentavalent ones.

### 1.1.3 Chromium

Chromium (chemical symbol *Cr*) is the first element of the sixth transition group in the periodic table. It shows oxidation states 0, +2, +3, +4, +5 and +6. However, the most stable compounds are the trivalent and the hexavalent ones.

The name has its origin in the Greek *chroma*, “color”, because of the variety of different colors shown by its compounds. Chromium was discovered as lead chromate ( $\text{PbCrO}_4$ ) in 1797 and isolated as metal in 1798 by Vauquelin [Downing *et al.*, 2001].

Chromium belongs to the group of the more abundant trace elements, with an average concentration in the earth crust of 0,01%. It is often found in magmatic intrusions and their crystallization. Although chromium is found in many minerals, the only commercial source of chromium is chromite, which is a spinel of the form  $\text{FeO}\cdot\text{Cr}_2\text{O}_3$ . The main producers are South Africa, Zimbabwe, Turkey, the states of the former Soviet Union, the United States of America and Finland.

Chromium has a great number of industrial applications, which can be roughly divided in three main categories: ferrous/non-ferrous alloys, production of refractory materials, chemical products.

For the production of stainless steel, chromium is usually added in form of ferrochrome (a master alloy of iron and chromium, containing 45-95% Cr), while the alloys made from pure chromium are referred to as superalloys.

The refractory industry has found chromite useful for forming bricks and shapes, for its high melting point, the moderate thermal expansion, and the stability of the crystalline structure.

Chromium compounds are in use in the chemical industry since the 19<sup>th</sup> century. Chromates yield yellow, red and green pigments. Moreover, chromium compounds are used in traces also in other pigments, ranging from black to blue [Endriss, 1997]. Dichromates are employed on base of their oxidizing properties in the textile and the photographic industry.

All of the chromium oxides have large applications: the trivalent oxide ( $\text{Cr}_2\text{O}_3$ ) is used as a green pigment and as a catalyst. Tetravalent oxide ( $\text{CrO}_2$ ) is used in the production of magnetic audio and video tapes. Hexavalent chromium oxide ( $\text{CrO}_3$ ) is used in chrome plating to produce a hard, beautiful surface and to prevent metal corrosion. It is also employed as a wood protecting and oxidizing agent. Basic chromium sulphates play an important role in leather tanning [Anger et al., 1997].

Chromium is essential for many life functions, it is necessary in enzymes, and it acts as an antidiabetogenic agent. Lack of chromium might induce diabetes [Endriss, 1997]. The recommended daily intake is estimated to be around 50 – 500  $\mu\text{g}$  (in adults). Excessive levels of chromium in vegetable or animal food are not known and supply of chromium tends to be rather too low than too high [Anger et al., 1997].

For the toxicological behavior, the speciation of chromium plays a crucial role. While trivalent compounds can be regarded as being rather harmless, hexavalent ones are much more toxic because of the oxidizing action they can exert on cell membranes. They also show carcinogenic effects.

#### 1.1.4 Molybdenum

Molybdenum (chemical symbol *Mo*) is the element just below chromium in the sixth transition group of the periodic table. As in other transition elements groups, the second element has quite a different behavior from the first element (Cr) but is very close to the third one (tungsten, W).

Molybdenum shows oxidation states 0, +2, +3, +4, +5, +6, although much of the familiar molybdenum chemistry is in the +5 and +6 oxidation states. Molybdenum thus exemplifies a further trend in transition metal groups: for the heavier elements (Mo, W) the higher oxidation states are more stable than the lower ones (i.e. more resistant to reduction), while the opposite holds for chromium. Moreover, hexavalent molybdates (as well as hexavalent tungstates) do not have

oxidizing properties, unlike hexavalent chromates. This fact has obviously a positive effect in view of their toxicity, as will be discussed further on.

Molybdenum shows a complicated aquatic chemistry. It is dominated by oxo-species which are prone to dimerize or polymerize.

Molybdenum derives its name from the Greek *molybdos*, “lead”. Until discovered by Scheele in 1778, molybdenum disulfide ( $\text{MoS}_2$ ) was confused with graphite and lead ore. After its discovery, for the next century, molybdenum was merely a laboratory curiosity. The first major use came during the first world war, when additions of molybdenum produced steel with excellent toughness and strength at high temperatures for utilization as tank armor in aircraft engines. In peace times after the war, new uses were developed, largely in the automotive industry [Sebenik et al., 1997].

The earth’s crust molybdenum content amounts to  $10^{-4}\%$ . Molybdenum does not occur native, but is obtained principally from molybdenite ( $\text{MoS}_2$ ), found in veins of quartz rock. Wulfenite ( $\text{PbMoO}_4$ ) and powellite ( $\text{CaMoO}_4$ ) are also minor commercial ores. The main suppliers of molybdenum are the United States of America, followed by the People's Republic of China, Chile, Mexico and Norway.

Today, molybdenum production can be divided in three major groups: primary mining production (40%), co-production from copper and tungsten mines (55%), processing of spent petroleum catalysts (2%) [Sebenik et al., 1997].

Molybdenum has a high elastic modulus and only tungsten and tantalum, of the more readily available metals, have higher melting points. Moreover, molybdenum shows a high heat resistance and a low coefficient of thermal expansion. Thus, it is mainly used as an alloying element in steel, cast iron and superalloys to increase hardenability, strength, toughness and corrosion resistance. Molybdenum materials like carbide-hardened alloys have a higher failure tolerance and ductility than ceramics and are less expensive than tantalum and niobium. Molybdenum wire is valuable for use as a filament, grid and screen material for electronic tubes and halogen lamps. Metallurgical uses make up for over 90% of the total molybdenum consumption [Sebenik et al., 1997]. On the other hand, there are plenty of chemical applications for other molybdenum compounds: molybdenum trioxide ( $\text{MoO}_3$ ) is widely employed as a catalyst in the desulfurization of petroleum and coal-derivatives. Furthermore, it is used as a less toxic substitute for antimony oxide in flame retardant agents for PVC [Starnes, 1984]. Molybdenum disulfide ( $\text{MoS}_2$ ) is used as a high-temperature solid lubricant as well as in the production of greases or motor and industrial oils. Alkali molybdates find their use as corrosion inhibitors, and can make up to 0,2 wt.-% of modern engine coolants. Only chromates resulted to be more effective, but molybdates are less toxic and have no oxidizing effect. The less soluble zinc, calcium and strontium molybdates are used as

pigments in anticorrosive paints for steel and aluminium. Lead molybdate ( $\text{PbMoO}_4$ ) has an extensive use as a yellow or orange pigment. Sodium molybdate ( $\text{Na}_2\text{MoO}_4$ ) is used as a soil additive and a fertilizer, as molybdenum is an essential trace element for enzymes which fix nitrogen in leguminous crops [Sebenik *et al.*, 1997].

Molybdenum compounds in general are of low order of toxicity. Molybdenum is an essential element which plays a key role in many enzymatic functions. Its metabolism is closely related to copper and sulfur metabolism. The estimated necessary body content of molybdenum amounts to about 0,07 mg/kg body weight. Lack of molybdenum is related with esophageal cancer and kidney failure [Endriss, 1997].

On the other hand, molybdenum has a profound effect on the absorption and metabolism of copper by ruminant animals. Raised molybdenum levels in the diet induce copper deficiency resulting in a scouring disease [Davis, 1982]. Since pasture herbage often contains barely enough copper for the nutrition of grazing animals, there is concern about molybdenum and molybdenum-to-copper ratio. For this reason, the Netherlands have adopted soil and groundwater contamination guidelines for molybdenum and included it in the “gray list”, which lists elements of general concern in the environment (whereas the “black list” lists very toxic and persistent elements).

## 1.2 Concentration of the elements in municipal solid waste

It is not easy to gather reliable data about trace elements in municipal solid waste. First, the composition of municipal solid waste is subject to strong variations, depending on the country, on the collection system, on local customs and regulations. This is especially true for many heavy metals that are, because of their peculiar industrial applications, enriched in certain fractions rather than in others. Furthermore, analytical results are affected by the inhomogeneity of the analyzed waste and by the sampling methods.

Brunner and Ernst point out [Brunner and Ernst, 1986] that it is more reliable to analyze the metal concentrations in the incineration residues, which can be regarded as more homogenous materials than the waste itself (although they still are rather inhomogeneous). Thus, the input concentration of a metal can be inferred as the sum of the concentrations of all residue streams. This method has been adopted by several other authors [Schneider, 1986; Reimann, 1989; Angenend and Trondt, 1990].

Table 1.1 is a compilation of literature data on concentrations of the investigated elements in municipal solid waste (data expressed in mg/kg). The line labeled as TAMARA indicates averaged values of the concentrations in the MSW fed to the TAMARA pilot plant at the *Institute for*

*Technical Chemistry - Division of Thermal Waste Treatment.* The sampling methods and the analytical techniques are discussed in *chapter 4*.

**Table 1.1:** Concentration of the elements in municipal solid waste (mg/kg)

Source	As	Sb	Cr	Mo
Schneider, 1986	9	59	390	
Clapp et al., 1988	11	4		28
Reimann, 1989	4		250	
Angenend and Trondt, 1990	5		41	
Bidlingmeier, 1990			30	
Chandler et al., 1993	8	33	92	
Nakamura et al., 1996		8		
Vehlow and Mark, 1997	17	31	109	7
Belevi, 1998	3	31	310	9
Van Velzen et al., 1998		42		
TAMARA	13	30	259	19

### 1.3 Enrichment of the elements in municipal solid waste

It is useful to evaluate not only the absolute concentration of an element in the input waste stream, but also its enrichment compared to other solid fuels (mainly coal) and to natural soils as well as to the earth's crust. The enrichment factor of an element is defined as the ratio between its concentration in a selected fuel and its concentration in the lithosphere.

*Table 1.2* lists the concentration of the elements in MSW, in coal and in the earth's crust (first ten miles in depth), as well as the respective enrichment factors.

**Table 1.2:** Concentrations of the elements in coal, soils and the earth's crust (mg/kg)

	As	Sb	Cr	Mo
MSW, mg/kg [ <i>see Table. 1.1</i> ]	13	30	259	19
Coal [ <i>Querol et al., 1995</i> ]	17	1	38	4
Lithosphere [ <i>Ullmann, 1997</i> ]	6	0,3	100	1
Enrichment factor in MSW	2	100	3	19
Enrichment factor in coal	3	3	< 1	4

Antimony shows a remarkable enrichment in MSW, as well as molybdenum. This is presumably related to the utilization of these two elements in the production of flame retarding agents for plastic materials and as colored pigments, as will be discussed in the next section. Arsenic and chromium show only a slight enrichment. None of the elements shows a particular enrichment in coal.

### 1.4 Origin and speciation of the elements in municipal solid waste

Studies on municipal solid waste composition in which the analyzed waste is subdivided into merceological fractions allow to estimate the origin of metals in MSW and allow speculations about the chemical speciation, which plays a key role in the fate of an element during incineration.

Figures 1.1, 1.2, and 1.3 are adapted from the Canadian WASTE program [Chandler et al., 1993] and show the percent distribution of metals among different waste fractions.

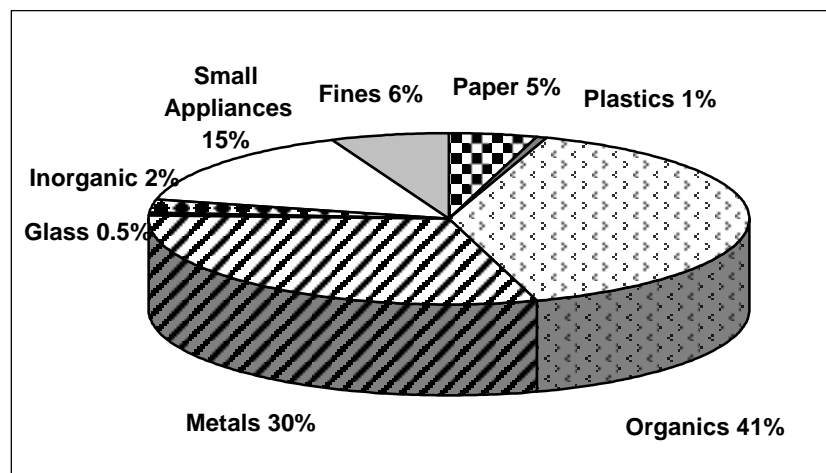


**Figure 1.1:** Distribution of As among MSW fractions [ad. from Chandler et al., 1993]

For arsenic (figure 1.1), the main contributions come from the organic fraction (41%) as well as from the metal (30%) and the small appliances fractions (15%). The first is probably related to the agricultural use of arsenic compounds, and yet such a high contribution may not be found in today's waste, as the use of arsenic in agriculture is restricted in most countries nowadays. The latter two contributions derive very likely from the metallurgical and electronic utilizations of arsenic compounds, respectively.

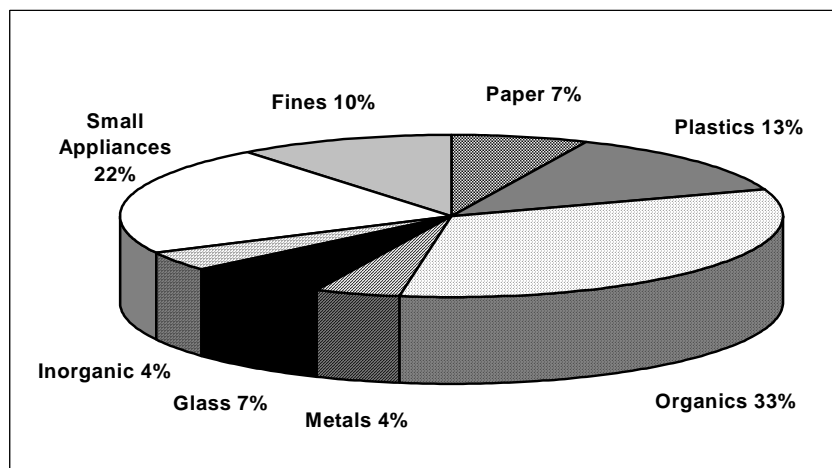


**Figure 1.2:** Distribution of Sb among MSW fractions [ad. from Chandler et al., 1993]

For antimony (figure 1.2), the main contribution comes from the organic, plastic and small appliances fractions, i.e. the fractions in which antimony is most likely present because of its utilization as a co-agent in brominated flame retardants. Electronical devices, as well as many common household plastic items are currently flame-retarded because of their fire risk and thus show very often remarkable antimony concentrations. This is confirmed by several investigations [Nakamura et al., 1996; Van Velzen et al., 1998; Vehlow et al. 2000; Paoletti et al., 2000]. The origin of the large share deriving from the organic fraction is not very clear.

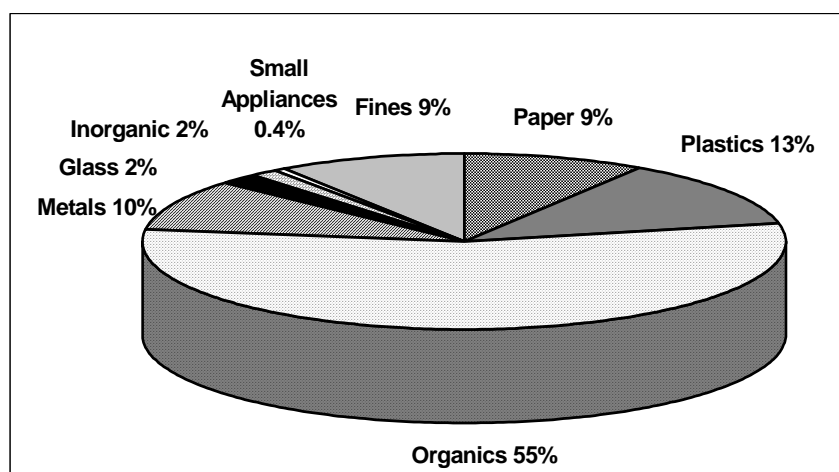


**Figure 1.3:** Distribution of Cr among MSW fractions [ad. from Chandler et al., 1993]

For chromium, more than half of the total MSW concentration derives from the organic fraction. This can be explained by the fact that in the WASTE investigation, leather and rubber materials have been added to the organic fraction. In fact other authors have pointed out that wood, leather and rubber are main sources of chromium in household waste [Lorber, 1983; Bidlingmeier, 1990].

Other contributions come from plastics and metal fractions, very likely on account of the utilization of chromium as a pigment and for chrome plating.

For molybdenum, there seems to be no indication of its origin in literature. Yet it can be expected that a large part of the molybdenum found in household waste will derive from its utilization as a pigment and to a minor extent also as a flame retardant. Thus, increased concentrations can be expected in the plastic fraction and in electronic devices. Moreover, the agricultural utilization of molybdenum must be kept in mind, too. In fact, *Mast et al.* point out that over 50% of the molybdenum analyzed in municipal solid waste can be found in the fines fraction (< 20 mm) [*Mast et al., 1996*]. This fraction is very difficult to define in its nature, but it can be assumed that a large part of it will consist of dust and soil.

These considerations, as well as the main industrial applications of the elements, allow to make speculations on the chemical form in which the elements enter a municipal solid waste incineration plant. This is the first step in defining their successive fate.

*Table 1.3* lists the main industrial applications and the estimated chemical form of the elements. It is interesting to observe that the elements might already enter the plant in their oxyanionic form. This seems to be especially true for arsenic.

**Table 1.3:** Industrial applications and speciation of the elements

<b>Element</b>	<b>Application</b>	<b>Speciation</b>
As	alloys (NF), batteries, semiconductors, wood protection, herbicides, insecticides	As, arsenates
Sb	batteries, flame retardants, ceramic, glass, pigment	Sb, Sb <sub>2</sub> O <sub>3</sub> , antimonates
Cr	steel, chrome plating, pigment, wood protection, leather tanning	Cr, Cr <sub>2</sub> O <sub>3</sub> , CrO <sub>3</sub> , chromates
Mo	steel, catalysts, lubricant, flame retardants, pigment	Mo, MoS <sub>2</sub> , MoO <sub>3</sub> , molybdates

## **Chapter 2**

### **Physical and chemical transformations during combustion**

#### **2.1 Pathways of metals through a combustion system**

An essential aspect to consider when talking about the fate of an element is its transfer factor, or partitioning coefficient. The transfer factor is defined by the fraction of the input inventory that exits the combustion chamber along with the flue gas [Brunner and Mönch, 1986; Belevi, 1998]. Thus, it indicates the fraction of the total elemental input which will be found in the boiler ashes, in the filter ashes, in the air pollution control residues and in the cleaned gas emitted through the stack. The transfer factor is the result of the complex chemical and physical transformations that an element undergoes on its way through the combustion chamber and it quantifies the transfer of the element (or its reaction products) from the solid to the (raw) gas phase both by means of evaporation or sublimation processes, as well as by the mechanical entrainment of those elements which are constituents of the fly ash matrix.

Theoretically, it is imaginable to define the transfer factor for each element under specific conditions [Morf and Brunner, 1998]. Thus, once the input inventory and the combustion parameters are defined (temperature, residence time, air excess, fuel composition etc.) it could be theoretically possible to predict the fate of an element during incineration.

On the other hand, the transfer factor is to a large extent influenced by undetermined factors, such as the exact input speciation of the element and local burning conditions (temperature, oxygen partial pressure), which determine whether and to which extent a chemical reaction will take place. Hence an exact prediction of the transfer factor is very difficult and only a global estimation is feasible.

Metals can be divided in two main groups, depending on their transfer factor. Lithophilic metals are those which will not be transferred out of the combustion chamber but will be mainly found in the grate ashes and the grate siftings [Vehlow, 1993]. Their transfer factor is extremely low (less than 0,05). Among these are: chromium, iron, manganese, nickel, vanadium.

On the contrary, volatile (or atmophilic) metals are those which show to some extent a mobilization out of the fuel bed and thus are enriched in the fly ashes. Volatile behavior is exhibited by such metals (and half-metals) as zinc, arsenic, cadmium, tin, antimony, mercury and lead.

For the classification of metals as volatile or non-volatile, the thermal behavior of all the compounds that are likely to be formed during combustion must be taken into account. Metals showing an extremely high melting point, such as, for example, molybdenum and tungsten, might,

under certain circumstances, show a more volatile behavior than metals with a much lower melting point, if the compounds they form during combustion are of sufficient volatility.

Chlorinated compounds of metals may be highly volatile, and, if they are formed, they will contribute strongly to the volatilization of an element [Barton *et al.*, 1990; Rizeq *et al.*, 1992; Vehlow, 1993; Watanabe *et al.*, 2000]. Other halogenated species, for example bromine compounds, might play an important role in metal volatilization, too [Vehlow and Mark, 2000].

In general, the main chemical reactions involving metals during combustion are assumed to be oxidation with formation of higher oxidation-state compounds and chlorination with formation of volatile chlorides. A further class of reactions can occur as a consequence of the formation of a reducing environment at high temperature in the fuel bed on the grate. This condition is very likely to be formed locally in nearly all combustion systems though the incinerator may be operated at overall excess air conditions [Quann and Sarofim, 1982].

However, as will be discussed further on, other reactions might play a crucial role in the fate of certain metals or half-metals, such as the formation of thermally stable oxyanionic compounds. Moreover, not always does the oxidation to a higher valence take place nor is the higher oxidation state compound thermally and chemically more stable, so that detailed knowledge of the chemical characteristics of any investigated metal and its compounds is indispensable to understand the partitioning of an element.

As the flue gases cool down on their way through the energy recovery and air pollution control sections, the volatilized compounds will condense both homogeneously to form new particles and heterogeneously on the surfaces of the entrained ash particles [Senior and Flagan, 1982]. Since the smaller particles have a high surface-to-volume ratio, they will offer a larger condensation surface and will be thus enriched in those metallic species that have vaporized during combustion [Neville and Sarofim, 1982].

On the other hand, the fact that a metal exhibits lithophilic behavior, does not imply that it will not be found in the fly ashes or in the APC residues. Metals can exit the combustion chamber also by means of mechanical entrainment, in form of matrix constituents of the fly ashes, which are carried out of the furnace along with the flue gas. The entrained particles generally range in size from 1 to 100  $\mu\text{m}$ . The quantity of material entrained is a function of the size, shape and density of the ash particles, of the fuel characteristics, as well as the incinerator operating conditions like air supply and distribution. Metals which exit the furnace by mechanical entrainment will show little or no enrichment on small size particles [Barton *et al.*, 1990].

## 2.2 Modeling the chemical equilibrium

In general, it is almost impossible to determinate exactly all the different chemical reactions taking place within the fuel bed. This is a result of the complexity of the chemical and physical interactions taking place. Furthermore, for numerical simulations, the investigated system must be assumed to be chemically and thermally homogeneous, i.e. each particle of any component of the system is accessible for chemical interaction with the particles of other components and the temperature is constant over the entire volume of the system [Shriyaev, 1994]. These assumptions are obviously far from reality in such systems like the extremely inhomogeneous fuel bed in waste incineration plants, with great temperature and reactant concentration gradients. Moreover, the chemical equilibrium is almost never reached.

Nevertheless, in spite of all of these obstacles, evaluation of chemical equilibria using simplified and idealized systems are very useful to indicate which reactions are more likely to take place.

All chemical systems can be described in terms of the state function Gibbs energy or free enthalpy  $G$  :

$$G = H - T \cdot S \quad [Eq. 2.1]$$

where:  $H$  = molar enthalpy [ $J/mol$ ]

$S$  = molar entropy [ $J/mol \cdot K$ ]

$T$  = temperature [ $K$ ]

In a closed system with constant pressure and temperature, chemical reactions take place spontaneously only if the variation of Gibbs energy for the reaction  $\Delta G$  has a negative value, i.e.:

$$\Delta G = \sum_i \nu_i G_{i_{prod.}} - \sum_j \nu_j G_{j_{react.}} \leq 0 \quad [Eq. 2.2]$$

where  $\nu$  = stoichiometric coefficient

$i$  = reaction products,

$j$  = reactants,

$G$  = Gibbs energy [ $J/mol$ ]

In a combustion chamber, the overall pressure is constant whilst the average temperature varies between an ambient temperature and about  $1000^\circ C$ . In this case,  $\Delta G$  is calculated using the Gibbs-Helmholtz equation:

$$\Delta G_T^0 = \Delta H_{298}^0 + \int_{298}^T \Delta c_p \cdot dT - T \cdot \Delta S_{298}^0 - T \cdot \int_{298}^T \frac{\Delta c_p}{T} \cdot dT \quad [Eq. 2.3]$$

where  $c_p$  = molar heat at constant pressure [ $J/mol \cdot K$ ]

The further fate of the stable reaction products during combustion - volatilization in the flue gases or fixation in the grate ashes - can be estimated by considering the shape of their vapor pressure curve. This curve can be approximated by:

$$\log p = -\frac{A}{T} + B + C \cdot \log T + D \cdot T \quad [\text{Eq. 2.4}]$$

where: T = temperature [K]

A, B, C, D: experimental constants

Thermodynamic models have been developed to evaluate the more likely reactions inside a combustion chamber. They are mainly based on the calculation of the variation of Gibbs energy  $\Delta G$  (Eqs. 2.2 and 2.3).

An equilibrium approach by means of minimization of the Gibbs energy as well as an extensive literature survey can be found in Frandsen et al. [Frandsen et al., 1994]. Another way of modeling the chemical equilibrium is to calculate the variation of the chemical potential  $\mu$  for the investigated reactions [Alvin et al., 1977; Wilde and Halbrook, 1977; Lee, 1988]. In a closed system, minimizing the chemical potential is equivalent to the minimization of the Gibbs energy.

A fundamental aspect in chemical modeling is the database which is used as the input for the model. Compilations of thermochemical data are available in literature [Barin, 1989; NIST-Janaf, 1998; Binnewies and Milke, 1999]. A useful survey over the available thermochemical databases can be found in the work of Bale and Eriksson [Bale and Eriksson, 1990]. Thermodynamic software packages for equilibrium calculations are available commercially. Some examples are CHEMSAGE [Eriksson and Hack, 1990] and EQUITHERM [Barin et al., 1996]. A comparison between different commercial software packages and the differences in the respective output results was carried out by Frandsen et al. [Frandsen et al., 1996].

The evaluation of the Gibbs energy gives an idea of the direction of the chemical reactions, however, it does not give any information about the kinetics of these reactions. Kinetic approaches to the prediction of chemical reactions can be found in the publications of Cosic and Fontijn and of Shriyaev [Cosic and Fontijn, 2000; Shriyaev, 1994].

### 2.3 Behavior of arsenic and antimony

Arsenic and antimony show a similar chemical behavior and therefore will be discussed in the same section. Both elements have weak metallic properties and are well known for the volatility of some of their compounds. *Figures 2.1 and 2.2* represent vapor pressure curves of arsenic and antimony compounds. The constants for *equation 2.4* and experimental vapor pressure data have been taken from literature [Landolt and Börnstein, 1960; Honig, 1962; Weast, 1975].

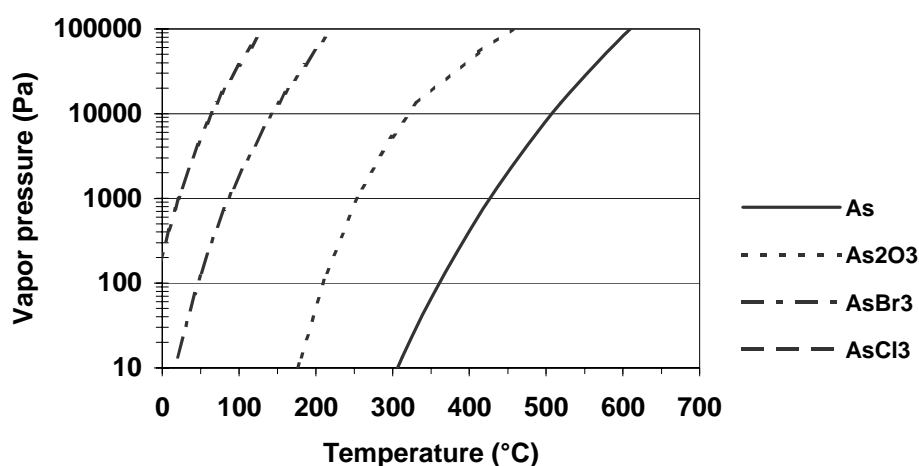


**Figure 2.1:** Vapor pressure of As compounds

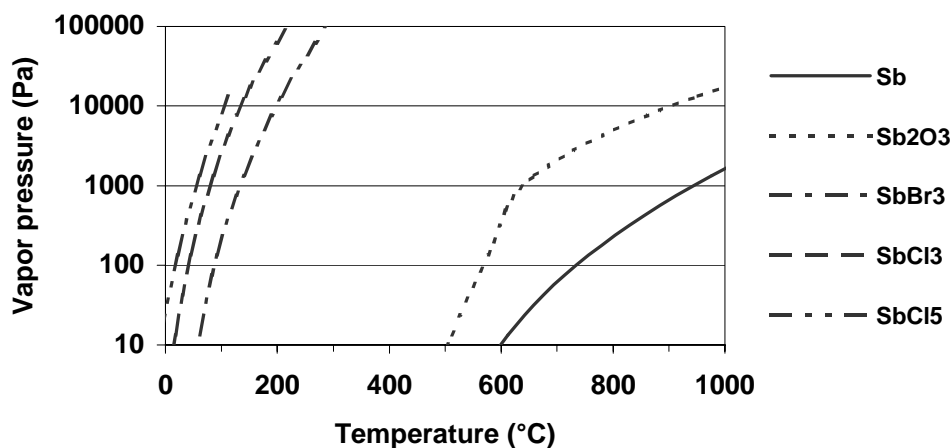


**Figure 2.2:** Vapor pressure of Sb compounds

Antimony and arsenic are both more stable in their trivalent oxidation state than in their pentavalent one. In aquatic systems, however, the pentavalent oxidation states are more stable, due to the formation of stable pentavalent oxo- and hydroxo-ions.

There are more thermodynamic data available for arsenic than for antimony. This situation might hopefully change in future, since the attention of the scientific community has increasingly been drawn on the chemistry of antimony, as a consequence of its large utilization in brominated flame retardants.

Figures 2.3 and 2.4 show the values for the variation of the Gibbs energy  $\Delta G$  at different temperatures for some highly probable reactions involving arsenic and antimony. The values were calculated following equation 2.2 and using data compilations available in literature [Barin, 1989]. As mentioned in the previous section, reactions will take place spontaneously only if  $\Delta G$  has a negative value. Furthermore, the reaction for which  $\Delta G$  has the lowest value, will be the most favored from a thermodynamical point of view.

Generally, it can be assumed that organic compounds of trace elements will behave like the respective metallic species while the sulfidic ones will behave in a similar way to oxides.

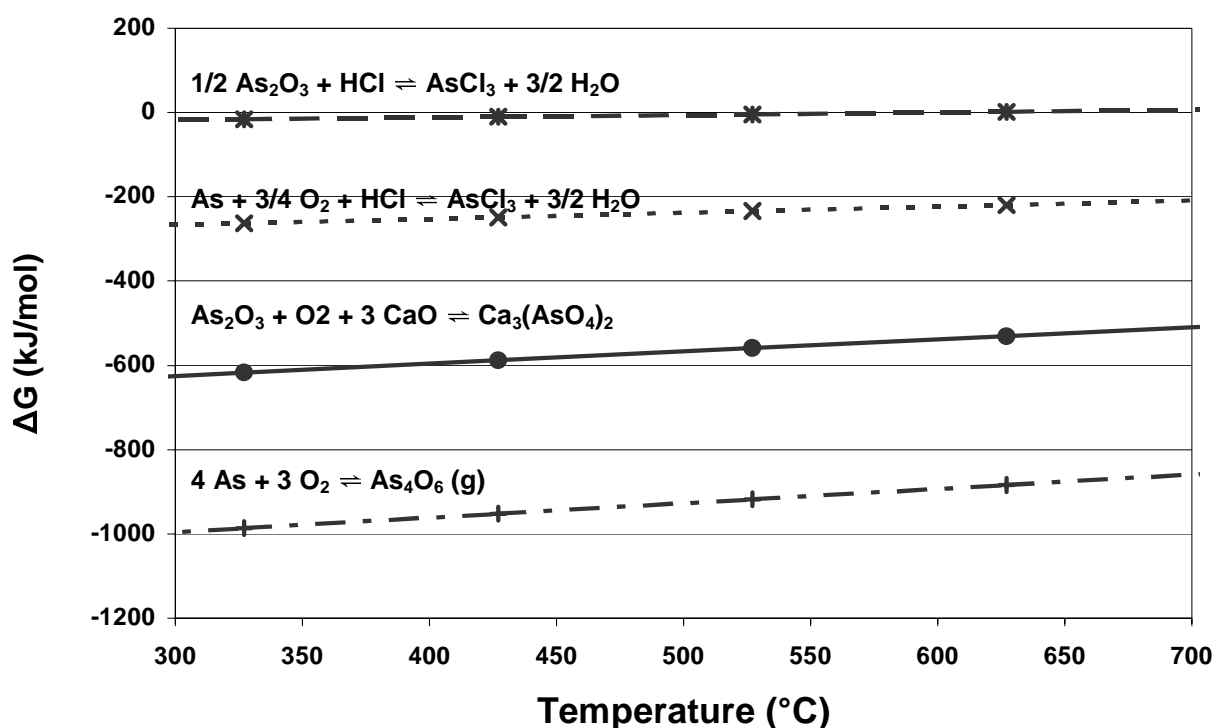


Figure 2.3:  $\Delta G$  values for As reactions

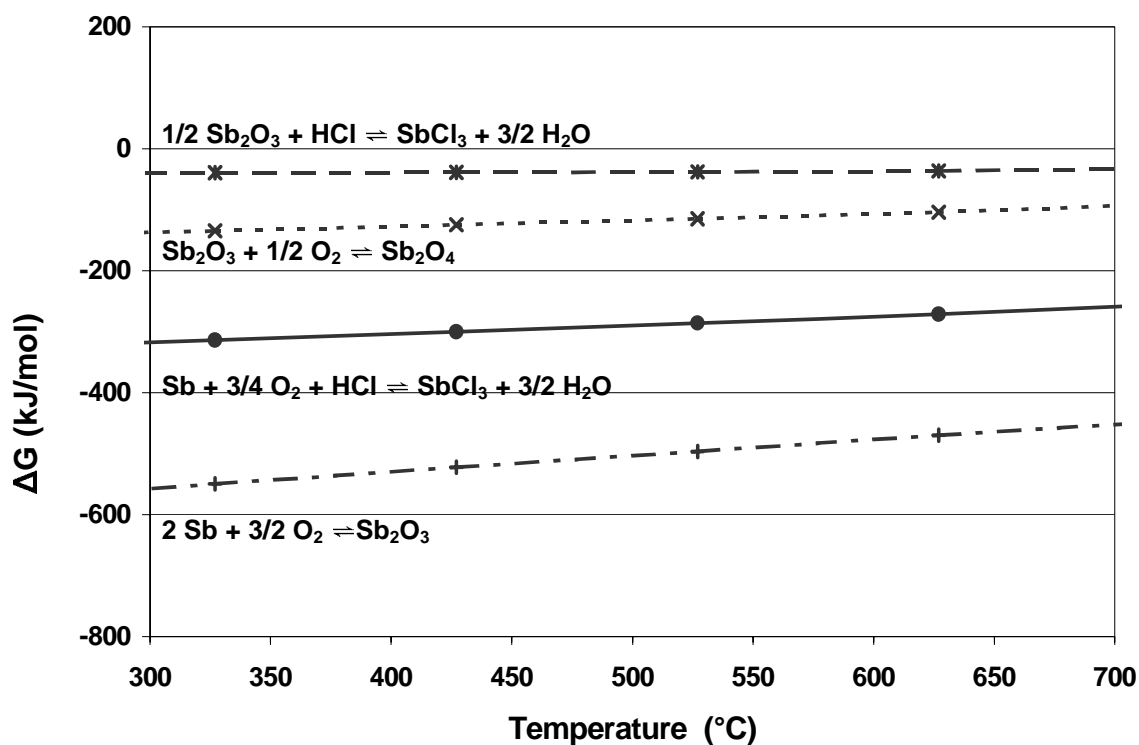


Figure 2.4:  $\Delta G$  values for Sb reactions

The calculations indicate that arsenic and antimony oxides are very likely to be formed in the combustion chamber and that antimony chlorides are easily formed if a local excess of chlorine is present in the fuel bed, as should be the case during municipal solid waste incineration. For arsenic the formation of chlorides seems to be less favored than for antimony. This is probably a consequence of the minor metallic character of arsenic, resulting in a lower affinity to chlorine. This fact might be the explanation for the higher transfer to the flue gas measured for antimony than for arsenic, as will be discussed in *chapter 5*.

The graph indicates that - especially if large amounts of antimony trichloride ( $\text{SbCl}_3$ ) were formed during the combustion process - it could be expected that nearly the entire amount of antimony entering the combustion chamber would be volatilized. This has been pointed out also in other thermodynamic calculations [Verhulst *et al.*, 1996; Watanabe, 1999].

In fact, though, the experimental results presented in *chapter 5* contradict these theory-based considerations. About 76% of the antimony input was found to remain in the grate ashes, which means that only part of the antimony inventory is transformed to  $\text{SbCl}_3$  in the combustion chamber.

Similarly, the low transfer factor shown by arsenic (about 0,2) is in contradiction with the thermodynamic data.

An explanation may be the formation of thermally stable oxyanionic compounds such as arsenates and antimonates. Thermodynamic evidence for the formation of calcium arsenates according to the reaction:



is shown by the values for  $\Delta G$  in *figure 2.3*.

The correlation between fuel calcium content and arsenic stability has been pointed out also in the work of *Watanabe [Watanabe et al., 1999]* as well as in several works concerning the behavior of arsenic in coal [*Haynes et al., 1982; Gullett and Ragnunathan, 1994; Bool and Helble, 1995; Clemens et al., 1999; Hirsch et al., 2000; Seames and Wendt, 2000; Senior et al., 2000*]. It is interesting to observe that generally partitioning analyses in coal combustion systems yield a much higher transfer coefficient for arsenic than those for municipal solid waste incinerators. On one side, this is related to the much higher temperature encountered in coal combustion systems. On the other hand, the discussion on arsenic speciation in municipal solid waste in *chapter 1* suggests the possibility that the lower transfer factor might be caused by a different input speciation, namely as arsenates, whereas arsenic in coal could be rather present in form of sulfides or organically bound. A theoretical prediction of arsenic behavior under reducing conditions has been carried out by *Williams et al.* Arsenic hydride ( $\text{AsH}_3$ ) resulted to be the dominant reaction product [*Williams et al., 2000*].

Unfortunately, no thermodynamic data are available for antimonates, but the close chemical relationship with arsenic gives rise to speculate about a similar mechanism. Thermogravimetric investigations shown in *chapter 3* give indeed strong evidence for the formation of thermally stable calcium antimonates as a results of a similar reaction as for arsenic.

## 2.4 Behavior of chromium

Toxicity and potential environmental hazard through chromium are strongly related to the oxidation state of this metal, as discussed in *chapter 1*. As hexavalent chromium compounds are much more toxic than trivalent ones, determining under which conditions trivalent chromium can be oxidized to its hexavalent forms is of fundamental importance. Trivalent chromium compounds are generally highly stable and not volatile, with high melting points. Furthermore, they are mostly scarcely soluble. On the contrary, hexavalent compounds are volatile, unstable and show high solubility. *Table 2.1* shows melting points of trivalent and hexavalent chromium compounds [Lide, 1994].

Trivalent chromium oxide ( $\text{Cr}_2\text{O}_3$ ) is an extremely stable compound. When heated in air, it is not oxidized to hexavalent oxide ( $\text{CrO}_3$ ) up to very high temperatures (over  $1500^\circ\text{C}$ ). On the other hand, because of their high oxidation potential, hexavalent compounds can be expected to be reduced easily to trivalent ones. In particular,  $\text{CrO}_3$  will be reduced to  $\text{Cr}_2\text{O}_3$  when heated in air.

**Table 2.1:** Melting points of chromium compounds [Lide, 1994]

Trivalent compounds		Hexavalent compounds	
Compound	Melting point	Compound	Melting point
$\text{Cr}_2\text{O}_3$	$2266^\circ\text{C}$	$\text{CrO}_3$	$193^\circ\text{C}$
$\text{CrCl}_3$	$1150^\circ\text{C}$	$\text{CrO}_2\text{Cl}_2$	$-96^\circ\text{C}$ (b.p.: $117^\circ\text{C}$ )
$\text{CrF}_3$	$1407^\circ\text{C}$	$\text{Cr}(\text{CO})_6$	$152^\circ\text{C}$
$\text{Cr}_2\text{S}_3$	$1350^\circ\text{C}$		

From a look at the values of the variation of the Gibbs energy  $\Delta G$  shown in *figure 2.5* for some chromium reactions, it is evident that the formation of trivalent compounds is more favored than the formation of hexavalent ones.

The formation of the very volatile hexavalent oxide  $\text{CrO}_3$  is highly unlikely. The reaction:



has a positive  $\Delta G$  value, which implies that the very stable trivalent oxide  $\text{Cr}_2\text{O}_3$  is formed instead.

Furthermore, the oxidation of metallic chromium to the trivalent oxide:



is the reaction showing the lowest value for  $\Delta G$ , and hence the most favored one.

Chlorination reactions do not seem to be very favored, too. This is a consequence of the rather weak metallic character of chromium. Formation of highly volatile (and toxic) chromylchloride ( $\text{CrO}_2\text{Cl}_2$ )

is favored only in case hexavalent oxide is formed, which seems unlikely, from a theoretical point of view.

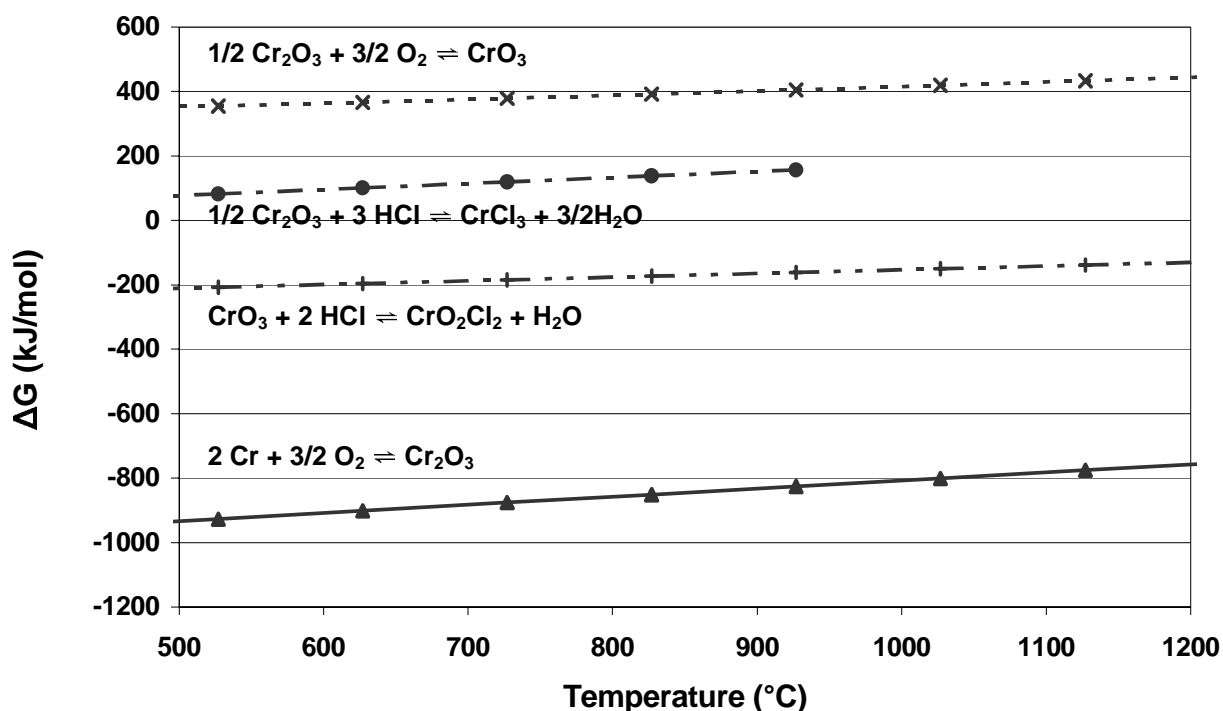


Figure 2.5:  $\Delta G$  values for Cr reactions

From the above mentioned considerations, it is evident that trivalent oxide  $\text{Cr}_2\text{O}_3$  is the most likely reaction product during combustion. As  $\text{Cr}_2\text{O}_3$  is a highly stable compound up to temperatures of around  $1200^\circ\text{C}$ , it follows that little or no chromium volatilization should be expected in a standard municipal solid waste incinerator, in which the average temperatures in the fuel bed hardly exceed  $1000^\circ\text{C}$ . In fact, as will be discussed in *chapter 5*, less than 5% of the chromium inventory is found in the fly ashes.

However, the remarkable leachability of chromium from the solid residues (both grate and fly ashes), and, most of all, the effect of the primary air ratio on the leaching trend, which were both encountered during the spiking incineration tests in the pilot plant TAMARA, as will be discussed in *chapters 6* and *7*, are a strong evidence of the fact that at least part of the chromium entering the combustion chamber must be converted into hexavalent chromium. Several different mechanisms might possibly be responsible for the presence of hexavalent chromium compounds in incineration residues.

First of all, chromium might already enter the incinerator in its hexavalent form, as discussed in *chapter 1*.

Furthermore, hexavalent compounds might be formed by a different pathway than the oxidation of  $\text{Cr}_2\text{O}_3$  to  $\text{CrO}_3$ .

The observed increased volatility of trivalent chromium in presence of water vapor has led to the discovery of the highly volatile pentavalent and hexavalent oxyhydroxides ( $\text{CrO}_2\text{OH}$  and  $\text{CrO}_2(\text{OH})_2$ ) [Glemser and Müller, 1964; Bulewicz and Padley, 1971; Kim and Belton, 1975].

Ebbinghaus provides thermodynamic data on volatile chromium species and on chromium volatility [Ebbinghaus, 1992; Ebbinghaus, 1993a; Ebbinghaus, 1993b] and calculates that at 1500 K most of the chromium volatilization in an incinerator takes place as a consequence of oxyhydroxide ( $\text{CrO}_2(\text{OH})_2$ ) formation [Ebbinghaus, 1992]. Moreover, the presence of excess chlorine in the combustion chamber might lead to the formation of highly volatile chromylchloride ( $\text{CrO}_2\text{Cl}_2$ ) in case part of the chromium inventory converts to hexavalent oxide ( $\text{CrO}_3$ ). This possibility has been investigated by Wu and Biswas [Wu and Biswas, 1993]. Kashireninov and Fontijn in their calculations, come to the conclusions that most of the volatilized chromium is in form of chromium trioxide  $\text{CrO}_3$  [Fontijn and Kashireninov, 1998].

On the other hand, it must be considered that the temperatures (above  $1200^\circ\text{C}$ ) and oxygen partial pressures needed for the beginning of the dissociation reaction of  $\text{Cr}_2\text{O}_3$  are almost never reached in normal municipal solid waste incinerator systems. However, in case fuel bed temperatures over  $1200^\circ\text{C}$  are reached (as for example in hazardous waste incineration plants), an increased volatilization of hexavalent chromium compounds should be expected.

Another possible mechanism for the formation of hexavalent chromium compounds is presented in this work. Trivalent chromium could react directly with alkali and earth alkali metal compounds present in the fuel bed with subsequent formation of hexavalent chromates, following similar reactions as those seen for arsenic and antimony in the precedent section. As will be discussed in *chapter 3*, these reactions take place at temperatures around  $800\text{-}900^\circ\text{C}$  and are thus highly plausible in municipal solid waste incinerator systems.

These reactions would not yield an increased chromium volatility but, as chromates are characterized by very high solubility, the consequence might be an unfavourably high leaching of chromium from the solid incineration residues.

## 2.5 Behavior of molybdenum

There has not many research work been done on the behavior of molybdenum in combustion systems. However, partitioning data relating to coal combustion can be found in the works of *Klein et al.*, *Alvin et al.*, and *Querol et al.* [*Klein et al.*, 1975; *Alvin et al.*, 1977; *Querol et al.*, 1995].

Molybdenum exhibits a very close similarity to tungsten, which is located just below in the periodical table of elements. Therefore, much of the experimental evidence presented in the next chapters about the fate of molybdenum in municipal solid waste incineration can be expected to apply for tungsten, too.

Molybdenum and tungsten belong to the metals with the highest melting points (2610°C and 3410°C, respectively), so it would seem surprising to speculate about their volatility during incineration. And yet, as will be discussed in *chapter 5*, the transfer factor exhibited by molybdenum is comparatively high. About 10% of the total molybdenum input was found in the fly ashes. Moreover, the high enrichment in the fly ashes supports strongly the probability of the formation of volatile species during combustion.

This fact is not surprising, if the volatility of some compounds of these two metals is considered. Hexavalent molybdenum oxide ( $\text{MoO}_3$ ) is a rather volatile oxide, which starts to sublime at 750°C, well below its melting point of 801°C. Moreover, molybdenum chlorides are extremely volatile, as can be seen in *table 2.2* [*Lide, 1994*]. For tungsten, the volatility is more limited. Hexavalent tungsten oxide ( $\text{WO}_3$ ) is not as volatile as  $\text{MoO}_3$ . However, tungsten chlorides are characterized by high volatility, too, so that some tungsten volatilization can be expected on the basis of chlorination reactions.

**Table 2.2:** Volatility of molybdenum and tungsten compounds [Lide, 1994]

<b>Molybdenum compounds</b>		<b>Tungsten compounds</b>	
<b>Compound</b>	<b>Melting point</b>	<b>Compound</b>	<b>Melting point</b>
MoO <sub>3</sub>	801°C	WCl <sub>5</sub>	248°C
MoCl <sub>5</sub>	194°C	WCl <sub>6</sub>	275°C
MoOCl <sub>3</sub>	subl. 100°C	WO <sub>2</sub> Cl <sub>2</sub>	subl. 260°C
MoO <sub>2</sub> Cl <sub>2</sub>	subl. 157°C	WOCl <sub>4</sub>	211°C
MoF <sub>5</sub>	46°C (b.p.: 275°C)	WF <sub>6</sub>	2°C (b.p.: 17°C)
MoF <sub>6</sub>	17°C (b.p.: 37°C)	WOF <sub>4</sub>	110°C (b.p.: 187°C)
MoO <sub>2</sub> F <sub>2</sub>	subl. 270°C	WBr <sub>5</sub>	232°C
MoOF <sub>4</sub>	98°C (b.p.: 180°C)	WBr <sub>6</sub>	232°C
		WOBBr <sub>4</sub>	277°C

Thermodynamic calculations on the formation of chlorinated compounds of molybdenum can be found in the works of *Strafford et al.* and of *Djona et al.* [Strafford et al., 1991; Djona et al., 1995].

Values of  $\Delta G$  for molybdenum reactions are depicted in *figure 2.6* and show that MoO<sub>3</sub> is very likely to be formed during combustion. Formation of calcium molybdate (CaMoO<sub>4</sub>) is very favored, too, and plays an important role in the fate of molybdenum, as will be discussed in *chapters 3, 6* and *7*.

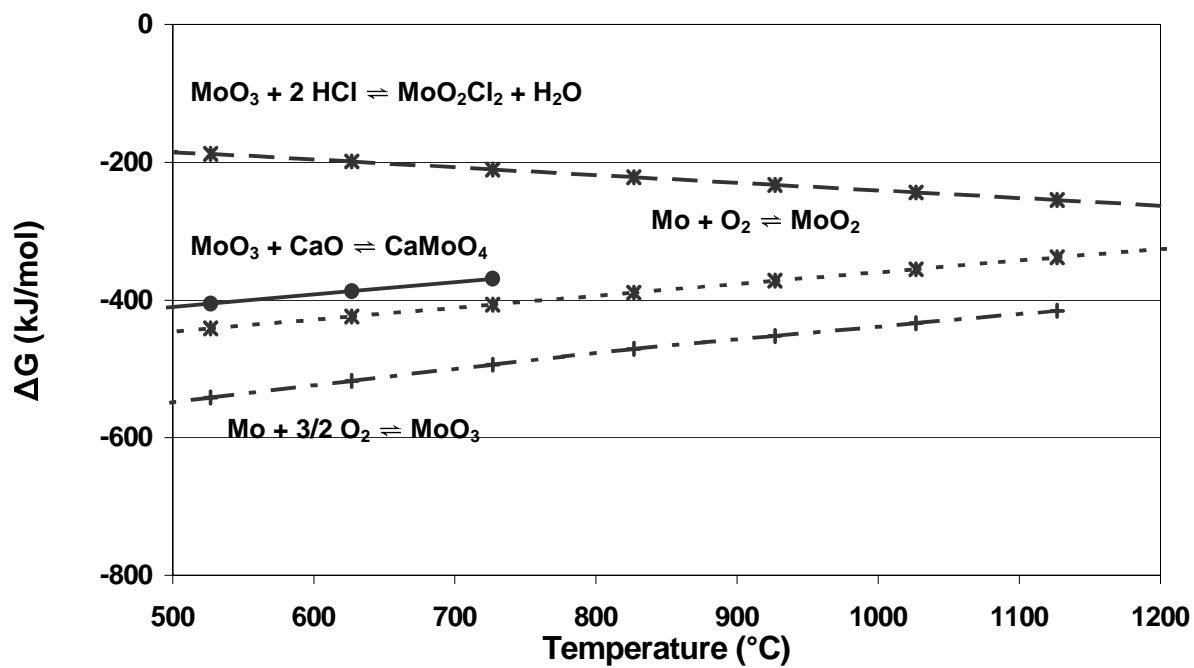


Figure 2.6:  $\Delta G$  values for Mo reactions

## **Chapter 3**

### **Oxyanion formation**

#### **3.1 Theoretical considerations**

The term oxyanions indicates oxygen containing anions. In an aquatic environment these will be found in their ionic state, whereas in the solid phase they will be bound to metallic cations to form oxyanionic salts (or oxy-salts).

The chemical process leading to the formation of oxyanionic compounds can be regarded as a Lewis acid-base neutralization reaction. A Lewis acid is defined as a substance which can employ an electron pair from another molecule to complete the stable octet group of one of its own atoms (electron pair acceptor). Thus, all metal ions can be classified as Lewis acids. On the other hand, a Lewis base is a substance having an electron pair which can be used to complete an octet group of another atom (electron donor). All ligands that form coordination compounds with metals are Lewis bases [*Jensen, 1980*].

Since the metal-oxygen bond in an oxyanion is a covalent one, it will be the more strong, the lower the values of the difference of the electronegativity ( $\Delta EN$ ) between the two elements. Electronegativity was defined in 1932 by *Pauling* as the ability of an atom to attract to itself an electron pair shared with another atom in a chemical bond [*Pauling, 1932*].

As oxygen is, after fluorine, the element showing the highest electron affinity, it follows that the tendency of a metal to form stable oxyanions increases with rising electronegativity. Generally, it can be stated that the electronegativity of a metal is inversely related to its metallic character, that means, the weaker the metallic properties, the higher its electronegativity [*Hardt, 1987*].

The oxyanions thus formed are Lewis bases and will therefore tend to react with Lewis acids to form oxyanionic salts. These are bound, as all salts, by a prevalently ionic bond and hence will be the more stable for higher values of the electronegativity difference  $\Delta EN$  between the metal cation and the oxyanion. It follows that the most stable oxyanionic salts are formed with alkaline and earth- alkaline metals, which exhibit the lowest values of electronegativity.

There are several methods to evaluate the electronegativity of an element, which can lead to different numerical results [*Gordy and Thomas, 1956*]. Moreover, an element showing more oxidation states, will have a different electronegativity value for each oxidation state, whereby, generally, the electronegativity can be assumed to be higher for higher oxidation states. *Table 3.1* lists electronegativity values for selected elements [*Gordy and Thomas, 1956*].

**Table 3.1:** Electronegativities of the elements [Gordy and Thomas, 1956]

Element	Oxidation state	Electronegativity	Element	Electronegativity
Cr	Cr <sup>6+</sup>	2,2	O	3,5
	Cr <sup>3+</sup>	1,6	Li	0,95
	Cr <sup>2+</sup>	1,4	Na	0,9
As		2,0	K	0,8
Mo	Mo <sup>6+</sup>	2,1	Rb	0,8
	Mo <sup>4+</sup>	1,6	Cs	0,75
Sb	Sb <sup>5+</sup>	2,1	Be	1,5
	Sb <sup>3+</sup>	1,8	Mg	1,2
			Ca	1,0
			Sr	1,0
			Ba	0,9

The purpose of the present chapter is to provide experimental evidence that reactions resulting in the formation of oxyanionic salts can take place in a solid-phase high-temperature environment and can thus be expected to take place in combustion systems.

For every investigated metal, some model reactions (in presence or absence of oxygen, respectively) were identified, as listed in *table 3.2*. For a better overview, the representation of the reaction products shows the oxidation states of the single elements within the oxyanionic molecule. Calcium oxide (CaO) was chosen as a reaction partner because of its relative abundance in municipal solid waste (about 3% [IAWG, 1997]). However, similar reactions can be expected to take place with other alkali or earth-alkali metals (Na, K, Mg, Sr, Ba), which are present at lower concentrations (less than 1%).

**Table 3.2:** Investigated model reactions

Element	Reaction	Reaction product
As	$\text{As}_2\text{O}_3 + 3 \text{CaO} + \text{O}_2 \rightleftharpoons \text{Ca}_3(\text{AsO}_4)_2$	Ca-arsenate (V), $\text{Ca}_3^{2+}[\text{As}^{5+}\text{O}_4^{2-}]_2^{3-}$
	$\text{As}_2\text{O}_3 + 3 \text{CaO} \rightleftharpoons \text{Ca}_3(\text{AsO}_3)_2$	Ca-arsenate (III), $\text{Ca}_3^{2+}[\text{As}^{3+}\text{O}_3^{2-}]_2^{3-}$
Sb	$\text{Sb}_2\text{O}_3 + 3 \text{CaO} + \text{O}_2 \rightleftharpoons \text{Ca}_3(\text{SbO}_4)_2$	Ca-antimonate (V), $\text{Ca}_3^{2+}[\text{Sb}^{5+}\text{O}_4^{2-}]_2^{3-}$
	$\text{Sb}_2\text{O}_3 + 3 \text{CaO} \rightleftharpoons \text{Ca}_3(\text{SbO}_3)_2$	Ca-antimonate (III), $\text{Ca}_3^{2+}[\text{Sb}^{3+}\text{O}_3^{2-}]_2^{3-}$
Cr	$\text{Cr}_2\text{O}_3 + 2 \text{CaO} + 3/2 \text{O}_2 \rightleftharpoons 2 \text{CaCrO}_4$	Ca-chromate (VI), $\text{Ca}^{2+}[\text{Cr}^{6+}\text{O}_4^{2-}]^{2-}$
	$\text{Cr}_2\text{O}_3 + \text{CaO} \rightleftharpoons \text{Ca}(\text{CrO}_2)_2$	Ca-chromate (III), $\text{Ca}^{2+}[\text{Cr}^{3+}\text{O}_2^{2-}]_2^{-}$
Mo	$\text{MoO}_2 + \text{CaO} \rightleftharpoons \text{CaMoO}_3$	Ca-molybdate (IV), $\text{Ca}^{2+}[\text{Mo}^{4+}\text{O}_3^{2-}]^{2-}$
	$\text{MoO}_2 + \text{CaO} + 1/2 \text{O}_2 \rightleftharpoons \text{CaMoO}_4$	Ca-molybdate (VI), $\text{Ca}^{2+}[\text{Mo}^{6+}\text{O}_4^{2-}]^{2-}$
	$\text{MoO}_3 + \text{CaO} \rightleftharpoons \text{CaMoO}_4$	Ca-molybdate (VI), $\text{Ca}^{2+}[\text{Mo}^{6+}\text{O}_4^{2-}]^{2-}$

### 3.2 Thermal analysis

The reactions leading to oxyanionic salts formation were investigated by means of thermal analytical methods. Thermal analysis is defined as a group of techniques in which a physical property of a substance and/or its reaction products is measured as a function of temperature while the substance is subjected to a controlled temperature program [Warrington and Höhne, 1994].

The experimental equipment used for thermal analysis was a thermobalance Netzsch STA 409 (figure 3.1). This apparatus allows to perform both thermogravimetric measurements (TG) as well as differential scanning calorimetry (DSC).

Thermogravimetry is used to measure variations in the mass of a sample as a function of temperature. Mass variations are a consequence of substance decomposition (mass loss) or oxidation, if oxygen is present in the system (mass increase).

Differential scanning calorimetry is concerned with the measurement of the energy release and heat exchange in a system. The heat exchange is quantified by means of the measurement of the temperature difference between the sample and an inert reference substance (normally aluminium oxide,  $\text{Al}_2\text{O}_3$ ) while the system temperature is varied under controlled conditions. If the sample mass is small, an empty crucible can be used instead of a reference material. Thus, the heat exchange during any physical or chemical process can be quantified [Warrington and Höhne, 1994].

The scheme of the experimental equipment is depicted in figure 3.2. Basically, it is constituted of two main units: the precision weighing system is located in the inferior part, while the upper part is constituted by a silicium carbide (SiC) furnace in which the temperature program is carried out, as dictated by the equipment controlling unit.

The sample to be analyzed is placed in an aluminium oxide crucible on top of the sample carrier. The latter constitutes the connecting part between the furnace and the weighing system. Choosing between two different kinds of sample carriers allows to perform TG and/or DSC measurements.

**Figure 3.1:** Netzsch Thermobalance STA 409

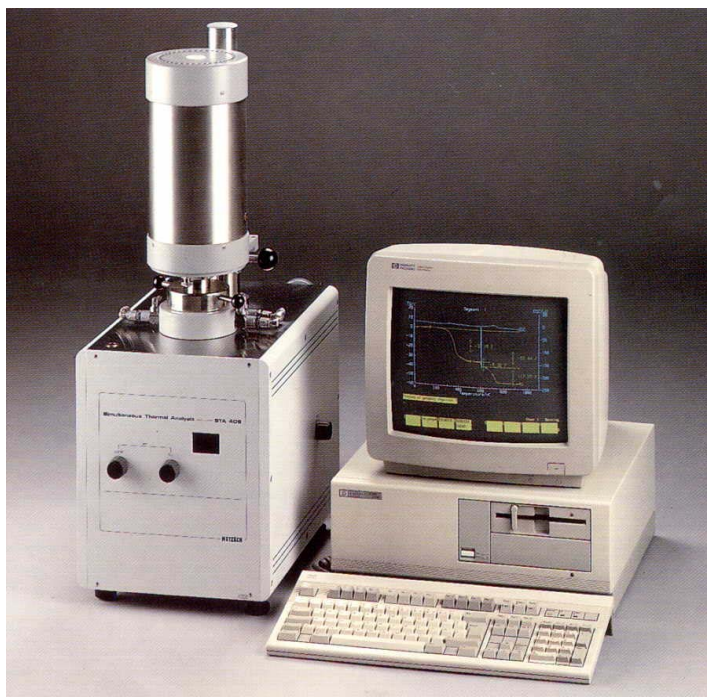
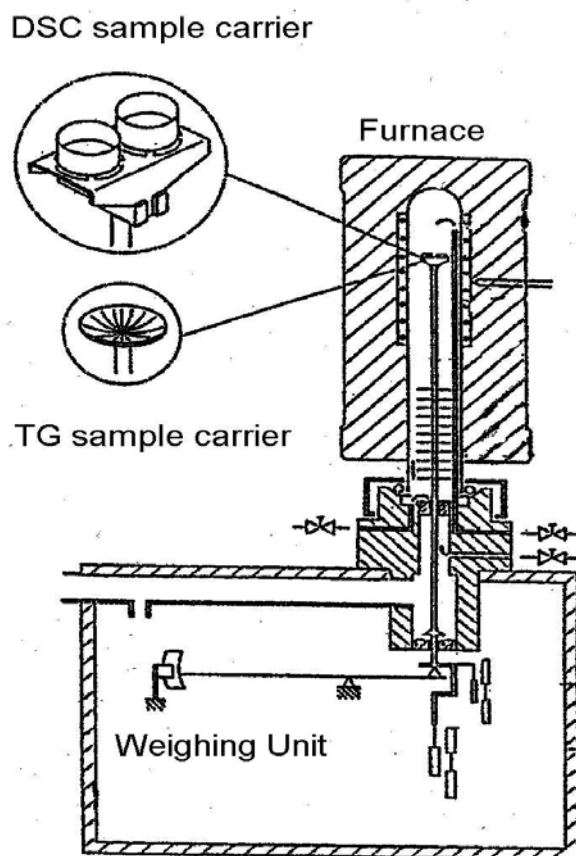


**Figure 3.2:** Scheme of the TG-DSC system



The calibration procedure of the thermobalance was carried out following the procedure prescribed by the German standard *DIN 51007* [*DIN 51007, 1994*].

The calibration materials were part of the calibration set supplied by Netzsch and are listed in *table 3.3*. The calibration curves were calculated with the aid of the Netzsch software package Proteus®, which was also used for measurement data analysis.

**Table 3.3:** Calibration substances

Substance	Melting Point (°C)	Fusion Enthalpy $\Delta H_f$ (J/g)
Tin	231,9	60,5
Zinc	419,5	107,5
Aluminium	660,3	397
Silver	961,8	107
Gold	1064,2	63,7
Nickel	1454,8	297,7

To further investigate the reaction products, some of the samples were heated in a laboratory chamber furnace (Linn High Therm, VMK-1600) with a similar temperature program as the one used for the thermal analysis.

The residues were then analyzed by means of X-ray diffractometry using a diffractometer Siemens Crystalloflex D500. X-ray diffractometry is a widely employed technique for analysis of solid crystalline phases [*Paulus and Gieren, 1999*]. It is based on the measurement of the diffraction of an x-ray passing through a crystal lattice, following the Bragg's equation:

$$n \cdot \lambda = 2d \cdot \sin\theta \quad [Eq. 3.1]$$

where  $\lambda$  is the ray wavelength,  $\theta$  the glancing angle,  $d$  the net plane spacing and  $n$  an integer number

Each crystal lattice will produce a characteristic diffractometric pattern, or spectrum, which allows crystallographic identification.

### 3.3 Experimental program

For thermal analysis, high-purity chemicals were used. Some problems were encountered with calcium oxide. Although the substance used was high-purity grade, the high hygroscopicity of CaO caused the formation of calcium hydroxide ( $\text{Ca(OH)}_2$ ) within a few days, even if the mixtures were kept in a closed vessel. This fact did not interfere with the formation of oxyanionic salts and with the reactions investigated but caused a weight loss when the sample was heated above 350°C, accompanied by a strong endothermic DSC signal, when the  $\text{Ca(OH)}_2$  lost water, as will be seen in the next section. Moreover,  $\text{Ca(OH)}_2$  absorbs readily carbon dioxide ( $\text{CO}_2$ ) from the atmosphere, thus leading to the formation of calcium carbonate ( $\text{CaCO}_3$ ). This process, however, is not as fast as

calcium hydroxide formation, and requires a time frame of some weeks. Calcium carbonate exhibited a weight loss step around 700°C (see *figure 3.13*).

All chemical mixtures were homogenized in a ball mill. Multiple experimental runs were performed to ensure reproducibility. *Table 3.4* lists the samples and their composition.

**Table 3.4:** Samples for thermal analysis

Sample	Mixture (stoichiometric ratio)	Composition
As1	As <sub>2</sub> O <sub>3</sub> + CaO, 1:7	2 g As <sub>2</sub> O <sub>3</sub> + 4 g CaO
As2	As <sub>2</sub> O <sub>3</sub> + CaO, 1:3	2 g As <sub>2</sub> O <sub>3</sub> + 1,7 g CaO
Sb1	Sb <sub>2</sub> O <sub>3</sub> + CaO, 1:10	2 g Sb <sub>2</sub> O <sub>3</sub> + 4 g CaO
Sb2	Sb <sub>2</sub> O <sub>3</sub> + CaO, 1:3	3 g Sb <sub>2</sub> O <sub>3</sub> + 1,7 g CaO
Cr1	Cr <sub>2</sub> O <sub>3</sub> + CaO 1:5	3 g Cr <sub>2</sub> O <sub>3</sub> + 2,2 g CaO
Cr2	Cr <sub>2</sub> O <sub>3</sub> + CaO 1:1	3 g Cr <sub>2</sub> O <sub>3</sub> + 1,1 g CaO
Mo1	MoO <sub>3</sub> +CaO 1:5	2 g MoO <sub>3</sub> + 0,8 g CaO
Mo2	MoO <sub>3</sub> + CaO 1:1	2 g MoO <sub>3</sub> + 0,8 g CaO

### 3.4 Results

#### 3.4.1 Arsenic and antimony

The first element to start with was antimony. Antimony oxide (Sb<sub>2</sub>O<sub>3</sub>) showed total volatilization if heated in inert (nitrogen) atmosphere. Volatilization started at about 550°C and was completed around 870°C (*figure 3.3*). On the other hand, when Sb<sub>2</sub>O<sub>3</sub> was heated in an oxidizing environment (synthetic air), oxidation to antimony tetraoxide (Sb<sub>2</sub>O<sub>4</sub>) took place between 400°C and 650°C with subsequent mass increase of about 5% (*figure 3.4*).

Actually, Sb<sub>2</sub>O<sub>4</sub> is not a "true" oxide with oxidation state +4, but has proven to be a double molecule of the antimony trioxide and the pentoxide (Sb<sub>2</sub>O<sub>3</sub>\*Sb<sub>2</sub>O<sub>5</sub>) and can be considered as an antimony antimonate [*Remy, 1960*]. However, at 900°C, Sb<sub>2</sub>O<sub>4</sub> decomposed back to Sb<sub>2</sub>O<sub>3</sub> and hence volatilized easily (*figure 3.4*).

Things looked completely different when a mixture of Sb<sub>2</sub>O<sub>3</sub> and CaO (sample *Sb1*) was analyzed. The addition of calcium oxide increased the thermal stability of antimony trioxide significantly. In nitrogen atmosphere, the mixture showed only very moderate mass losses up to 1100°C (less than 2%, *figure 3.5*). A moderate weight loss occurred above 1100°C and the residual mass at 1400°C amounted to 95%. Thus it can be speculated that in absence or scarcity of oxygen antimonate(III) formation could take place by means of direct interaction between Sb<sub>2</sub>O<sub>3</sub> and CaO.

In synthetic air atmosphere (*figure 3.6*) the first reaction was an oxidation to Sb<sub>2</sub>O<sub>4</sub> (up to 600°C). At 800°C the formation of a new compound could be seen which is presumably a pentavalent calcium antimonate. This substance is very stable and the total mass increase at 1400°C amounted to 3%.

The finding that pentavalent antimonate is more stable than the trivalent one is consistent with the data shown in *table 3.1*: the elements in their higher oxidation states have higher electronegativity values and hence form more stable oxyanions, whereas in their metallic compounds, the lower oxidation states show a higher stability, as discussed in *section 2.3*.

No volatilization of the  $\text{Sb}_2\text{O}_3$ -CaO mixture (*Sb1*) was found up to temperatures exceeding  $1400^\circ\text{C}$ .

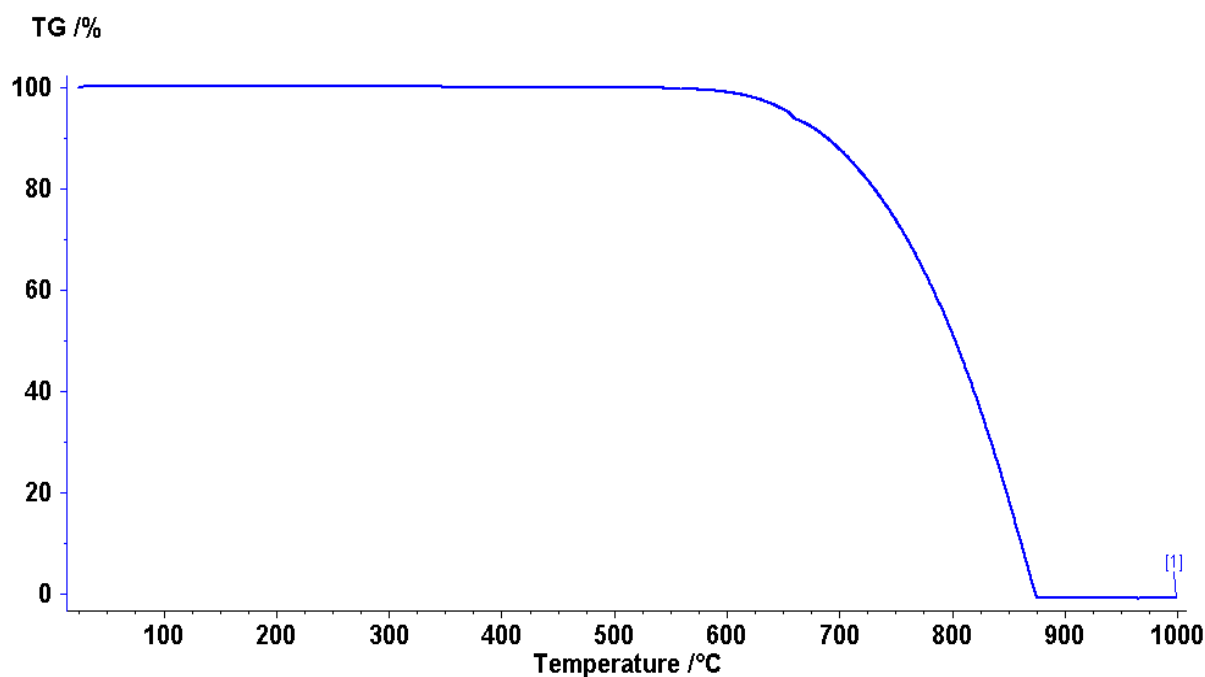


**Figure 3.3:**  $\text{Sb}_2\text{O}_3$  in nitrogen atmosphere

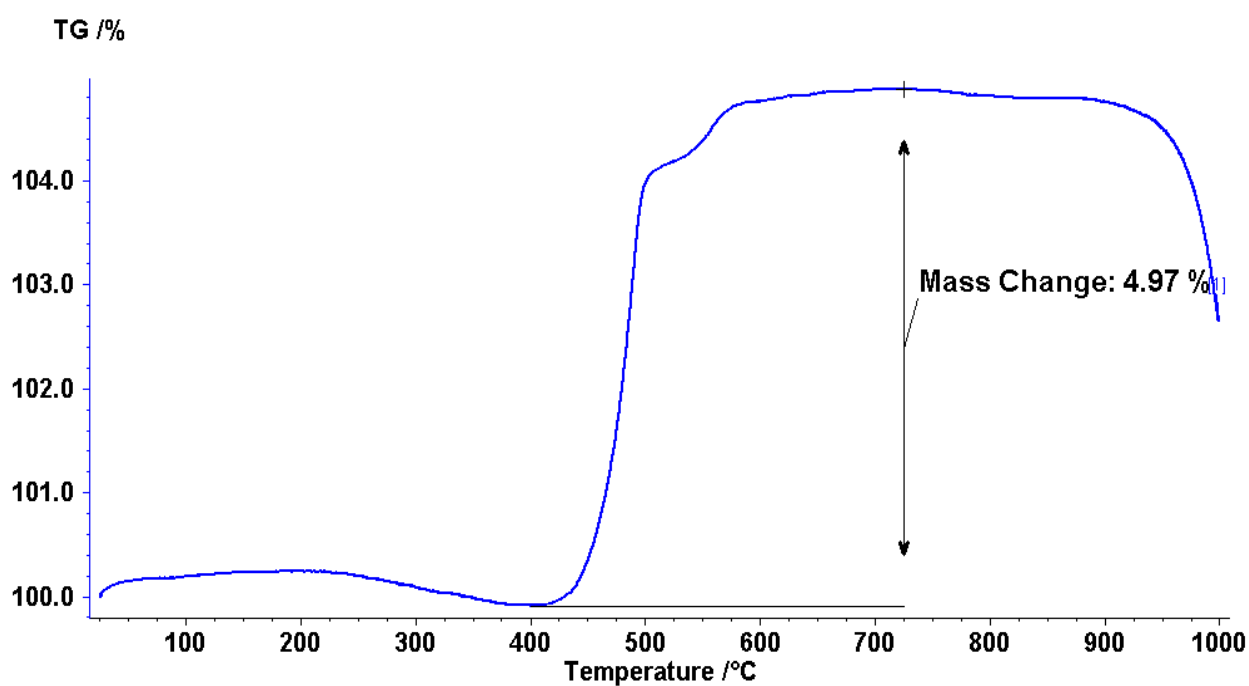


**Figure 3.4:**  $\text{Sb}_2\text{O}_3$  in synthetic air atmosphere

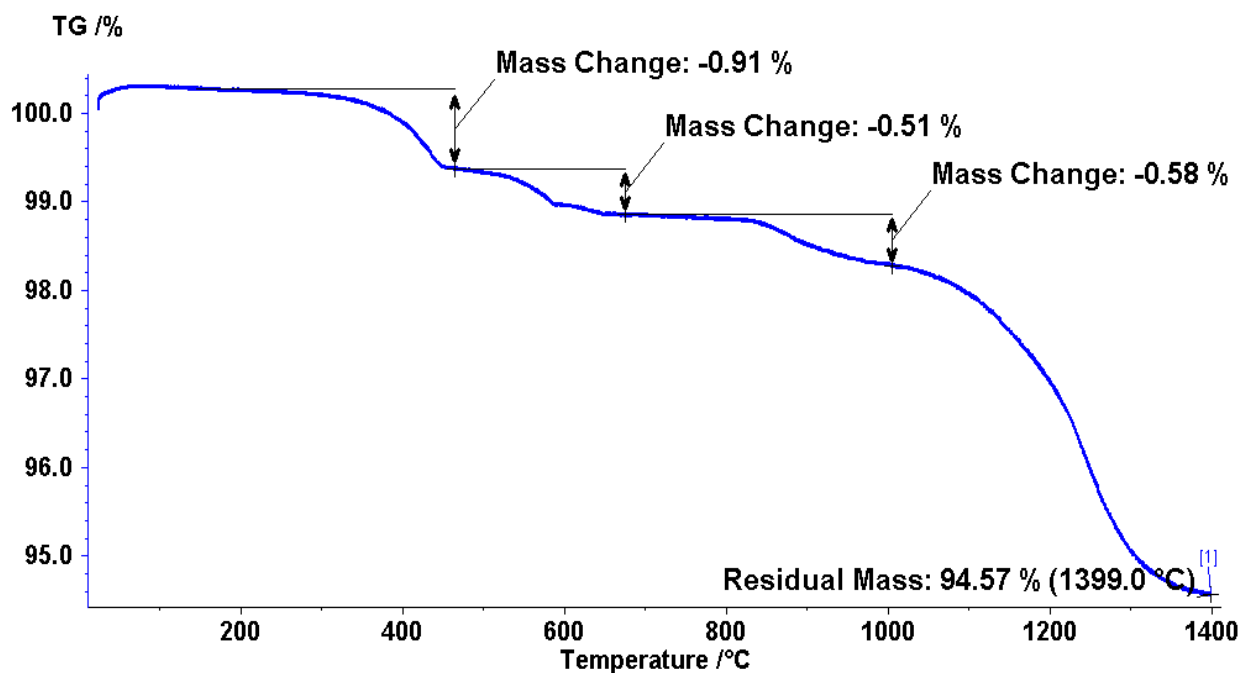


Figure 3.5:  $\text{Sb}_2\text{O}_3 + \text{CaO}$  in nitrogen atmosphere (sample *Sb1*)

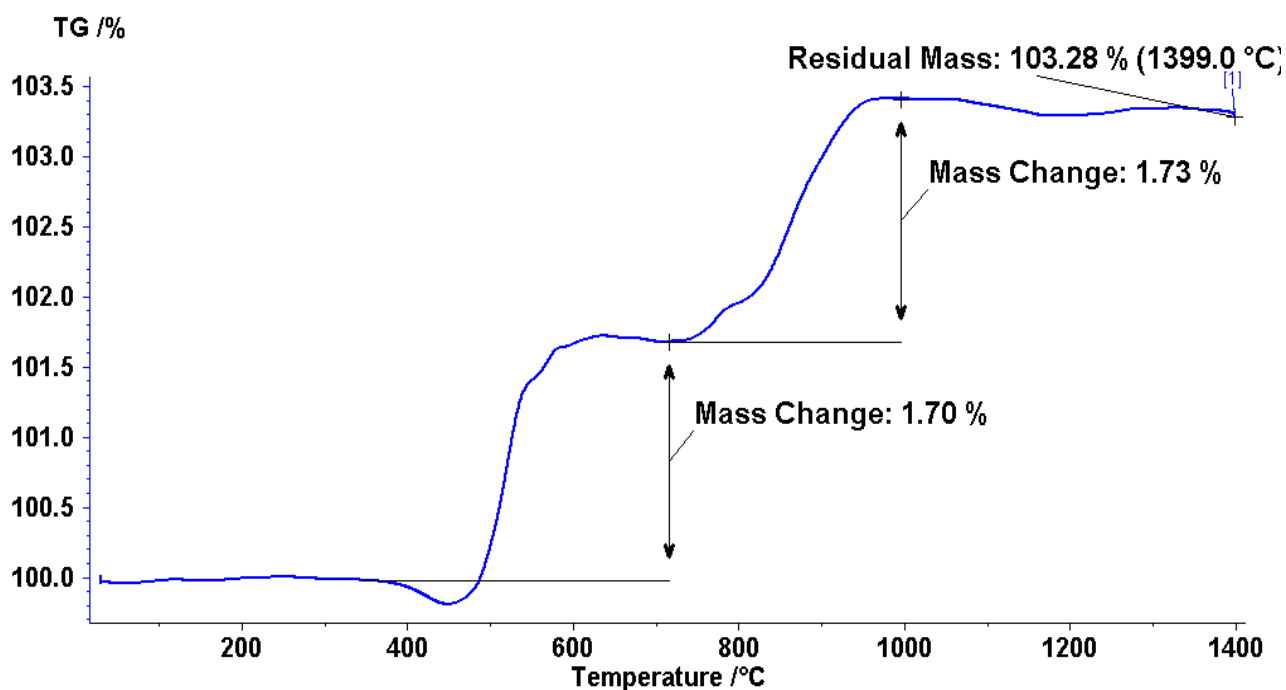


Figure 3.6:  $\text{Sb}_2\text{O}_3 + \text{CaO}$  in synthetic air atmosphere (sample *Sb1*)

After thermal treatment in the laboratory furnace, mixture samples were analyzed by means of X-ray diffractometric analysis (XRD) to further identify the compounds formed. The diffractometric spectrum of the sample *Sb2* annealed for 1 hour at 1000°C is shown in *figure 3.7*.

For diffractometric analysis, sample *Sb2* was chosen because of its lower Ca/Sb ratio (see *table 3.4*): an excess of unreacted calcium would have generated large CaO peaks which would have

possibly hidden antimonate peaks. The same consideration applies for all the other investigated elements, too (see *sections 3.4.2 and 3.4.3*).

Not all of the peaks could be identified, and some unreacted CaO seemed to be present, too. However, peaks of two mixed antimony-calcium oxidic compounds,  $\text{Ca}_5\text{Sb}_5\text{O}_{17}$  and  $\text{Ca}(\text{SbO}_3)_2$ , could be identified. The reference spectra used for the interpretation are part of the 1994 JCPDS Reference system (*International Centre for Diffraction Data*). Unfortunately, no reference spectra for other antimonates were available.

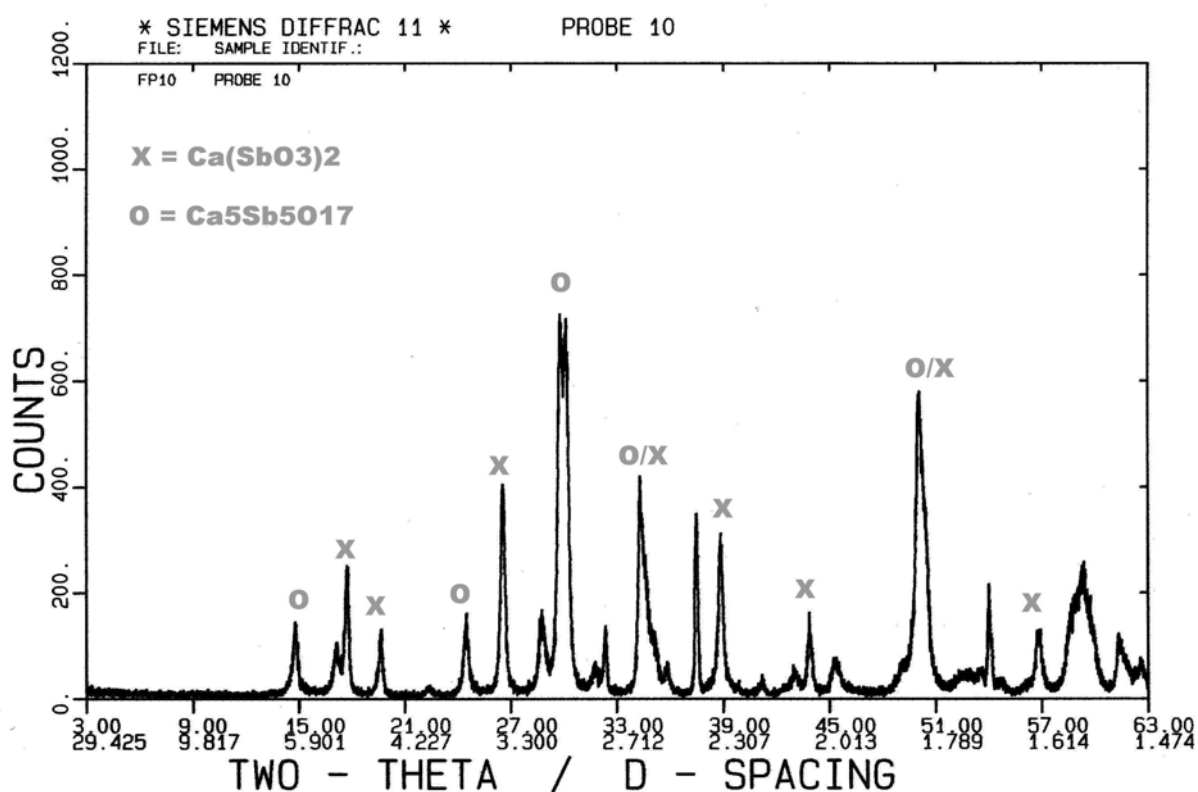


**Figure 3.7:** XRD spectrum of sample *Sb2*

For arsenic, the results were less satisfying. Arsenic trioxide ( $\text{As}_2\text{O}_3$ ) is a highly volatile compound and was completely volatilized at around  $450^\circ\text{C}$ . At this temperature, no formation of oxyanionic salts had yet started. Thus, the main reactant exited the system before the reaction actually started and a completely different experimental equipment would have been needed to investigate this reaction (for example, a tightly closed crucible). However, an attempt to "trap"  $\text{As}_2\text{O}_3$  in the crucible was carried out by pressing a layer of CaO over a layer of  $\text{As}_2\text{O}_3$ , to hinder volatilization. The result is shown in *figure 3.8*. Even if most of the arsenic oxide was volatilized, at about  $500^\circ\text{C}$  a slow mass increase started (1,7% at  $1000^\circ\text{C}$ ), which means that part of the arsenic trioxide was presumably involved in the formation of arsenates.

This was confirmed by the XRD analysis of sample As2 (1hour at 1000°C), depicted in *figure 3.9*. Even if CaO peaks prevailed, peaks of a calcium arsenate ( $\text{Ca}_5(\text{AsO}_4)_3(\text{OH})$ ) can nonetheless be identified.

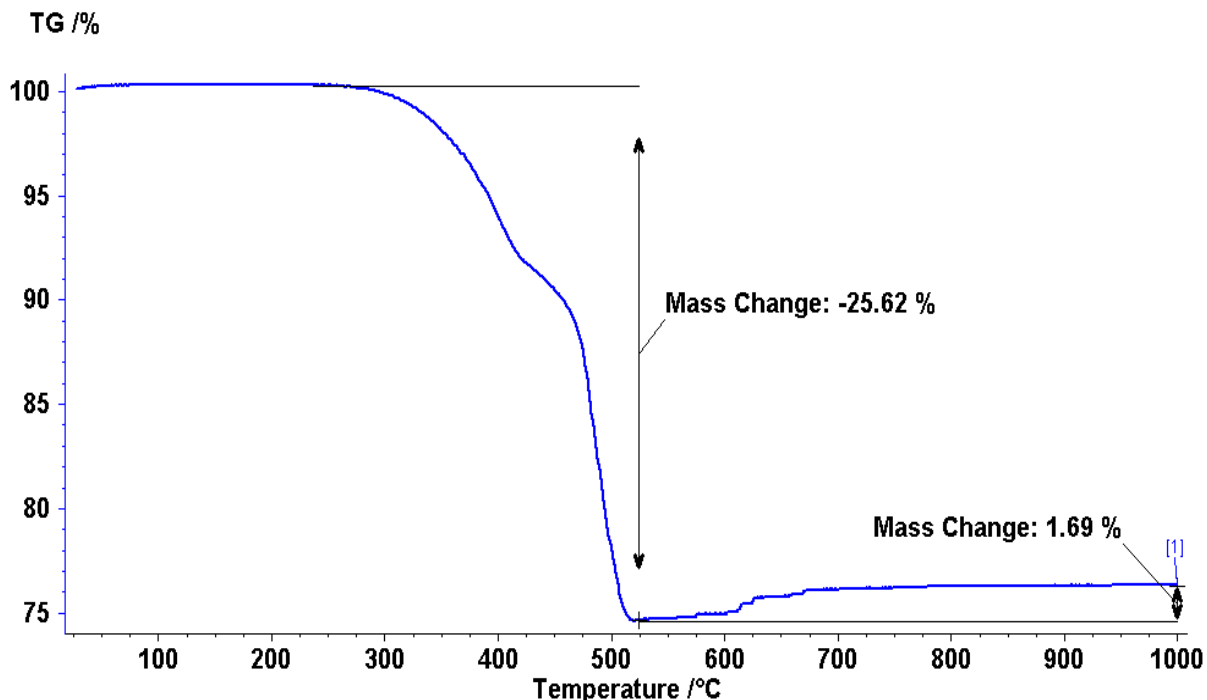


**Figure 3.8:**  $\text{As}_2\text{O}_3 + \text{CaO}$  in synthetic air atmosphere (sample As1)

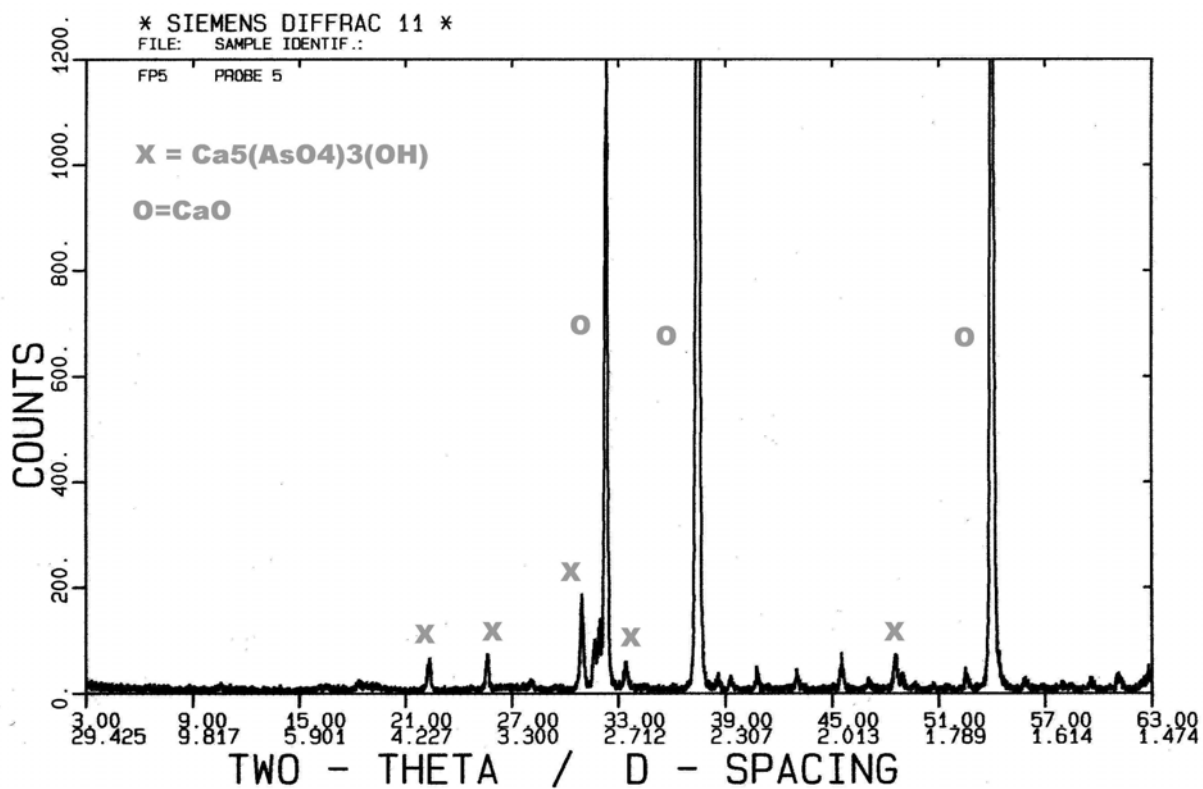


**Figure 3.9:** XRD spectrum of sample As2

### 3.4.2 Chromium

As discussed in *chapter 2* trivalent chromium oxide ( $\text{Cr}_2\text{O}_3$ ) is a very stable compound and showed no signs of oxidation or thermal decomposition in synthetic air up to  $1400^\circ\text{C}$ . However, the mixture of  $\text{Cr}_2\text{O}_3$  and  $\text{CaO}$  (sample *Cr1*) exhibited a very interesting thermal behavior (*figure 3.10*).

At  $500^\circ\text{C}$  (air atmosphere) a very fast mass increase started which was completed at  $850^\circ\text{C}$  (+9,5%). At this temperature the sample mass started to decrease again until  $1000^\circ\text{C}$  were reached (-2%). This behavior could be explained by the formation and subsequent decomposition of an oxidized reaction product. However, not all of the reaction product seemed to decompose, as the mass loss was not as high as the mass increase.

This interpretation was confirmed by the XRD analysis of the residues. The analysis of sample *Cr2*, which was heated for one hour at  $850^\circ\text{C}$  allowed to detect hexavalent calcium chromate ( $\text{CaCrO}_4$ ) (*figure 3.11*) while the spectrum of the same sample heated up to  $1250^\circ\text{C}$  (*figure 3.12*) showed the presence of the trivalent chromate ( $\text{Ca}(\text{CrO}_2)_2$ ), as well as hexavalent chromate.

This experimental evidence is of high importance because as the average fuel bed temperatures in a municipal solid waste incinerator range generally between  $800^\circ\text{C}$  and  $1000^\circ\text{C}$  there is a chance that at least part of the total chromium inventory is converted to hexavalent chromates.

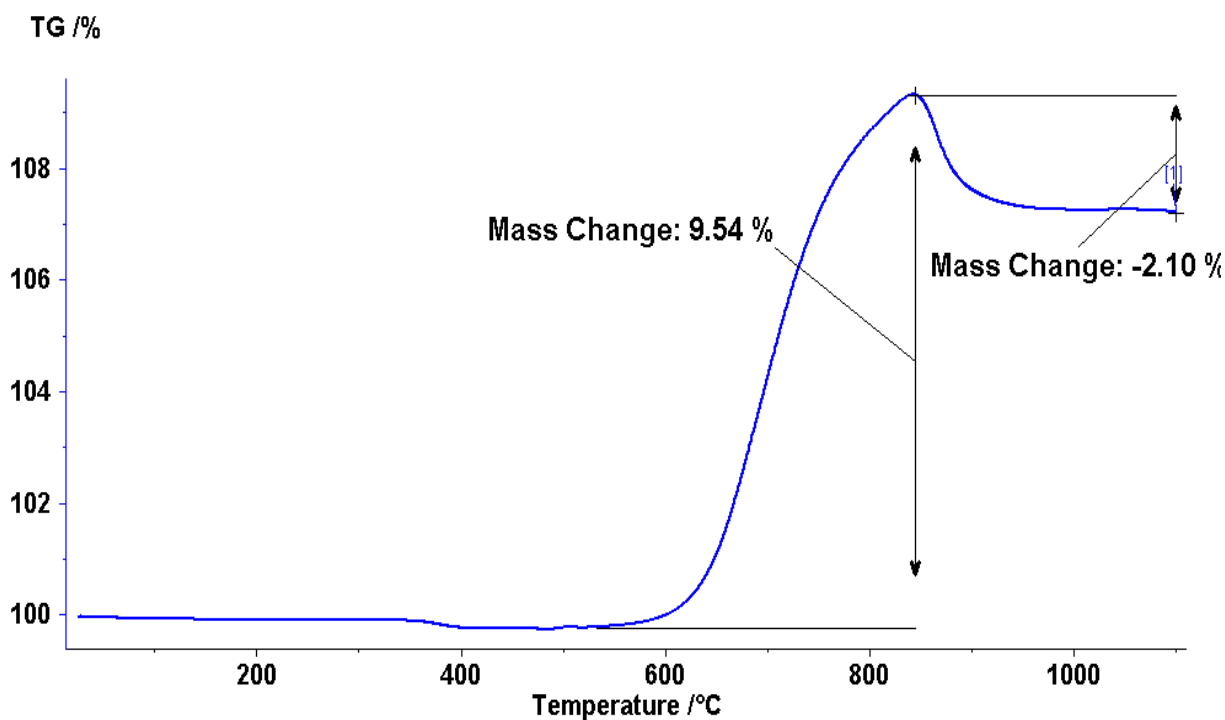


**Figure 3.10:**  $\text{Cr}_2\text{O}_3 + \text{CaO}$  in synthetic air atmosphere (sample *Cr1*)

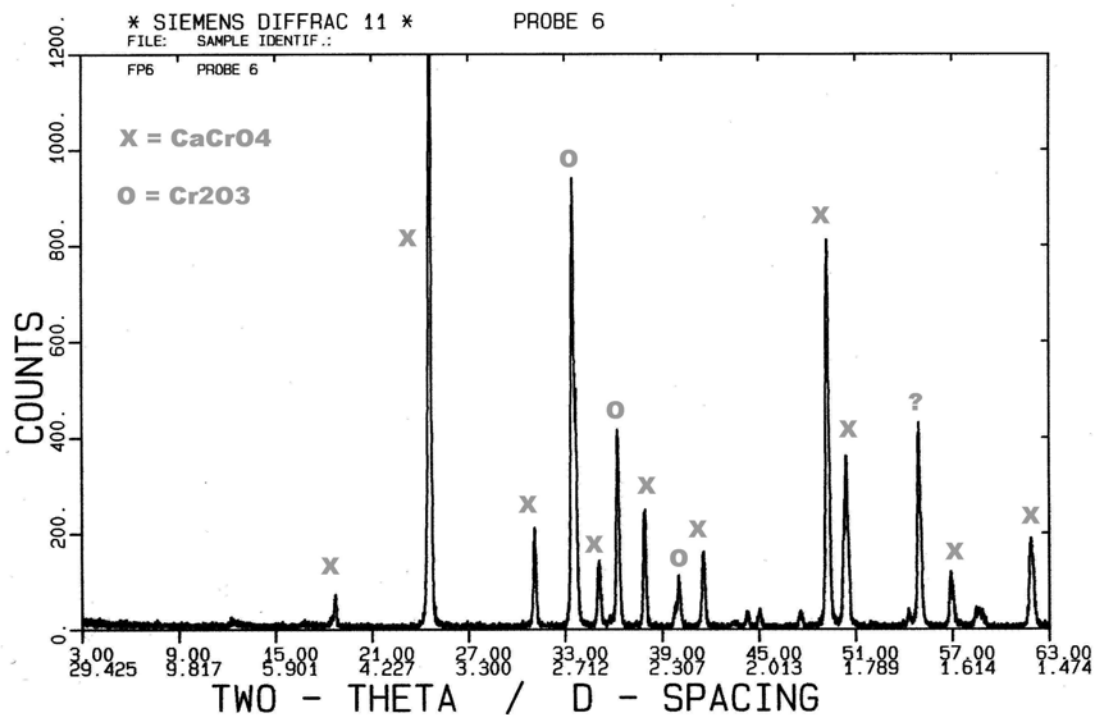


Figure 3.11: XRD spectrum of sample Cr2 (1 hour @ 850°C)

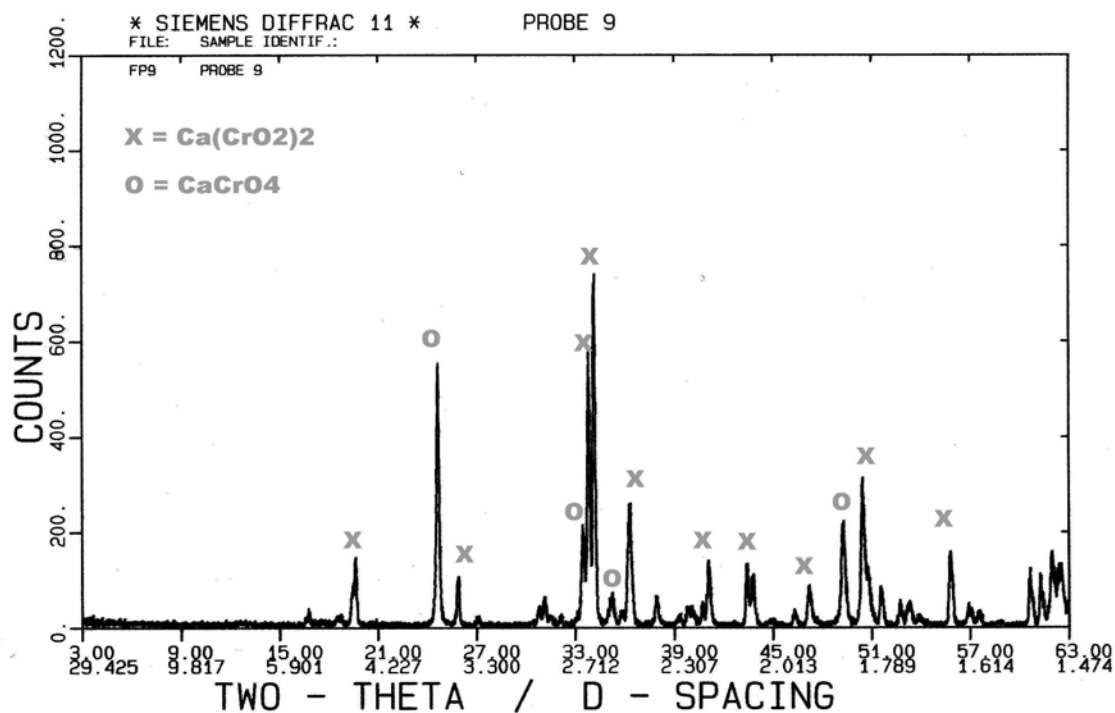


Figure 3.12: XRD spectrum of sample Cr2 (1 hour @ 1250°C)

The thermal analysis of sample Cr1 in inert atmosphere (nitrogen) showed no signs of relevant mass changes (figure 3.13). The two mass loss steps around 450°C and 600°C were caused by the loss of water and carbon dioxide from the calcium oxide sample discussed in the previous section. The dotted line in figure 3.13 represents the thermal analysis of a CaO sample for comparison.

However, it was striking to notice that the sample residues after thermal analysis showed a slight change in color, having turned from emerald green ( $\text{Cr}_2\text{O}_3$ ) to olive green. The XRD spectrum of the sample heated in inert atmosphere up to  $1000^\circ\text{C}$  (figure 3.14) revealed the presence of trivalent calcium chromate ( $\text{Ca}(\text{CrO}_2)_2$ ) as well as chromium oxide ( $\text{Cr}_2\text{O}_3$ ). Thus, chromate formation seems to take place even in inert atmosphere.

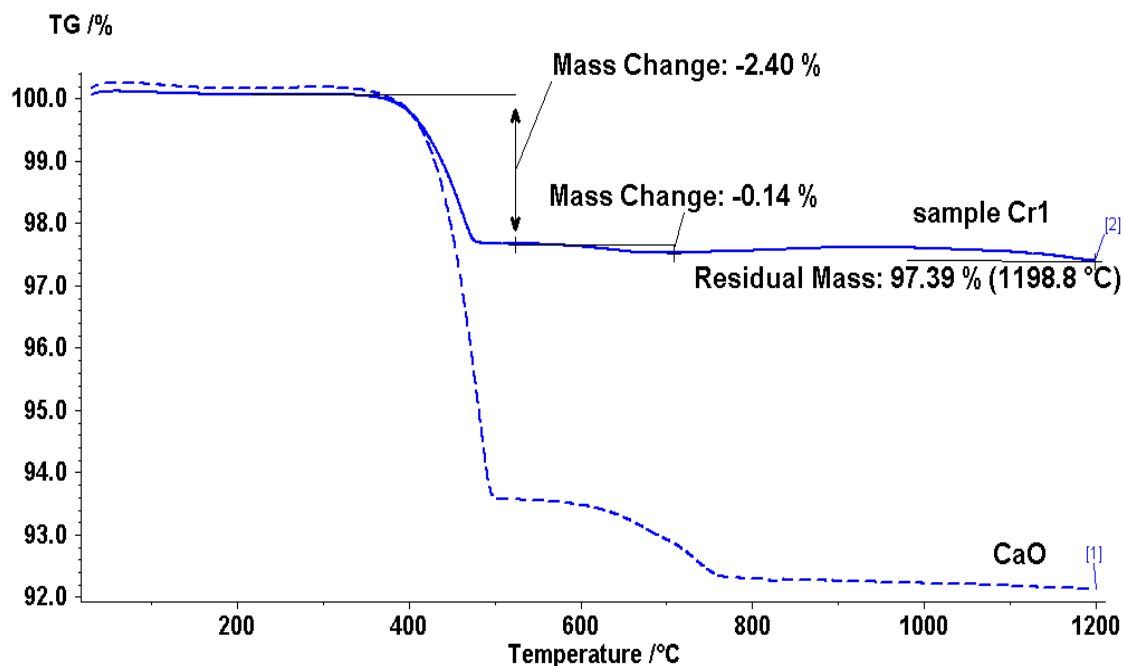


Figure 3.13:  $\text{Cr}_2\text{O}_3 + \text{CaO}$  in inert atmosphere (sample Cr1)

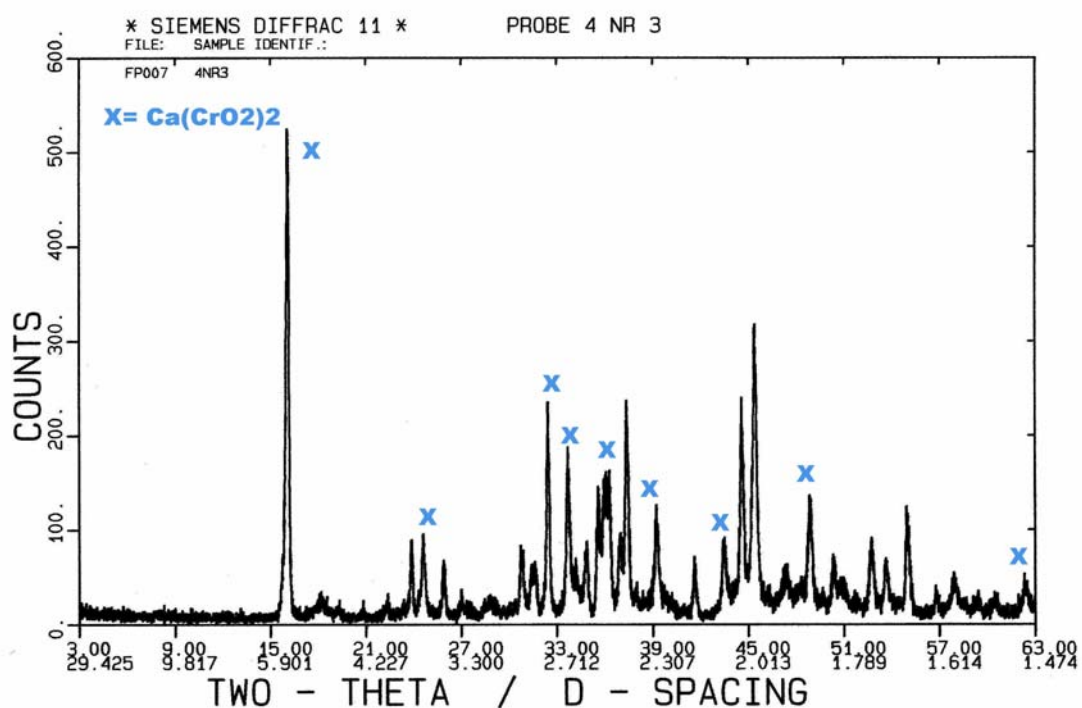
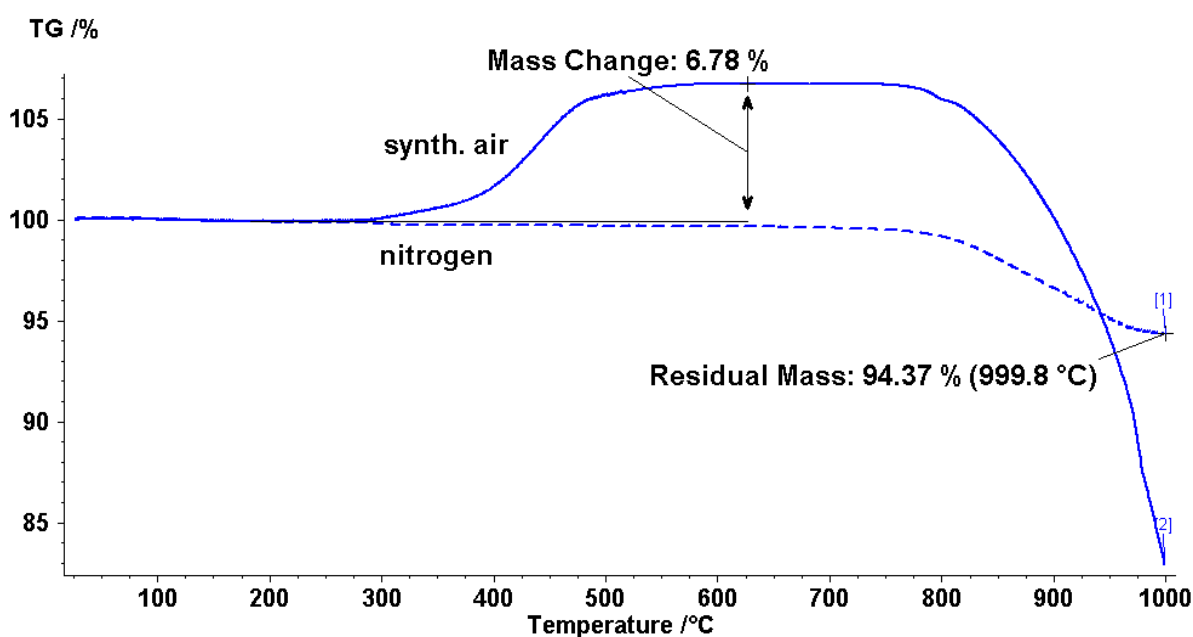


Figure 3.14: XRD spectrum of sample Cr2 (1 hour @  $1000^\circ\text{C}$ , inert atmosphere)

### 3.4.3 Molybdenum

Two molybdenum compounds have been considered for thermal analysis: tetravalent molybdenum oxide ( $\text{MoO}_2$ ) and hexavalent molybdenum oxide ( $\text{MoO}_3$ ).

$\text{MoO}_2$  was quite stable in inert atmosphere showing a moderate weight loss in nitrogen atmosphere (5%, dotted line in *figure 3.15*). In synthetic air, instead,  $\text{MoO}_2$  was oxidized to the much more volatile  $\text{MoO}_3$  and was quickly volatilized at temperatures above  $750^\circ\text{C}$  (solid line in *figure 3.15*). Oxidation started around  $300^\circ\text{C}$  and was completed at  $500^\circ\text{C}$ . Thus, it can be assumed that in synthetic air  $\text{MoO}_2$  and  $\text{MoO}_3$  will show the same behavior for temperatures above  $500^\circ\text{C}$ .



**Figure 3.15:**  $\text{MoO}_2$  in synthetic air (solid line) and in nitrogen atmosphere (dotted line)

The mixture of  $\text{MoO}_3$  and  $\text{CaO}$  (sample *MoI*) showed no mass losses in air atmosphere up to  $1400^\circ\text{C}$  which was interesting, since a volatilization of  $\text{MoO}_3$  was expected to start at approx.  $800^\circ\text{C}$ . Moreover, the residues showed a color change from white-turquoise to white-orange.

In fact, if calcium molybdate formation had taken place instead of  $\text{MoO}_3$  volatilization this would imply no mass change (see *table 3.3*). In this case DSC analysis would be more suited to provide evidence for the reaction. The results of the DSC analysis of sample *MoI* are depicted in *figure 3.16*. The thin dotted line represents the TG analysis while the thicker line represents the DSC curve. The dotted line represents the DSC baseline (empty crucible). Water loss from calcium oxide was characterized by a strong endothermic peak at  $428^\circ\text{C}$  (mass loss 7,2%). At  $450^\circ\text{C}$  an exothermic signal started, showing a maximum at  $575^\circ\text{C}$ . This signal was evidently caused by the heat of reaction of molybdate formation.

Sample *Mo2* was then heated up in the laboratory furnace and kept for one hour at 850°C. The XRD-spectrum of the residue is depicted in *figure 3.17*.

The diffractometric analysis revealed unmistakably the formation of calcium molybdate ( $\text{CaMoO}_4$ ), with no traces of unreacted materials. Thus, the residence time of the fuel bed in the combustion chamber should be sufficient to allow molybdate formation.

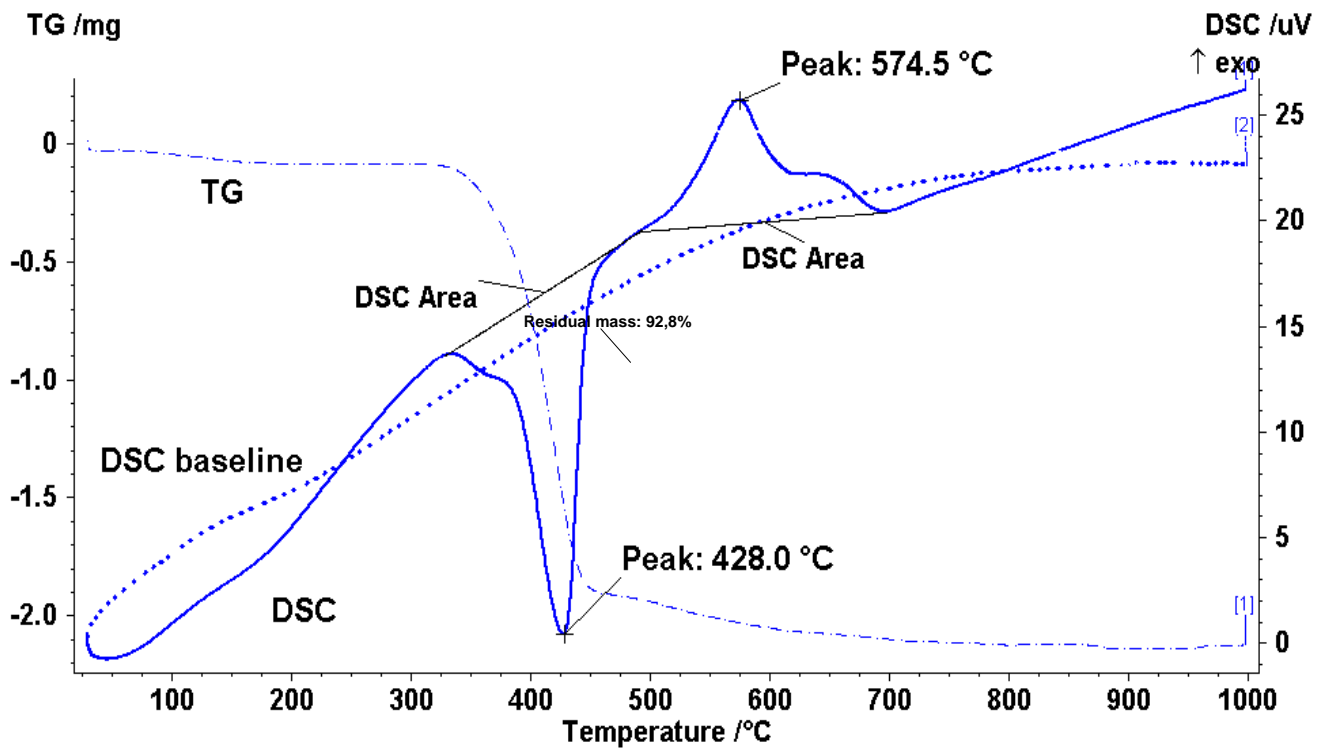


**Figure 3.16:**  $\text{MoO}_3 + \text{CaO}$  in synthetic air atmosphere (sample *Mo1*)

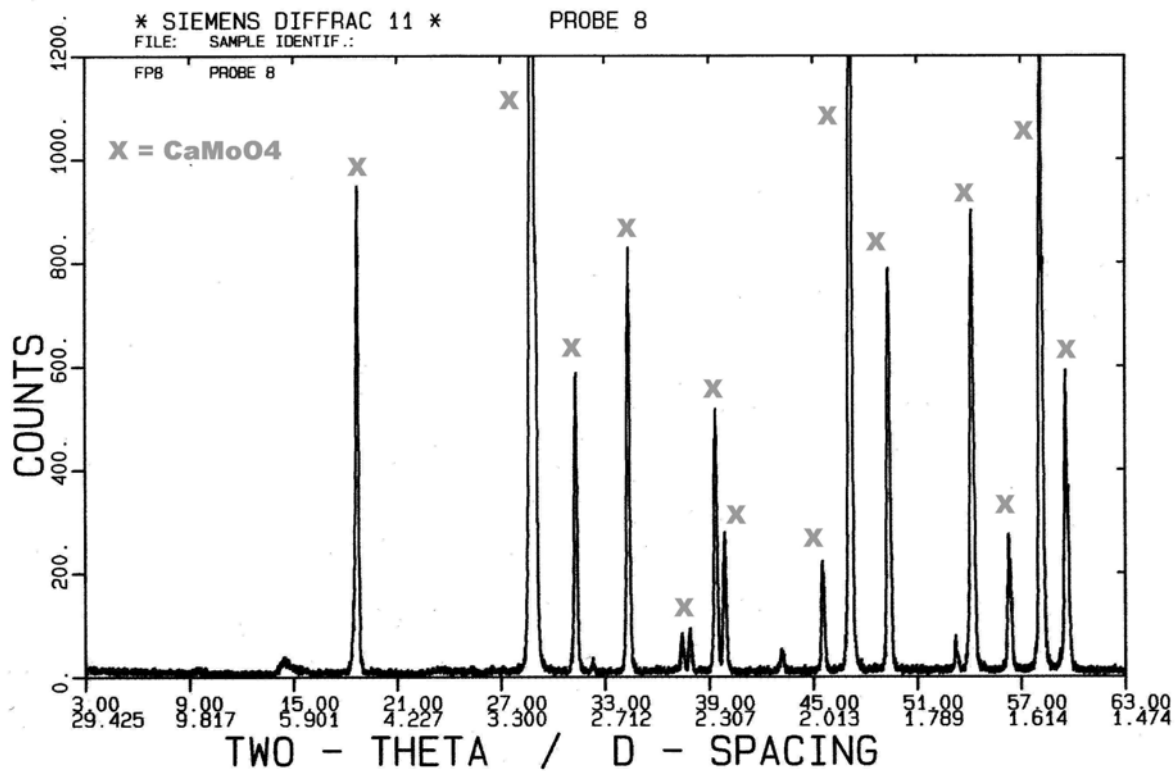


Figure 3.17: XRD spectrum of sample Mo2 (1 hour @ 850°C)

## Chapter 4

### Experimental methods

#### 4.1 TAMARA test facility for waste incineration

TAMARA is a pilot plant for the incineration of municipal solid waste located at the *Institute for Technical Chemistry - Division of Thermal Waste Treatment*. It was taken in operation in 1987. The name of the plant is a German acronym that stands for "test facility for waste combustion, flue gas cleaning, residue treatment and wastewater purification".

TAMARA (*figure 4.1*) is a grate incinerator with a throughput of approx. 250 kg/h. The feed is typically composed of 75% preconditioned solid waste (shredded, sieved to <60 mm, lower heating value about 6 MJ/kg) and 25% of refuse derived fuel (lower heating value about 16 MJ/kg). The average heating value of the fuel mixture amounts to about 8,5 MJ/kg. The composition of this mixture is representative of an average German municipal solid waste.

The reciprocating grate measures 3,2 m in length and 0,8 m in width and has a grate load of 65 kg/m<sup>2</sup>. The residence time varies between 45 and 60 minutes. It is divided in four sections equal in space with independent control for primary air supply, stroke and feed rate.

The geometry of the combustion chamber can be varied in order to realize either co-current-, middle- or counter-flow conditions by the installation of roof elements. *Figure 4.1* shows the co-current-flow configuration. *Figure 4.2* shows the interior of the TAMARA combustion chamber.

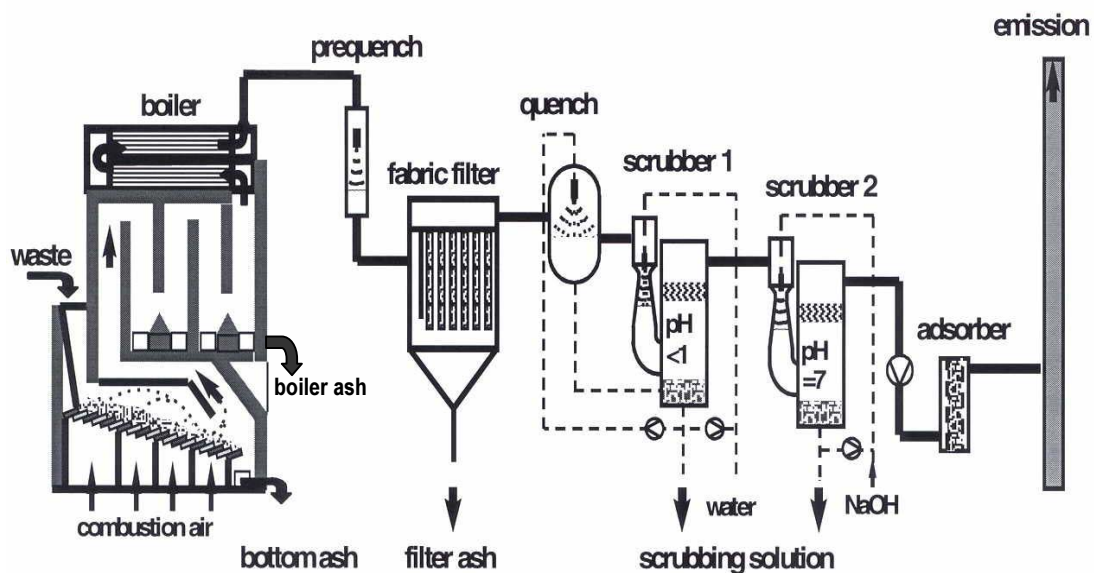


Figure 4.1: TAMARA test facility



**Figure 4.2:** TAMARA combustion chamber

For the cooling of the gases a boiler is installed on top of the furnace which consists of 5 radiation sections followed by a horizontal water wall tube boiler. After exiting the boiler, a prequencher reduces the flue gas temperature from some 230°C to about 180°C.

Dedusting is performed by means of a fabric filter (consisting of 36 PTFE fabric tubes coated by Goretex® membrane). The filter has an active area of 40 m<sup>2</sup> and the operation temperature is 160-180°C. The flue gas cleaning system consists of a two-stage wet scrubber with a separate initial quench stage. In the first stage, the scrubbing solution is kept at a pH value <1 for acid gases and mercury removal. The second stage is operated at pH = 7 (by addition of sodium hydroxide) for SO<sub>2</sub> removal. The scrubbers operate at a temperature of about 65°C.

Before exiting the stack the flue gases pass through a fixed bed carbon filter which guarantees compliance with emission regulations even under extreme conditions, especially in regard to dioxins and furans.

## 4.2 Sampling strategies

The TAMARA test facility allows the collection of representative samples of all solid combustion residues (grate ashes, grate siftings, boiler ashes, fly ashes).

The different mass streams require different sampling strategies. Especially the sampling and size reduction of inhomogeneous materials such as solid waste and grate ashes is always a compromise between theory and practice. The methods applied here follow recommendations made by the International Ash Working Group [IAWG, 1997]. The sampling time was always 3 h.

The grate ashes were sampled in a separate bin which replaced the original grate ash bin for five minutes every hour. The total sample per test run was typically 30-40 kg. For analytical reasons no grate ash quenching like in full scale plants was performed.

On account of their small amounts, the entire grate sifting and boiler ash streams were collected. The boiler ashes were taken from four different sampling ports located in the inferior part of the radiation part of the boiler (see *figure 4.1*). This allowed the classification of the boiler ashes on behalf of their deposition temperature and thus a separate analysis and characterization.

The fly ashes in the raw gas were sampled isokinetically directly out of the gas stream. These particulate samples are more representative than collecting dust from the fabric filter discharge. The filter ashes may suffer from tailing effects as a result of deposits not removed by the periodical cleaning. By means of a long-term isokinetic sampling system [Kahanek *et al.* 1988, Patent Document DE 3422052 C2, 1988, Patent Document DE 3520380 C2, 1994] approx. 15 m<sup>3</sup> of raw gas were sampled. The dust was collected by means of a plane PTFE/Goretex filter, which was located in a heated chamber where the temperature was kept at approx. 180°C. The plane filter and the heated chamber are depicted in *figure 4.3*.

For the sampling of filter-passing gaseous species a flow of 4-5 m<sup>3</sup>/h of filtered gas was drawn from the main gas stream, cooled down to 5°C and then led through a series of impingers filled with two absorbing solutions (first absorption solution: HNO<sub>3</sub> + HCl, second absorption solution: HNO<sub>3</sub> + H<sub>2</sub>O<sub>2</sub>) as recommended by the German Engineering Association [VDI, 1984]. All chemicals used were high-purity grade. The gas condensate and the absorbing solutions in the impingers were analyzed for anions to get information about the HF, HCl, and HBr concentrations in the raw gas and for gaseous and/or filter passing heavy metals. The gas sampling system (impinger) is depicted in *figure 4.4*.



**Figure 4.3:** Plane filter chamber



**Figure 4.4:** Absorption system

### 4.3 Sample treatment

All solid samples needed a pretreatment prior to analysis such as subdividing, size reduction, and digestion.

The solid waste fraction as well as the refuse derived fuel were dried at 106 °C [DIN 51718, 1995] and then shredded. The metal scrap in the solid waste fraction, in the grate ash, and in the grate siftings were manually separated. Ash samples (except for the isokinetically collected particulate) were sub-divided using a riffle (figure 4.5). A first rough size reduction of the grate ashes down to a grain size of approximately 1-2 mm was carried out by means of a crusher before grinding.

A subsample of about 100 g of each fraction was ground in a tungsten carbide ball mill and sieved using a sieve with a mesh size of 0,125 mm (figure 4.6). Further subdivision is carried out in a rotating sample divider.

Because of the small sample size (generally 3-8 g) and the very fine grain size, the isokinetically collected fly ash was manually separated from the PTFE filter and ground in an agate mortar without any further treatment.

For analyzing heavy metals about 100-300 mg of each sample have been digested using a HNO<sub>3</sub>/HF (ratio 6:1) mixture in a PTFE bomb at 200 °C.



**Figure 4.5:** Riffle for sample subdivision



**Figure 4.6:** Ball mills and sieves

#### 4.4 Analytical methods

Metal concentrations in liquid (or digested) samples were analyzed by means of total reflection X-ray fluorescence analysis (TRFA) [Knoth and Schwenke, 1978; Prange, 1987] with a spectrometer 8300C by Atomika. This analytical method offers the great advantage of simultaneous analysis of most trace elements present in the sample.

Some leachates were analyzed for their chromium speciation. This was the case for the leachates obtained by the German leaching procedure DEV S4 (see next section).

There are several methods to determine the chromium speciation in aqueous samples, especially the fraction of total chromium ( $Cr_{tot}$ ) present as hexavalent chromium (Cr(VI)) [DIN 38405, 1987; Harzdorf, 1990; Bittner and Broekaert, 1998]. Generally, these methods are based on the determination of the total chromium content in the sample, followed by the selective separation of trivalent species and subsequent analysis of the remaining hexavalent species.

However, these detection methods are often not very sensitive and, moreover, are hampered by cross-effects with other metallic species. Hence these data must be regarded with a certain caution. Unfortunately it is not possible to determine the chromium speciation in the solid residue samples since the digestion process (acid digestion or alkali digestion with sodium peroxide) alters the oxidation state of the element thus rendering the determination of hexavalent chromium impossible. For the DEV S4 leachates, precipitation of trivalent chromium species was carried out following the procedure prescribed by the German Normalization Institute [DIN 38405, 1987]. The samples were then stirred overnight in nitrogen atmosphere and then filtrated using a 0,2  $\mu\text{m}$  membrane filter. After filtration, the leachates were analyzed for hexavalent chromium species.

Concentration of anionic species ( $Br^-$ ,  $Cl^-$ ,  $F^-$ ,  $NO_3^-$ ,  $SO_4^{2-}$ ) in liquid samples were analyzed by means of ionic chromatography (IC) [Weiss, 1984] using a Dionex DX 500 ion chromatograph.

The ultimate analysis of the TAMARA fuel mixture was carried out by means of a Leco CHNS-VTF 900 analyzer while the total carbon content (TC) of the residues was determined by burning the sample in an oxygen flow and subsequent infra-red (IR) carbon dioxide measurement.

For total organic carbon content (TOC) determination the carbonates present in the residues were previously eliminated by means of sample acidification with concentrated hydrochloric acid.

#### 4.5 Leaching procedures

To investigate the leaching behavior of the elements, several leaching test procedures were carried out on the incineration residues (grate ashes, boiler ashes and filter ashes).

For leaching purposes filter ash samples collected directly from the dedusting unit were used since the limited amounts of the isokinetically collected fly ashes would not be sufficient to carry out leaching procedures.

Table 4.1 shows the different leaching test methods adopted for the various residues. The procedures differ greatly from each other in respect to the most important leaching parameters (agitation, time, sample mass and grain size, liquid-to-solid ratio, leachant and pH control). An overview on leaching test procedures can be found in the works of the *International Ash Working Group* and of Fällmann [Fällmann, 1990; IAWG, 1997].

**Table 4.1:** Leaching procedures carried out

<b>Grate ashes</b>	<b>Boiler ashes</b>	<b>Filter ashes</b>
availability test [NEN 7341] column leaching test [NEN 7343] DEV-S4 test [DIN 38414] TVA test [TVA] Ep Tox test [USEPA 1310] pH-stat test	availability test [NEN 7341] pH-stat test	availability test [NEN 7341] pH-stat test

The **Dutch availability test (AVA)** [NEN 7341, 1995] is used to determine the maximum quantity of a residue constituent that can be released into solution under aggressive leaching conditions (i.e. its availability for leaching) and thus is assumed to represent a maximum leaching potential.

The test consists of two successive extractions (of 3 hours each) of a finely ground (<0,125 mm) sample with a total liquid-to-solid ratio of 100. The suspension (ground sample and deionized water) is kept in agitation by means of a magnetic stirrer, and the pH value is kept constant to 7 (first extraction step) and 4 (second extraction step) by addition of 1M HNO<sub>3</sub> with the automatic titration apparatus shown in figure 4.7 (Metrohm Titrino 719 S).

The **Dutch column leaching test (CLT)** [NEN 7343, 1995], instead, is a dynamic leaching test and simulates the time resolution of the leaching process. The leachant is pumped through a column filled with the residues (flow-through test). By collection of different amounts of the leachate the liquid-to-solid ratio (L/S) is varied between 0,1 and 5 (for a cumulative value of 10) and the effect of rain or groundwater on the residues under a long-term scenario is simulated. The experimental equipment for the column leaching test is depicted in figure 4.8.

The **German regulatory test DEV S4** [DIN 38414, 1984] is an agitated extraction test. Approximately 100 g of a crushed sample (< 10 mm) are put in a closed vessel with de-ionized water in a liquid-to-solid ratio of 10 and then kept in agitation on a roller bench for 24 hours. In general, the final leachate pH depends on the alkaline properties of the residue being tested and ranges typically between 9 and 12 for municipal solid waste incinerator grate ashes [IAWG, 1997].

In the **Swiss TVA test** [Bundesamt für Umweltschutz, 1991] 100 grams of a crushed sample are put in contact with deionized water (L/S ratio: 10) and CO<sub>2</sub> is insufflated in the leaching vessel at a flow rate of 100 ml/minute. The bubbling of CO<sub>2</sub> keeps the pH of the leachate in the neutral range (about 6-7) and at the same time provides agitation of the system. The leaching vessel is provided with openings on the upper side to avoid over-pressure caused by the gas. The procedure consists of two extraction steps of 24 hours each.

The **US EPA Ep Tox test** [US EPA 1310, 1984] is an agitated extraction procedure. A suspension of 100 g of a crushed sample and deionized water (L/S: 20) is kept in agitation for 24 hours (on a roller bench). At the beginning of the test the pH value of the suspension is adjusted to 5 by addition of 0,5 N acetic acid (CH<sub>3</sub>COOH). The pH is then periodically adjusted to this value. After 24 hours, if the pH differed from 5 by more than ±0,2 units, the test is carried on for further 4 hours.

Finally, the **pH-stat** leaching test is a non-standardized procedure in which a finely ground sample is put in a leaching vessel with distilled water (L/S ratio: 20) and the suspension pH kept constant to a prefixed value (varying between 4 and 12) for 24 hours by titration of 1 M HNO<sub>3</sub> or 1M NaOH (depending on the pH value of the suspension). The titration and agitation equipment used for this procedure is the same as for the availability test.

The main leaching parameters of the applied procedures are summarized in *table 4.2*. All chemicals used were high-purity grade.

**Table 4.2:** Leaching parameters

test name	AVA	CLT	DEV	TVA	EpTox	pH-Stat
test type	extraction (2 steps)	flow-through	extraction	extraction (2 steps)	extraction	extraction
test purpose	maximum leaching potential	time resolution	no pH control	carbonation effects	effect of organic acids	effect of pH
agitation	magnetic stirrer	none	roller bench	gas bubbles	roller bench	magnetic stirrer
sample mass	7 g	300-400 g	100 g	100 g	100 g	8-15 g
grain size	<125 µm	<3 mm	<10 mm	<3 mm	<10 mm	<125 µm
L/S	100	0,1...10	10	10	20	20
time	3 + 3 h	6 - 7 d	24 h	24 + 24 h	24 + 4 h	24 h
leachant	H <sub>2</sub> O+HNO <sub>3</sub>	H <sub>2</sub> O+HNO <sub>3</sub>	H <sub>2</sub> O	H <sub>2</sub> O+CO <sub>2</sub> (100 ml/min)	H <sub>2</sub> O+ acetic acid	H <sub>2</sub> O+HNO <sub>3</sub> H <sub>2</sub> O+NaOH
pH	7 + 4	12-13	12-13	6-7	5 ± 0,2	4...12



**Figure 4.7:** Automatic titration unit (Metrohm Titrino 719 S)

After leaching the liquid was separated by a vacuum filter using a membrane with pore width  $0,45\ \mu\text{m}$  (figure 4.9). The pH value of the leachate was successively recorded by means of a glass electrode (in the availability and the pH-stat test, the pH was recorded automatically by the titration unit). The leachate was then divided in two portions: the first for analysis of anionic species (ionic chromatography), the second for TRFA metal analysis. To avoid precipitation of metallic species 1 ml of  $\text{HNO}_3$  (65%) was added for sample stabilization.



**Figure 4.8:** Column leaching test equipment



**Figure 4.9:** Vacuum filtration equipment

## **Chapter 5**

### **Incineration tests on pilot plant TAMARA**

#### **5.1 Incineration campaign**

The objective of this incineration campaign was to investigate the influence of the primary air ratio, i.e. the ratio of the combustion air supplied through the grate to the theoretical air demand, on the behavior of the investigated metals. It was assumed that the air ratio does not only influence the fuel bed temperature profile, but also the transfer out of the combustion chamber as well as the potential for leaching of the metals. The fuel bed residence time in the high-temperature zone as well as the oxygen availability play an important role in the oxyanion formation process.

The air ratio  $\lambda$  is defined as the ratio between primary combustion air and the theoretical air demand:

$$\lambda = \text{primary combustion air} / \text{theoretical air demand} \quad [\text{Eq. 5.1}]$$

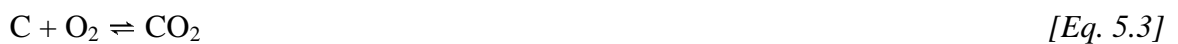
The theoretical air demand,  $l_{min,vol}$ , is calculated on dry fuel basis by:

$$l_{min,vol} = O_{2min,vol} / 0,21 \quad [\text{Eq. 5.2}]$$

where:  $O_{2min,vol}$  = stoichiometric oxygen demand [ $Nm^3/kg$ ]

0,21 = volume fraction of oxygen in air

The stoichiometric oxygen demand  $O_{2min,vol}$  is calculated on the assumption that all the required oxygen is consumed for the oxidation reactions of carbon, hydrogen, sulphur and nitrogen, respectively, following the reactions:



Furthermore, the fuel oxygen content must be detracted from the stoichiometric oxygen demand.

This yields an oxygen demand in terms of mass:

$$O_{2min,vol} = 22,41 \left( \frac{C}{12} + \frac{H}{4 \cdot 1} + \frac{S}{32} + \frac{N}{2 \cdot 15} - \frac{O}{2 \cdot 16} \right) \quad [\text{Eq. 5.7}]$$

where: 22,41 =  $Nm^3 O_2 / kg_{air}$

C = fuel carbon content [ $kg_C / kg_{dry fuel}$ ]

H = fuel hydrogen content [ $kg_H / kg_{dry fuel}$ ]

S = fuel sulphur content [ $kg_S / kg_{dry fuel}$ ]

N = fuel nitrogen content [ $kg_N/kg_{dry\ fuel}$ ]

O = fuel oxygen content [ $kg_O/kg_{dry\ fuel}$ ]

12 = carbon atomic weight

1 = hydrogen atomic weight

32 = sulphur atomic weight

15 = nitrogen atomic weight

16 = oxygen atomic weight

It follows that the theoretical air demand  $l_{min,vol}$  can be calculated as:

$$l_{min,vol} = \frac{22,41}{0,21} \left( \frac{C}{12} + \frac{H}{4 \cdot 1} + \frac{S}{32} + \frac{N}{2 \cdot 15} - \frac{O}{2 \cdot 16} \right) \quad [Eq. 5.8]$$

The values for C, H, S, N, O are gathered from the fuel ultimate analysis. However, in the case of municipal solid waste, the contribution of sulfur and nitrogen is very small (less than 0,5% and 1%, respectively) and can hence in a first approach be neglected in estimating the theoretical air demand.

The experimental data were gathered during one incineration campaign performed on the pilot plant TAMARA (see *chapter 4*). The combustion chamber was in middle flow geometry. The campaign consisted of five days, with two sampling periods every day. On each day, the combustion parameters (fuel input, combustion air, grate velocity) were kept constant. Of the two sampling periods each day, the first one was under reference conditions (no metal spiking, see next section), while during the second period a spiking was performed, i.e. metal compounds were added to the fuel. Reference sampling periods will be, from now on, referred to as *ref.1*, *ref.2*, *ref.3*, *ref.4*, *ref.5* (the number indicates the campaign day), while spiking periods will be termed *sp.1*, *sp.2*, *sp.3*, *sp.4*, *sp.5*.

To investigate the effect of combustion air variation on metal behavior, the amount of primary air was reduced on every successive campaign day so as to shift the air ratio  $\lambda$  from 1,5 (reference value) down to a value of 0,6.

To guarantee a complete burnout and a high furnace exit gas temperature, secondary air was insufflated so as to compensate for the reduced amount of primary air. Thus the total air ratio (as calculated from the primary and secondary air contribution) was kept at an overall constant value.

*Table 5.1* summarizes the combustion air flows and the calculated air ratio for each run and each campaign day.

**Table 5.1:** Combustion air

day	run	prim. air (Nm <sup>3</sup> /h)	prim. air ratio $\lambda_{\text{prim.}}$	sec. air (Nm <sup>3</sup> /h)	tot. air (Nm <sup>3</sup> /h)	tot. air ratio $\lambda_{\text{tot}}$
1	ref.1	450	1,5	0	450	1,5
	sp.1	440	1,5	0	440	1,5
2	ref.2	380	1,3	100	380	1,6
	sp.2	375	1,2	100	475	1,6
3	ref.3	300	1,0	200	500	1,7
	sp.3	300	1,0	200	500	1,7
4	ref.4	215	0,7	266	481	1,6
	sp.4	215	0,7	300	515	1,7
5	ref.5	185	0,6	250	435	1,4
	sp.5	175	0,6	250	425	1,4

The variation of the insufflated primary air flow had obviously a strong effect on the fuel bed temperature. *Figure 5.1* shows the temperature profile along the grate length for the five campaign days. It can be clearly recognized that with decreasing primary air flow, the fuel ignition point was shifted towards the end of the grate. Moreover, as the excess air diminished, the carbon oxidation reaction proceeded more slowly and the temperature profile became less steep and broader. On the other hand, as the area of the profile became larger, the residence time of the fuel bed in the high temperature zone increased, so that the delayed ignition could be compensated by this beneficial effect. This is particularly evident on day 3 ( $\lambda = 1$ ), while on day 5 ( $\lambda = 0,6$ ) no definite ignition point can be pointed out on the temperature profile and the high-temperature zone was reached nearly at the end of the grate. Thus, the carbon oxidation in the fuel bed resulted to be incomplete, as will be discussed in *chapter 6*.

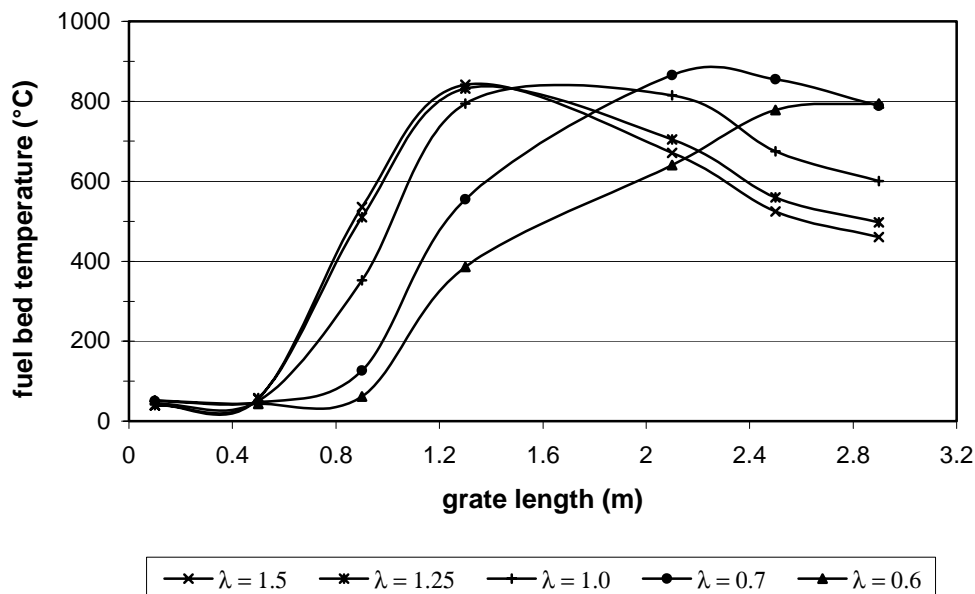
**Figure 5.1:** Temperature profiles along the grate ( $\lambda$ : primary air ratio)

Table 5.2 shows the temperatures measured at the end of the post-combustion zone. The 17. BImSchV. [Bundesministerium für Umwelt, Naturschutz und Reaktorsicherheit, 1990], the German ordinance for air emissions from waste combustion plants, requires that the flue gas must have a temperature not lower than 850°C for a residence time not inferior to 2 seconds after the last air injection. The effect of these regulatory requirements and other combustion parameters on burnout efficiency and PIC (products of incomplete combustion) concentrations in the raw gas were investigated in a project carried out at TAMARA and sponsored by the German Association of Power Plant Operators (VGB, *Vereinigung der Großkraftwerksbetreiber*) [Merz and Seifert, 1999]. The results obtained from the TAMARA incineration tests were validated in a successive project on a full-scale incineration plant [Merz and Seifert, 2000].

The columns labeled as boiler 1, boiler 2, boiler 3 and boiler 4, respectively, in table 5.2 indicate the temperatures at the boiler ash deposition and sampling points (located in the inferior part of the radiation boiler, see figure 4.1). It can be seen that, as the primary air flow in the combustion chamber decreased, the temperatures in the boiler increased. The carbon species which did not have sufficient time to be completely oxidized in the furnace continued reacting while being transported by the flue gas.

**Table 5.2:** Temperatures in the boiler (°C)

day	post-combustion zone	boiler 1	boiler 2	boiler 3	boiler 4
1	915	792	762	702	612
2	934	797	771	716	633
3	897	762	742	695	610
4	960	810	783	740	655
5	970	827	788	731	646

## 5.2 Spiking experiments

Spiking experiments consist in artificially increasing the concentration of an element in the input stream of an incineration plant. This is particularly useful in the case of those elements the concentration of which in municipal solid waste is normally very low. Partitioning effects as well as the influence of combustion conditions or interactions with other elements are thus more clearly pointed out. The first step in planning a spiking experiment is to estimate the reference input concentration of the element. This has been discussed in chapter 1. For the elements of interest a spiking factor of 5-10 was selected.

For spiking purposes, a mixture of those chemical compounds which are assumed to represent best the speciation of the elements in municipal solid waste has been used. For practical reasons, the spiking factor was adjusted depending upon the molecular weight of the compounds chosen: for

"heavier" compounds (like  $\text{Sb}_2\text{S}_3$ ) a lower spiking factor than for "lighter" compounds (like  $\text{As}_2\text{O}_3$ ) was chosen. For chromium, a low spiking factor was chosen because of its relative abundance in MSW. The compounds were dosed directly into the feeding hopper of TAMARA in a dry pulverized form by means of a dosing scale. The dosing scale automatically adjusted the mass flow of the mixture as a function of the fuel input.

Table 5.3 shows the fuel input flows for each sampling period of the campaign as well as averaged values over the whole campaign (bottom line).

**Table 5.3:** Input mass flows

Run	MSW (kg/h)	humidity (%)	MSW <sub>dry</sub> (kg/h)	RDF (kg/h)	total dry input (kg/h)
1	140	43	80	38	118
2	140	41	83	38	121
3	143	42	83	39	122
4	143	41	85	38	123
5	143	40	85	39	124
6	143	43	82	39	121
7	143	42	83	38	121
8	143	42	83	39	122
9	143	43	82	38	120
10	143	44	79	39	118
<b>Average</b>	143	42	82	38	121

The spiking factors of the investigated metals, the compounds used for the spiking experiments as well as their respective mass flows (average values) are listed in table 5.4. The reference concentrations in MSW are taken from literature (see table 1.1).

**Table 5.4:** Spiking experiments

Element	ref. conc. in MSW	spiking factor	compound	mass flow
As	10 mg <sub>As</sub> /kg d.f.	10	As <sub>2</sub> O <sub>3</sub>	14 g <sub>As2O3</sub> /h
Sb	50 mg <sub>Sb</sub> /kg d.f.	4	Sb <sub>2</sub> S <sub>3</sub>	27 g <sub>Sb2S3</sub> /h
Cr	200 mg <sub>Cr</sub> /kg d.f.	5	Cr <sub>2</sub> O <sub>3</sub>	123 g <sub>Cr2O3</sub> /h
Mo	20 mg <sub>Mo</sub> /kg d.f.	8	MoS <sub>2</sub>	27 g <sub>MoS2</sub> /h

Thus the total input of each metal (input inventory) consisted of three contributions: the metal concentration in municipal solid waste, the metal concentration in refuse derived fuel and the amount dosed. The total input of the four metals in the spiking tests (averaged values over the whole campaign) is listed in table 5.5. The values are expressed as mg/kg dry fuel and are gathered from the analysis of fuel (MSW and RDF) samples.

**Table 5.5:** Input inventory of the metals (averaged values)

Element	MSW	RDF	spiked amount	total input
As, mg <sub>As</sub> /kg <sub>d.f.</sub>	10	3	86	99
Sb, mg <sub>Sb</sub> /kg <sub>d.f.</sub>	15	15	162	192
Cr, mg <sub>Cr</sub> /kg <sub>d.f.</sub>	385	28	695	1108
Mo, mg <sub>Mo</sub> /kg <sub>d.f.</sub>	21	7	136	164

Table 5.6 shows the output mass flows for each run, respectively, as well as the averaged values over the whole campaign (bottom line).

**Table 5.6:** Output mass flows

Run	g.a. (kg/h)	g.s. (kg/h)	b.1 (kg/h)	b.2 (kg/h)	b.3 (kg/h)	b.4 (kg/h)	flue gas (Nm <sup>3</sup> /h)	dust (mg/Nm <sup>3</sup> )
1	38	6	0,41	0,20	0,21	0,01	881	548
2	39	6	0,25	0,09	0,26	0,004	866	545
3	33	6	0,35	0,30	0,39	0,11	841	524
4	33	5	0,19	0,36	0,30	0,04	953	563
5	41	6	0,22	0,04	0,01	0,003	943	391
6	38	6	0,42	0,06	0,15	0,05	929	518
7	44	6	0,11	0,04	0,16	0,04	819	473
8	38	4	0,34	0,02	0,04	0,02	814	576
9	40	5	0,29	0,05	0,06	0,02	706	356
10	44	5	0,20	0,05	0,07	0,02	709	364
<b>Average</b>	39	5	0,3	0,12	0,16	0,04	852	491

g.a.: grate ashes, g.s.: grate siftings, b.1, b.2, b.3, b.4: boiler ash fractions 1, 2, 3, 4

### 5.3 Relevance of test results

Before proceeding to the evaluation of the partitioning data, some considerations on the experimental error are necessary. If the accuracy of the analysis and the quality of the test performance is to be evaluated, then the ratio between output and input inventory (mass balance) needs to be considered.

There are many factors that might cause a mass balance not to be closed exactly at 100%, even in a comparatively small-scale plant like TAMARA. Some of these are plant-specific, some are element-specific, some are due to the digestion and analytical techniques employed and, last but not least, some are due to the general error that is part of every experimental work.

The incineration fuel, the municipal solid waste, is an extremely inhomogeneous material that hardly allows to collect a sample that can be regarded as representative. Large amounts of material over extended periods of time would be necessary and this would go far beyond the purpose of this work. Instead, as pointed out by other authors [Brunner and Ernst, 1986; Schneider, 1986; Vehlow and Mark, 2000] it is much more effective and reliable to leave the input data aside and evaluate the output data only, as the incineration residues are much more homogeneous in their nature than the

original solid waste. Moreover, except for the grate ashes the entire residue streams are sampled so that the sampling error for these residues can be neglected. For this reason from now on all partitioning data will be based on the evaluation of the output data only and the total output will be assumed to be equal to the total elemental inventory.

Apart from the above mentioned difficulty of getting a representative sample, one plant-specific cause of error is the fact that it is not possible to collect samples in all parts of the plant. For example, the fly ashes which are deposited in the horizontal water tube boiler cannot be collected. Thus the fly ash fraction which deposits between 600°C and 200°C is not represented in the balances. This is especially a problem for those elements, like arsenic and antimony, which form compounds that condensate in this temperature range.

On the other side, it must be considered that, despite some limitations in the sampling strategy, a pilot plant like TAMARA offers a unique possibility to sample different residue streams at locations which were especially designed for this purpose. Sampling of full-scale plants is a much more difficult task, as many residue deposition points are not accessible for sampling and furthermore it is not always possible to collect separate residue streams. Such is often the case for boiler ashes which might fall upon the fuel bed if the boiler banks are located directly above the furnace or are otherwise mixed with the grate ashes.

Scale-ups of the experimental results gathered from TAMARA incineration tests have been performed in the past in the *Institute for Technical Chemistry - Division of Thermal Waste Treatment*. The results showed that TAMARA data, despite some obvious differences caused by the limited furnace size, can be considered to be quite representative of full-scale conditions [Mark, 1996; Merz and Seifert, 2000].

Other errors might occur while handling the samples, especially during the laborious work of sample size reduction (sample division, grinding and sieving). Parts of the sample might be lost during handling and cleaning of the laboratory equipment, some fractions of the elemental inventory might be lost because of the separation of metal scrap (which is accomplished to avoid damage to the laboratory equipment). Moreover, even if all treatment steps are conducted as carefully and cleanly as possible a certain degree of contamination of the samples from the equipment used is unavoidable.

The analytical error is caused to a large extent by the extremely small amount of material which is analyzed (100-200 mg). Even in such a small amount of material it must be assumed that the element distribution is the same as for the whole sample.

Furthermore, the digestion process might be incomplete thus resulting in a reduced amount of the inventory being analyzed. On the other hand, some elements form highly volatile species during the digestion process which may be lost when opening the digestion vessel.

Finally, another error source lies in the multi-elemental TRFA analytical technique. While it is surely true that a great advantage consists in having all the trace elements present in the sample analyzed in one analytical run, on the other side the interference between the spectra of the elements can cause a sensible increase of the detection limit. This is especially true for arsenic, the spectrum of which is very close to that of lead.

Table 5.7 gives an overview of some of the most frequent error causes, grouped in systematic and causal error causes.

**Table 5.7:** Frequent error causes

<b>Systematic error causes</b>	<b>Casual error causes</b>
plant configuration (sampling locations)	inhomogeneous materials
mixed residue stream flows	tailing effect (fly ash deposits)
sampling strategy	sample handling and storage
contamination from handling equipment	sample contamination during pretreatment
size reduction steps	loss of material during size reduction and pretreatment
analytical interference	incomplete digestion of lithophilic species
analytical detection limit	loss of volatile species from digestion vessel

For all the above mentioned reasons, the level of error tolerance when evaluating the mass balance closure for a MSWI pilot scale plant like TAMARA for trace metals should be set at not less than  $\pm 10\text{-}15\%$  [Vehlow and Mark, 2000]. For full-scale plants, the error tolerance should be even higher, to account for the sampling difficulties.

Table 5.8 lists the output/input ratios for the investigated elements for every run as well as the campaign average value and the normalized standard deviation  $\sigma_N$ .

**Table 5.8:** Test performance (output/input ratio)

<b>Run</b>	<b>As</b>	<b>Sb</b>	<b>Cr</b>	<b>Mo</b>
1	1,4	1,4	0,5	0,6
2	0,5	1,0	0,6	0,65
3	0,7	2,3	0,4	0,55
4	0,4	0,7	0,4	0,5
5	1,1	1,5	0,4	0,5
6	0,6	0,9	0,6	0,6
7	1,6	0,9	0,7	0,6
8	0,6	0,8	0,8	0,8
9	1,5	0,6	0,5	0,7
10	0,6	0,8	0,8	0,7
<b>Average</b>	0,9	1,1	0,6	0,6
<b><math>\sigma_N</math></b>	0,4	0,4	0,2	0,1

Arsenic and antimony seemed to perform rather well. However, the data are widely scattered around the mean value. On the contrary, chromium and molybdenum showed a critical test performance which is more uniformly distributed. The low output amounts are typical for these and other lithophilic metals as the extremely stable compounds they form during combustion (spinel, chromites) cause difficulties in sample pretreatment and digestion.

#### 5.4 Transfer factor of the elements

The percent partitioning of the four investigated elements among the incineration residues (averaged over the whole incineration campaign) is depicted in *figure 5.2*. For a better overview in this section the four boiler ash fractions have been grouped together. A more detailed discussion concerning the boiler ashes will follow in the next section.

The concentrations in the flue gas absorbing solutions were always near or below the analytical detection limit, which means that almost no gaseous species could be detected. This will be discussed in *section 6* more in detail.

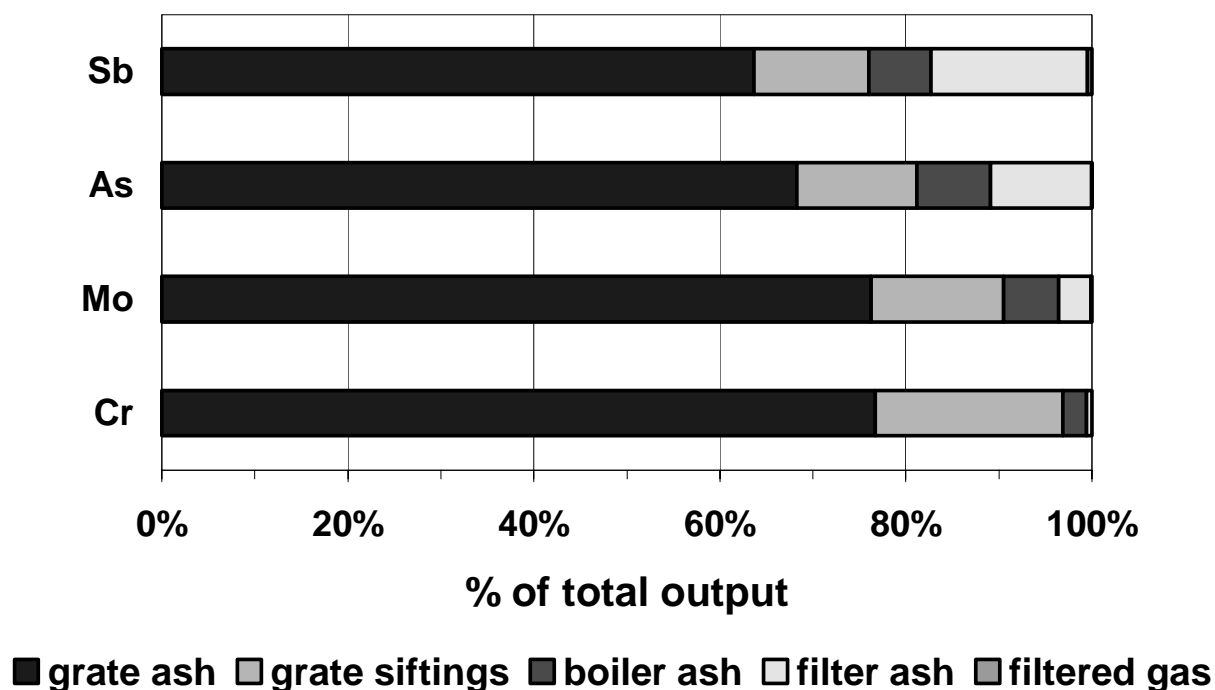


**Figure 5.2:** Percent partitioning of the elements (campaign average)

*Table 5.9* shows the partitioning data and the transfer factor (averaged values over the whole campaign) for the four metals.

As mentioned in *chapter 2*, the transfer factor is an essential element for the evaluation of the fate of metals in municipal solid waste incineration. It is defined as the fraction of the inventory of an

element that exits the combustion chamber along with the flue gas. In the case of the present experimental data, the transfer factor was calculated by addition of the inventory fractions found in the fly ashes -i.e. in the boiler ashes and in the filter ashes- and in the impinger absorbing solutions (columns labeled 3, 4, and 5 in *table 5.9*, respectively).

Data for calcium are included in *table 5.9*, since calcium is assumed to represent the behavior of ash matrix constituents and will hence be used as a reference element for standardization purposes. This will be discussed more in detail later on.

**Table 5.9:** Partitioning data and transfer factor of the elements (campaign average)

element	grate ash (1)	grate siftings (2)	boiler ash (3)	filter ash (4)	filtered gas (5)	transfer factor (3+4+5)
Sb	63,7%	12,3%	6,7%	16,8%	0,5%	24%
As	68,5%	12,9%	8%	10,6%	0,03%	18,6%
Mo	76,3%	14,2%	5,9%	3,5%	0,1%	9,5%
Cr	76,7%	20,1%	2,6%	0,6%	0,01%	3,2%
Ca	85,8%	11,4%	2,6%	0,2%	0,01%	2,8%

The elements can be divided in two groups on the base of their transfer out of the combustion chamber, as volatile (As and Sb) or lithophilic (Cr and Mo). It was surprising to see a rather limited transfer factor for arsenic, which is normally well-known for its volatility. This should be interpreted as a further evidence of its speciation in form of stable arsenates. These results are confirmed by other literature works [*Angenend and Trondt, 1990; Vehlow, 1993; IAWG,1997; Vehlow et al, 1997; Watanabe et al, 1999*].

The effect of the air ratio variation on the transfer factor of the elements is depicted in *figure 5.3*. Only the spiked incineration tests are considered for a better overview. The results are obviously similar for the reference runs. The data values are reported in *table 5.10*.

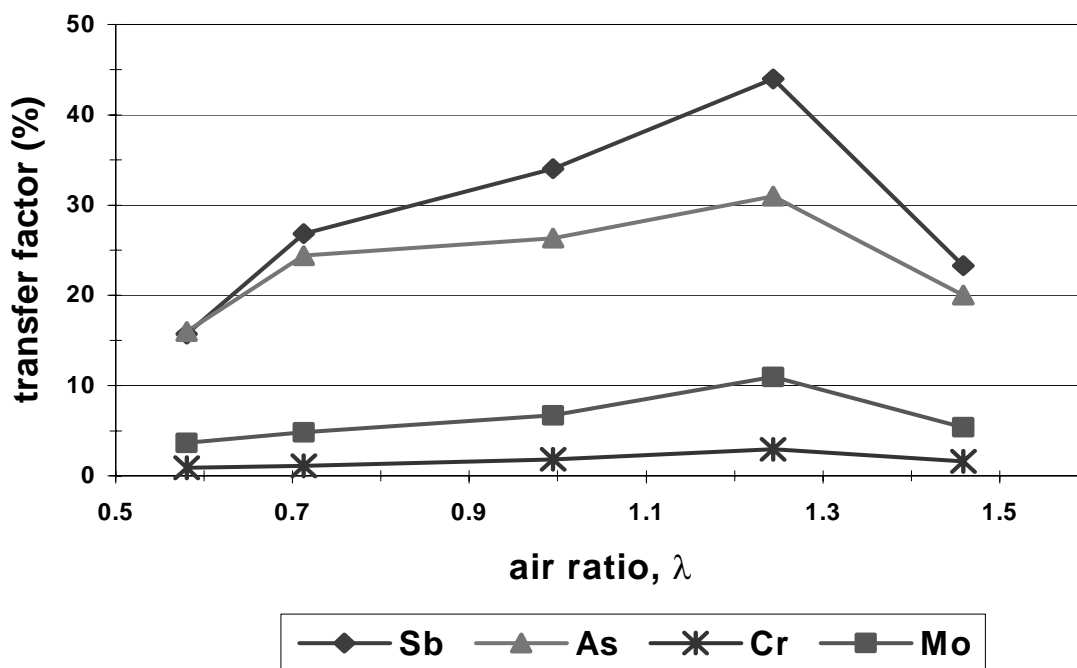


Figure 5.3: Transfer factor (as % of the inventory)

Table 5.10: Transfer factor of the elements (as % of the inventory, spiked runs)

	Sb	As	Cr	Mo	Ca
$\lambda = 0,6$	16	16	1	4	1
$\lambda = 0,7$	27	24	1	5	1
$\lambda = 1,0$	34	26	2	7	2
$\lambda = 1,25$	44	31	3	11	4
$\lambda = 1,5$	23	20	2	5	3

This data presentation reflects the amount of an element which is transferred out of the combustion chamber (i.e. the inventory fractions found in the boiler ashes, in the filter ashes and in the impinger solutions). Hence it includes both the fraction which is transferred by mechanical entrainment as well as the fraction which is volatilized to the gas phase.

For this reason, the interpretation of these data is influenced by the fact that the residue mass flows varied considerably between each run. A maximum in the transferred amount of an element does not necessary imply a maximum in element volatility. For example, the maximum values in the curves exhibited for  $\lambda = 1,25$  are most likely caused by the high mechanical fly ash transfer recorded on day 2 (runs 3 and 4, see *table 5.6*). Variations of the residue mass flows (especially for the fly ashes) are normal and depend on the plant operation as well as on the nature of the solid waste feed.

To separate the effect of mechanical entrainment, the transfer factor of the elements was standardized relatively to the calcium transfer. Calcium was chosen as a reference element because

it is one of the main constituents of the ash matrix and does not form any volatile compounds and hence it is assumed to be transferred out of the combustion chamber solely by means of mechanical entrainment [IAWG, 1997].

The standardized transfer factor was calculated using the following equation:

$$TF_{stand} = \text{element TF (\%)/calcium TF (\%)} \quad [Eq.5.9]$$

The results are shown in figure 5.4. Table 5.11 shows the data values.

**Table 5.11:** Transfer factor of the elements (standardized to calcium transfer, spiked runs)

	<b>Sb</b>	<b>As</b>	<b>Cr</b>	<b>Mo</b>	<b>Ca</b>
$\lambda = 0,6$	19	20	2	5	1
$\lambda = 0,7$	22	20	2	4	1
$\lambda = 1,0$	14	11	1	3	1
$\lambda = 1,25$	11	8	1	3	1
$\lambda = 1,5$	8	7	1	2	1

A standardized transfer factor of about 1 indicates that an element mainly exits the combustion chamber by means of mechanical entrainment, whereas a high standardized transfer factor shows that the element volatilized out of the combustion chamber in form of volatile compounds. Obviously calcium has a standardized transfer factor of 1.

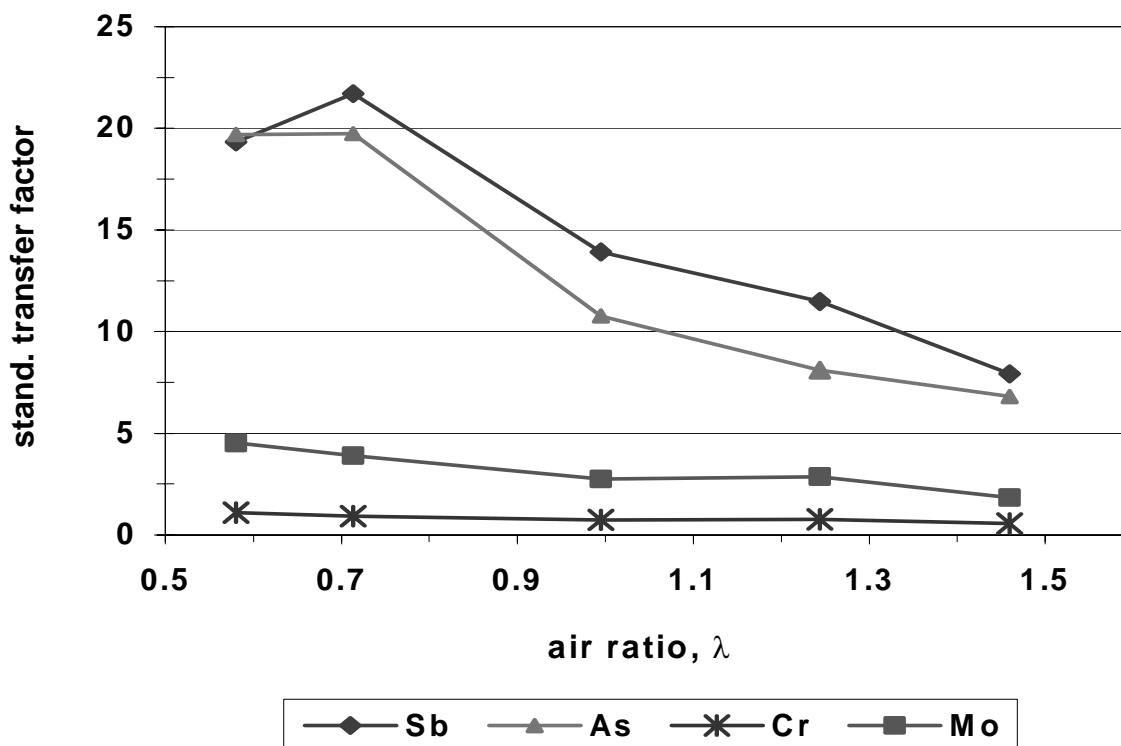


**Figure 5.4:** Transfer factor standardized to calcium transfer

The analysis of the standardized transfer factor (*figure 5.4*) showed that the air ratio variation had only a very slight effect on chromium volatility (which is very low in all runs), and a rather moderate effect on molybdenum. Instead, the effect on arsenic and antimony was very strong. A reduction of the air ratio from the reference value 1,5 to 0,7 implies an increase of the element transfer by a factor exceeding two.

This important fact can be interpreted by considering two facts: on one side, the presence of high amounts of oxygen in the fuel bed allowed the formation of thermally stable oxides (for example  $\text{Sb}_2\text{O}_4$ ) and oxyanionic salts (arsenates and antimonates), as discussed in *chapter 3*.

On the other hand, if the temperature profiles of *figure 5.1* are considered, it is evident that the less steep the temperature profile, the longer is the residence time of the fuel bed at high temperature.

If the total fuel bed residence time on the grate amounts to approximately 50 minutes and the grate length to 3,2 meters, then the fuel bed velocity can be estimated. Hence, from the temperature profiles it can be estimated, for example, that the residence time at temperatures greater than  $800^\circ\text{C}$  will be twice as high on day 4 ( $\lambda = 0,7$ ) as in the case of day one ( $\lambda = 1,5$ ).

These are only first estimates and obviously an exact mathematical integration of the temperature profiles would be needed for a more exact analysis. Moreover, a further insight in the kinetics of the fuel bed reactions which control metal volatilization would be needed. Nevertheless, these experimental results make clear that the time available for volatilization reactions was markedly higher in the case of a broader temperature profile (such as for  $\lambda = 0,7$ ) and thus the overall element transfer was increased. On the last day ( $\lambda = 0,6$ ), the transfer started decreasing again. The fuel ignition took place when the fuel was already near the end of the grate and the residence time was not sufficient to complete the reactions, as previously discussed in *section 2*.

## 5.5 Condensation on fly ashes

The sampling of boiler ashes at different locations (and temperatures) along the flue gas cooling path allows to gather information on condensation mechanisms of those chemical species that were transferred out of the combustion chamber by means of volatilization processes. The collected fly ash samples cover a temperature range from about  $800^\circ\text{C}$  down to  $190^\circ\text{C}$  (filter ashes).

For the same reasons mentioned in the previous section, the inventory fractions in the fly ashes are standardized to the calcium transfer to separate the effect of mechanical entrainment. Furthermore, considering the pure element concentration in the single residues might be misleading, since the mass of the fly ash increases as a consequence of surface condensation phenomena.

In the following diagrams, the data are presented in form of the enrichment factor of the metals related to the calcium transfer, i.e.:

$$EF = \frac{\% \text{ of element inventory in dust fraction}}{\% \text{ of calcium inventory in dust fraction}} \quad [Eq.5.10]$$

The values for the accumulated enrichment factors of the elements are listed in *table 5.12* (campaign average values). As in the case of the standardized transfer factor, calcium obviously shows an enrichment factor of 1. The temperature values indicates the sample collection temperature (flue gas temperature at the sampling point). Temperatures in the range from 800°C to 650°C refer to the four boiler ash fractions. The sampling point at 190°C refers to the filter ashes (isokinetic sampling system, see *section 4.2*).

**Table 5.12:** Accumulated enrichment factor of the elements (campaign average)

	800 °C	750 °C	700 °C	650 °C	190 °C
<b>EF<sub>Sb</sub></b>	3,3	7,6	12,2	18,85	91,5
<b>EF<sub>As</sub></b>	3,8	9,4	15,2	19,1	64,45
<b>EF<sub>Mo</sub></b>	2,8	5,2	7,75	10,0	25,04
<b>EF<sub>Cr</sub></b>	1,1	2,3	3,4	4,5	6,9
<b>EF<sub>Ca</sub></b>	1	1	1	1	1

Similarly to the standardized transfer factor, an enrichment factor close to 1 (no enrichment) is typical for lithophilic elements (high mechanical entrainment), whereas a high enrichment factor is typical for volatile elements that evaporate and subsequently condensate upon the fly ashes. However, these data should be interpreted only as a general tendency and not as a quantitative analysis of condensation phenomena. More detailed experimental investigation, such as particle size analysis and the determination of the specific surface of the particles, would be necessary to make a more definite assessment.

*Figure 5.5* represents the accumulated enrichment factors of the four investigated elements on the fly ashes (averaged values over the whole campaign). These data depict the condensation path of the volatilized species as they are transported by the flue gas in its cooling path through the energy recovery (boiler ashes) and air pollution control sections (filter ashes). As the flue gas cools down, the volatile species condense on the surface of the fly ashes, causing an increase in the enrichment factor.

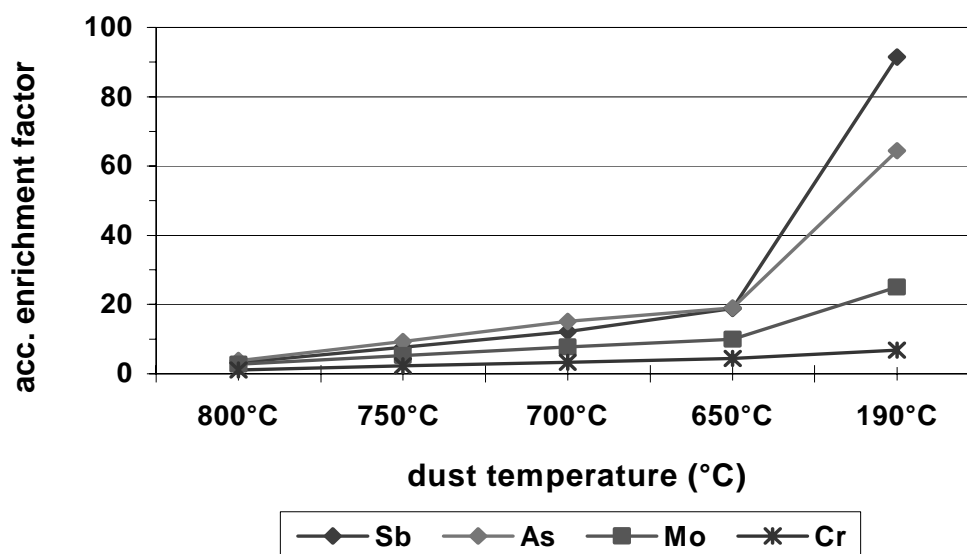


**Figure 5.5:** Enrichment of the elements on fly ashes (campaign average)

The volatile metals antimony and arsenic showed both remarkably high enrichment factors on the filter ashes (92 and 64, respectively) which indicates that volatilization out of the fuel bed probably took place by means of formation of volatile halogenated compounds.

Among the mainly lithophilic metals molybdenum can be further distinguished for its enrichment on low temperature fly ashes (accumulated enrichment factor 25), probably because of the formation of volatile halogenated compounds.

Chromium showed only a marginal enrichment (accumulated enrichment factor 7). This means that formation of volatile compounds took place only in very limited amounts (as might be the case of chromium oxychloride) or rather does not seem to take place at all.

*Figures 5.6, 5.7, 5.8, and 5.9* show the enrichment on the fly ashes of the single elements for the single spiked runs (effect of air ratio variation).

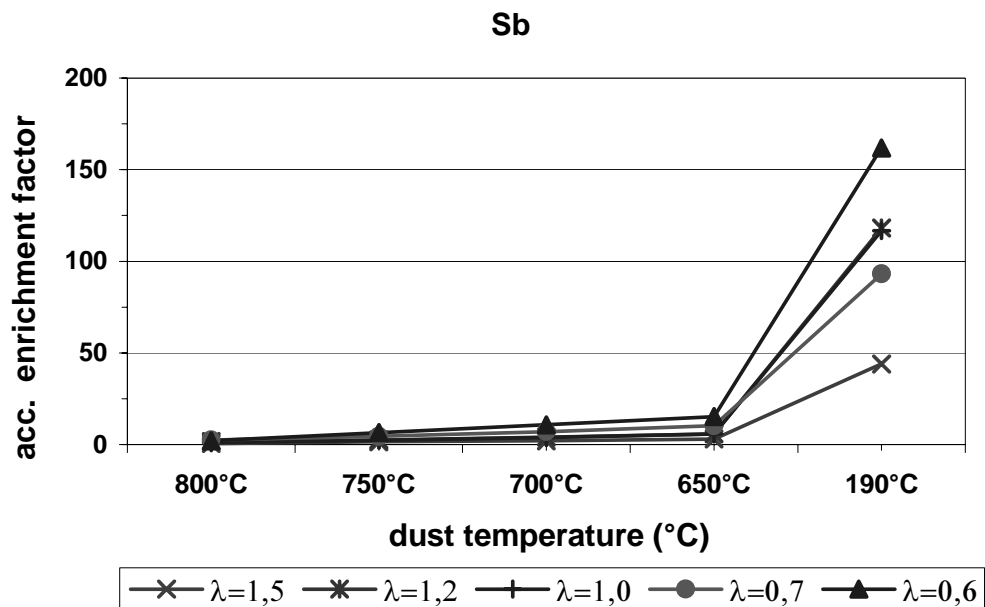


Figure 5.6: Enrichment on fly ashes of Sb

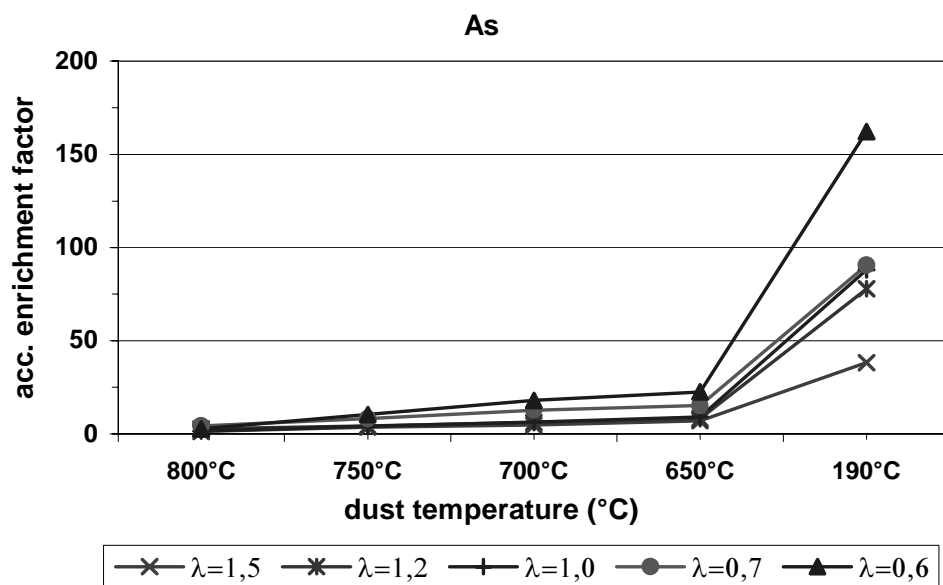
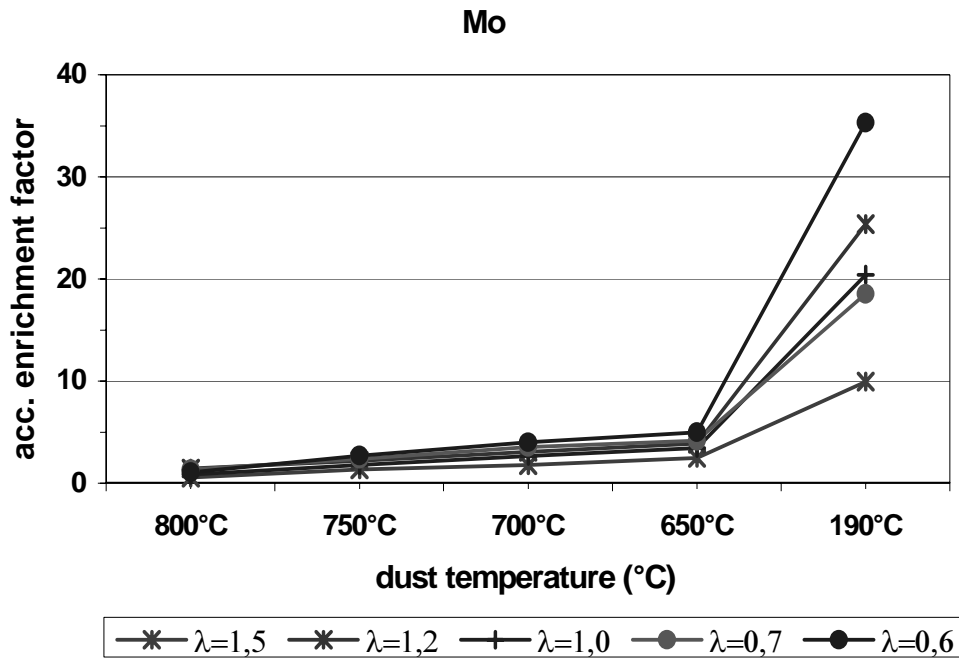
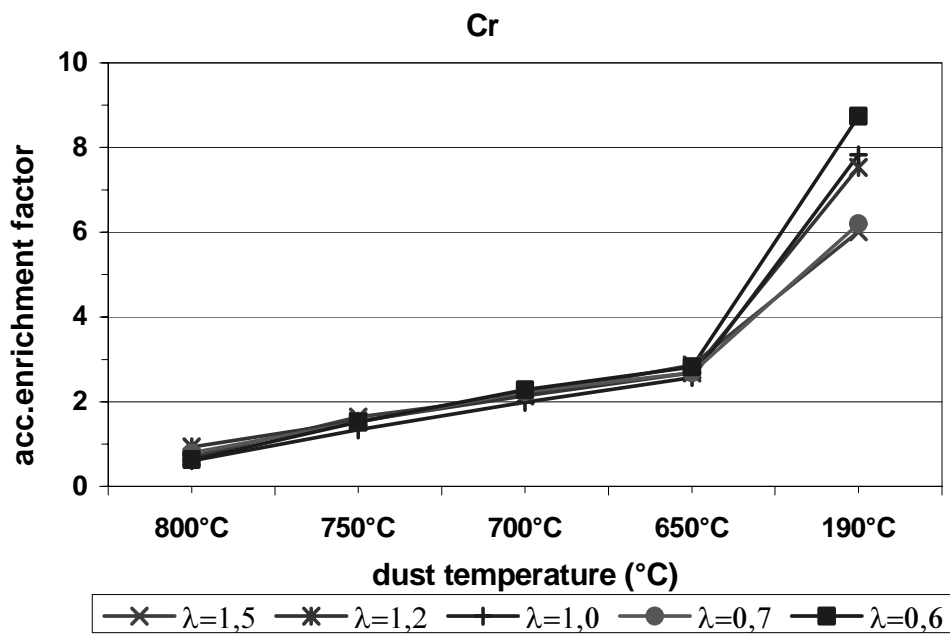


Figure 5.7: Enrichment on fly ashes of As



**Figure 5.8:** Enrichment on fly ashes of Mo



**Figure 5.9:** Enrichment on fly ashes of Cr

All elements showed an increasing enrichment factor on fly ashes with decreasing air ratio. This effect is rather limited for chromium, while it is very strong for arsenic. This is in accord with the results from the transfer factor analysis (previous section). The rather volatile behavior of molybdenum is, anyway, remarkable.

## 5.6 Filter-passing species

Table 5.13 lists the total metal concentrations in the gas sampling system (gas condensates and the two absorption solutions) for the five spiked trials. The concentrations were always near (or below) the analytical detection limit. Values for reference tests were always below detection limit and hence are not listed.

From a theoretical point of view, the volatilized metallic species should totally be condensated on the fly ash surface at temperatures below 200°C, as discussed in *chapter 2*. Thus, it is very likely that the metal concentrations analyzed in the gas condensates and in the absorbing solutions derive from fine particulate or aerosols that might slip through the particle separation system. However, the chosen detection procedure for sampling of filtered gas does not allow to distinguish between gaseous and fine particulate species. Therefore, the term filter-passing species will be used here, as no further speculation is possible on the physical state of the compounds analyzed.

**Table 5.13:** Filter-passing species ( $\mu\text{g}/\text{Nm}^3$ )

<b>Run</b>	<b>Sb</b>	<b>As</b>	<b>Mo</b>	<b>Cr</b>
$\lambda= 1,5$ ( <i>sp.1</i> )	37	3	7	5
$\lambda= 1,2$ ( <i>sp.2</i> )	74	1	14	n.d.
$\lambda= 1,0$ ( <i>sp.3</i> )	44	3	3	1
$\lambda= 0,7$ ( <i>sp.4</i> )	94	15	4	3
$\lambda= 0,6$ ( <i>sp.5</i> )	42	1	n.d.	n.d.

The low values measured for arsenic are consistent with the prediction that chlorination plays a minor role in arsenic partitioning (*chapter 2*). The only element which might be of some concern is antimony. This has been reported also by *Enders et al.* [*Enders et al.*, 1990]. However, the values listed must be regarded with a certain precaution. On one side, the numbers relate to spiked runs, so that the antimony inventory under normal conditions will be considerably lower. Second, the values are very close to the analytical detection limit and therefore in a concentration range in which the analytical error might be relevant.

Finally, it must be remembered that these samples are collected before the flue gas enters the scrubbing system. Thus, the remaining concentration of antimony in the flue gas will be removed in the first acid scrubbing stage and no stack emission should be expected.

## **Chapter 6**

### **Characterization of grate ashes**

#### **6.1 Characteristics of municipal solid waste incinerator grate ashes**

Grate ashes are the largest residue fraction in a municipal solid waste incinerator, constituting about 20 - 30% of the input mass flow and 85-95% of all residues produced during incineration [IAWG, 1997].

In full-scale plants, grate ashes are normally discarded in a quench tank and from there on a conveyor belt. For analytical reasons (balances of soluble salts), this quenching procedure is not employed for TAMARA grate ashes, which are collected directly from the bin at the end of the grate. This might result in a slightly higher ash alkalinity and pH value, as will be seen further on.

There are two ways to characterize grate ashes: by their chemical/mineralogical properties or by their behavior in an aqueous environment, which means by their leaching stability. Both characteristics are to some extent inter-correlated [IAWG, 1997]. In the present work, the grate ashes were characterized by means of leaching tests. The leaching procedures adopted have been described in *chapter 4*.

Grate ash is a complex mixture of different materials which reflects the inhomogeneity of the fuel fed to the incinerator. *Pfrang-Stotz and Schneider* distinguish three types of grate ashes: vitreous-type grate ashes, which are partly black, with a very dense structure and conchoidal fracture patterns similar to obsidian (volcanic glass). These grate ashes arise in incinerators the grate ashes of which are re-molten after incineration. The second type are the porous-type grate ashes, which are light brown, gray, or reddish in color with frequent degassing voids. These are typical for lower fuel bed temperatures. The last type of grate ashes is the most frequent and characteristic of medium waste bed temperatures and consists of microcrystalline-type grate ashes. These are very dense in structure and contain only few degassing voids. The color ranges from medium gray to black [Pfrang-Stotz and Schneider, 1995]. TAMARA grate ashes belong mainly to the second type of grate ashes and are depicted in *figure 6.1*.

A petrographic and mineralogical analysis conducted by *Eusden et al.* showed that the ash constituents can be divided in two major groups, on one side the refractory waste products, which include fragments of glass, metal, minerals, and lithic fragments that survived the incineration process, and on the other the melt products, which consist of glasses (slags) and crystalline phases. The slag fraction can be further subdivided in isotropic glasses and opaque glasses, while the

crystalline phases can be classified as complex silicates of the melilite group or complex oxides of the spinel group [Eusden et al., 1999].



**Figure 6.1:** TAMARA grate ash

From a chemical point of view, grate ashes consist mainly of oxides of the major constituents with near half of the total being silicium oxide ( $\text{SiO}_2$ ), followed, in order of abundance, by calcium oxide ( $\text{CaO}$ ), iron oxide ( $\text{Fe}_2\text{O}_3$ ), aluminium oxide ( $\text{Al}_2\text{O}_3$ ), sodium oxide, ( $\text{Na}_2\text{O}$ ), magnesium oxide ( $\text{MgO}$ ), potassium oxide ( $\text{K}_2\text{O}$ ) [Angenend and Trondt, 1990]. A more detailed survey of grate ash mineralogical and chemical composition can be found in the work of the *International Ash Working Group* [IAWG, 1997].

Table 6.1 lists the main characteristics of the grate ashes collected during the ten TAMARA incineration runs as well as the air ratio  $\lambda$  of the single runs (see chapter 5). The table contains two different carbon concentrations, the total carbon (TC), which summarizes organic and inorganic carbon, and the total organic carbon (TOC), which is the concentration of elementary and organically bound carbon. In grate ashes the inorganic carbon is present in form of carbonates and amounts typically - as long as the total carbon stays in the order of 1% - for about 50-60% of the total carbon [Hunsinger, 1999]. Hence only in the case of TC numbers exceeding 1% a separate determination of the TOC was performed.

It is evident that a reduction of the air ratio implied an increase in the total carbon content, which became remarkable in the last two runs, reaching approx. a 10-fold value compared to the reference

value. This fact can be correlated with the temperature profiles shown in *figure 5.1*. The ignition point of the fuel was shifted towards the end of the grate which implies that the time for the carbon oxidation reactions was not sufficient and a higher amount remains unburnt. In fact, in samples showing high TC values most of the carbon present was in the form of organic carbon TOC (unburnt fraction) while the inorganic carbon stays almost constant with 0,3 - 0,5%.

The values for the pH in aqueous solution were measured by putting a finely ground (<0,125 mm) grate ash sample in contact with deionized water (liquid-to-solid ratio: 20) under agitation. The values were recorded after 1 minute and 10 minutes, respectively, and give a measure of the grate ash alkalinity and reactivity. The air ratio variation did not seem to have a marked effect on the alkalinity.

**Table 6.1:** Characteristics of TAMARA grate ashes

test	air ratio, $\lambda$	TC (%)	TOC (%)	pH <sub>1 min</sub>	pH <sub>10 min</sub>
<i>ref. 1</i>	1,5	0,5	n.a.	11,7	11,7
<i>sp. 1</i>	1,5	0,5	n.a.	11,7	11,7
<i>ref. 2</i>	1,3	0,5	n.a.	10,9	11,3
<i>sp. 2</i>	1,2	0,4	n.a.	11,7	11,7
<i>ref. 3</i>	1,0	0,3	n.a.	11,8	11,8
<i>sp. 3</i>	1,0	0,4	n.a.	11,1	11,5
<i>ref. 4</i>	0,7	0,7	n.a.	11,6	11,6
<i>sp. 4</i>	0,7	1,3	1,0	11,5	11,6
<i>ref. 5</i>	0,6	5,5	5,1	10,7	11,9
<i>sp. 5</i>	0,6	3,5	3,0	11,3	11,6

n.a.: not available

*Table 6.2* lists the averaged concentrations of the elements investigated in the present work as resulting from the analysis of the TAMARA reference test grate ashes as well as other data taken from literature [*Schneider, 1986; Reimann, 1989; Angenend and Trondt, 1990; IAWG, 1997; Belevi, 1998*]. For comparison the average content in the earth's crust is included in the table (see *chapter 1*) [*Ullmann, 1997*].

**Table 6.2:** Concentrations of the investigated elements in grate ashes (mg/kg)

	present work (unspiked values)	Angenend	Belevi	Reimann	Schneider	IAWG	earth's crust
As	35	11	10	3,3	25	0,1-189	6
Sb	80		41		80	10-432	0,3
Cr	457	100	1100	655	900	23-3170	100
Mo	38		31			2,5-276	1

Of the four elements chromium can be considered to be only slightly enriched compared to the lithosphere. Arsenic shows a moderate enrichment while the enrichment of antimony and molybdenum is considerable.

## 6.2 Availability of the elements

As mentioned in *chapter 4*, the availability of an element in a residue, which is determined by the availability test AVA [NEN 7341, 1995], is assumed to be the maximum amount of an element which can be leached from a residue fraction under long-term conditions (worst-case scenario). It will in the following be expressed as the percentage of the total inventory in the respective residue fraction. *Figure 6.2* shows the availability of the elements for the five spiked incineration runs as a function of the air ratio.

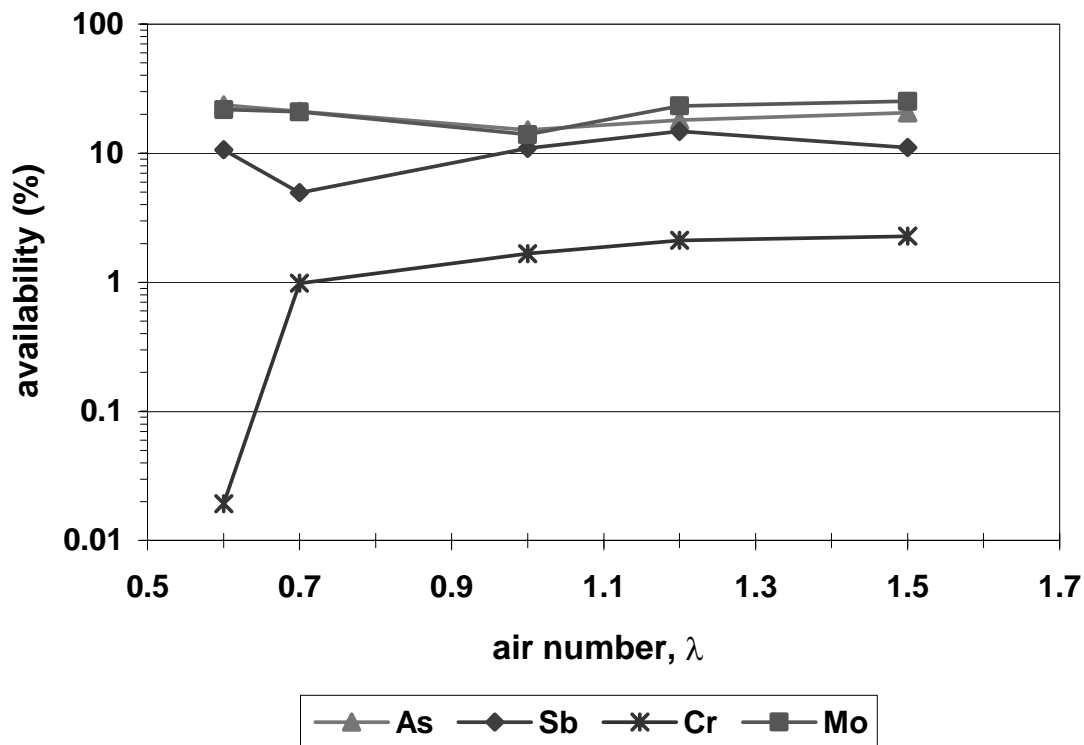


**Figure 6.2:** Availability of the elements in grate ashes

Arsenic, antimony and molybdenum showed availability values which can be considered in the normal range for most metals, between 10 and 20% of the total inventory. The dependence on the air ratio did not seem to be particularly marked. The minimum value shown by antimony on the fourth day ( $\lambda = 0,7$ ) was consistent with the increased transfer factor shown in the same incineration runs (see *chapter 5*).

Chromium, on the other hand, showed a very limited availability of a few percent only for the reference air ratio ( $\lambda = 1,5$ ). With decreasing air ratio, the availability of this element decreased gradually and then exhibited a sharp decline down to 0,02% for  $\lambda = 0,6$ . This behavior is a clear indication of the speciation of chromium in the residues: trivalent chromium compounds are mainly insoluble while hexavalent ones are characterized by high solubility (see *section 1.1.3*). The finding confirms that the formation of hexavalent compounds in the fuel bed takes place only to a very limited extent. A further evidence for this fact is the dramatic effect on the chromium availability once the air ratio reaches 0,6.

### 6.3 Regulatory leaching tests

A series of leaching tests have been carried out as prescribed by the residue management regulations of different European countries. In particular, the German DEV S4 [DIN 38414, 1984], the Swiss TVA [Bundesamt für Umweltschutz, 1991] and the U.S. EpTox [US EPA 1310, 1984] procedures were chosen. The test procedures are described in detail in *chapter 4*.

Figure 6.3 shows the results of the different regulatory tests and of the availability test expressed as % of the grate ash inventory (campaign average values).

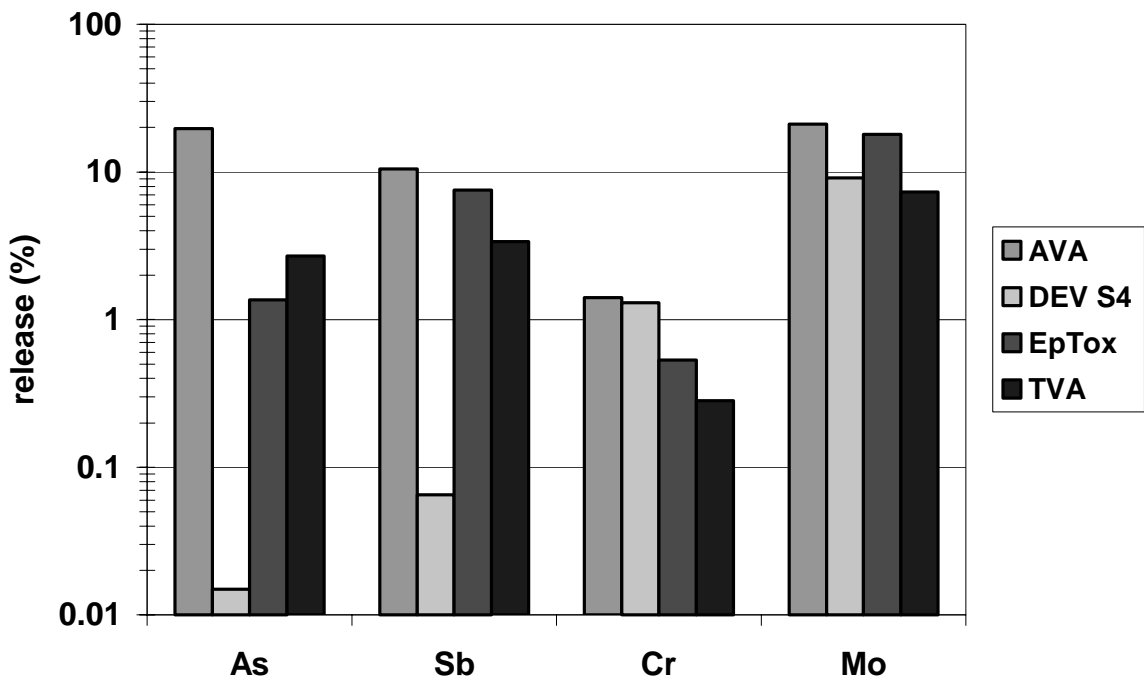


Figure 6.3: Regulatory leaching tests (averaged values)

It is striking to note the differences in the results of the various procedures for the same samples. For example, the German leaching procedures gave extremely low values for arsenic and antimony,

with the subsequent possibility of an underestimation of the mobility potential in reality. This is caused by the rather strong dependence of the leachability from the leachate pH for these two elements, as will be discussed in the next section. On the other hand, the utilization of acetic acid as a leaching medium (EpTox procedure) could imply the formation of soluble organic complexes, thus overestimating the actual potential for leaching. This might be the case for antimony and molybdenum.

For chromium the amount released during the German DEV S4 procedure is very close to the availability (1,3% and 1,4% respectively). As described for arsenic and antimony, this is probably related to the leachant pH rather than to the nature of the leachant. Chromium shows a relatively weak dependence on pH, as will be discussed in the next section.

The leachate samples obtained by the German DEV S4 leaching test were analyzed for chromium speciation to determine the fraction of hexavalent species of the total released Cr. The analytical procedure described in *chapter 4* delivered the results listed in *table 6.3*.

The Cr(VI) concentrations analyzed in the grate ashes of the reference tests were too close to the detection limit to be considered reliable and will hence not be considered here. However, the Cr<sub>tot</sub> concentrations were in the order of magnitude of 10-30 µg/l. These concentration values comply with the regulation limit for the German Class I landfill of 50 µg/l [TA Siedlungsabfall, 1993].

The results of the chromium speciation analysis for the spiked runs give strong evidence for the fact that, even if the total chromium amount released from the grate ashes can be considered rather limited (a few percent of the total inventory), yet this amount may consist nearly entirely of the toxic hexavalent chromium.

**Table 6.3:** Hexavalent chromium concentrations in DEV S4 leachates (spiked runs)

air ratio, $\lambda$	Cr <sub>tot</sub> , µg/l	Cr(VI), µg/l	Cr(VI)/Cr <sub>tot</sub> ratio
1,5	1805	1799	0,99
1,25	2216	1898	0,85
1,0	1841	1841	1
0,7	787	777	0,98
0,6	10	10 (d.l.)	n.a.

n.a.: not available

The correlation between air ratio and chromium leaching is evident. This result is of great practical importance, as it suggests the idea that chromium release from grate ashes could be controlled by primary air ratio reduction. On the other hand, the effect of a reduced air ratio on other ash characteristics (for example TOC) must be considered, too, and hence a process optimization is

necessary. More investigation is also required on other important process parameters which might influence chromium leaching behavior, such as the oxygen partial pressure in the furnace (flue gas recirculation), and the distribution of primary air below the grate (air staging).

Another important aspect to be considered is that TAMARA grate ashes are collected in dry form, i.e. with no quench stage. This might have a direct influence on the chromium concentrations in the leachates since a large part of the chromium release can be assumed to take place on account of wash-off processes (as will be discussed in *section 5*).

Thus, if the grate ash is discarded in a quench tank, the chromium concentration in the leachates can be expected to be lower. At the same time the quench water should exhibit higher chromium concentrations. This is confirmed by former investigations carried out at the *Institute for Technical Chemistry - Division of Thermal Waste Treatment [Wiese, 1996]*. A possible treatment option for the quench water could be the recirculation and its reutilization in the first stage of a wet flue gas cleaning system (with subsequent neutralization and metal precipitation). Furthermore, the possibility of the reduction of the chromium release by means of a separate grate ash washing step should be considered, too. Such secondary treatment, however, increases the cost of waste incineration to a greater extent than the washing in the quench tank.

Although these results were mainly obtained from artificially elevated chromium concentrations in the fuel (using compounds which may even not model the typical chemical speciation in municipal solid waste) they indicate nevertheless a potential environmental risk associated with this element and a need for further investigation.

#### **6.4 Effect of leachate pH on leaching behavior**

The pH of the leaching system is one of the dominant factors controlling the release of an element from incineration residues. The data gathered by means of the pH-stat leaching tests (see *chapter 4*) allow to point out the release pattern of the elements as a function of the leachate pH.

*Figure 6.4 and 6.5* show the results for arsenic and antimony, respectively. The trend of these two elements is typical for anionic species. Metallic cations usually show a maximum release in an acid environment and a minimum solubility in the low alkaline range. Anionic species, on the contrary, show a weaker dependence from the pH and have a maximum release in the neutral range [*Paoletti et al, 2001*].

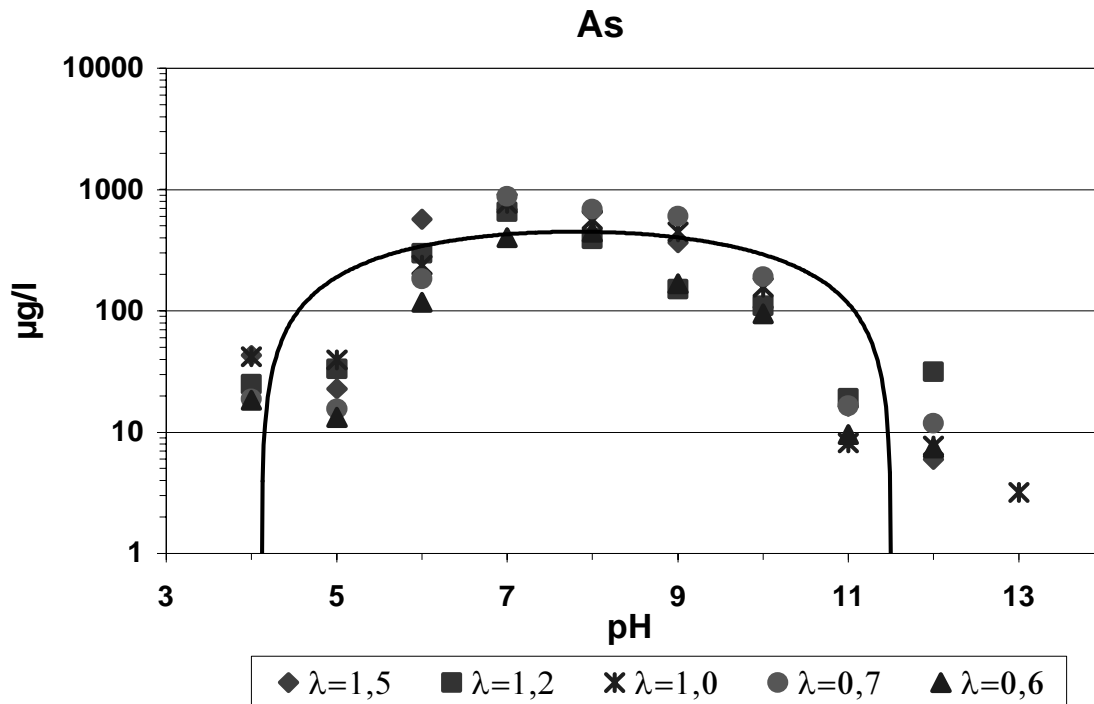


Figure 6.4: Leaching of As as a function of pH ( $\lambda$ : primary air ratio)

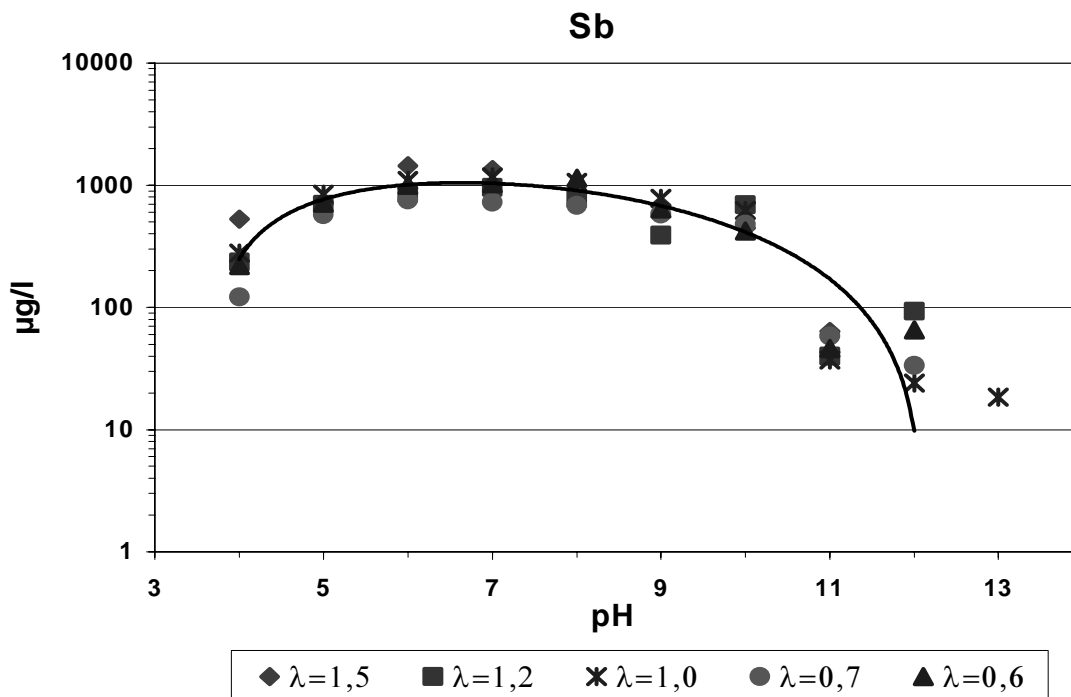


Figure 6.5: Leaching of Sb as a function of pH ( $\lambda$ : primary air ratio)

**Arsenic** showed a very strong dependence on the pH, decreasing quickly to values around the detection limit in the strongly acid and alkaline pH range. This behavior is documented also by other authors [Carbonell-Barrachina et al., 1999].

**Antimony** follows a very similar trend, even if the dependence on the pH is not as marked as for arsenic. Meima and Comans [Meima and Comans, 1998] point out that the leaching behavior of antimony could be mainly controlled by sorption processes. Since the affinity of oxyanions for oxide surfaces increases with decreasing pH, these elements might undergo sorption to amorphous iron and/or aluminium hydroxides at low pH.

On the other hand, at alkaline pH, the leaching of these elements might be controlled by a mechanism in which the respective oxyanions are incorporated in crystal structures by substitution of other anions. In particular, ettringite ( $\text{Ca}_6\text{Al}_2(\text{SO}_4)_3(\text{OH})_{12}\cdot 26\text{H}_2\text{O}$ ) has been shown to act as a host for various trace elements and oxyanions in particular [Kumarathasan et al, 1990; McCarthy et al., 1992; Gougar et al., 1996]. Ettringite can only persist at alkaline pH and is supposed to play a crucial role in controlling the grate ash pH [Meima and Comans, 1997]. Thus, a consequence of oxyanions incorporation by ettringite structures is the possibility of a delayed release after residue aging when carbonation and hydration processes have lowered the pH value from originally 11-13 to about 8-10 [Meima and Comans, 1993].

Figures 6.6 and 6.7 show the results of the pH-static tests for chromium and molybdenum, respectively.

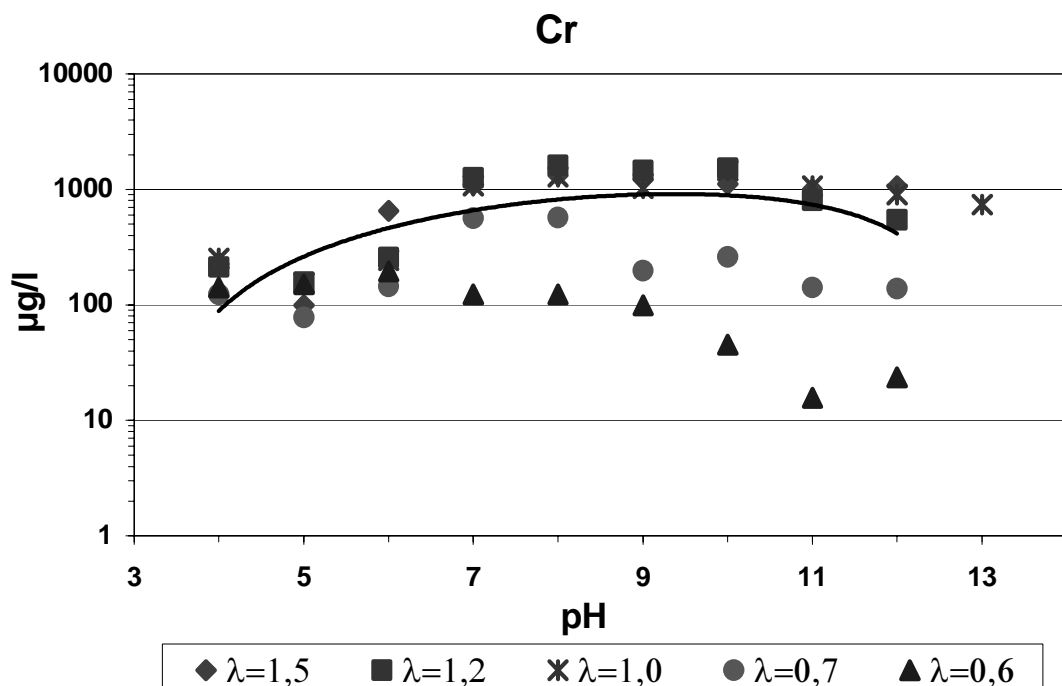


**Figure 6.6:** Leaching of Cr as a function of pH ( $\lambda$ : primary air ratio)

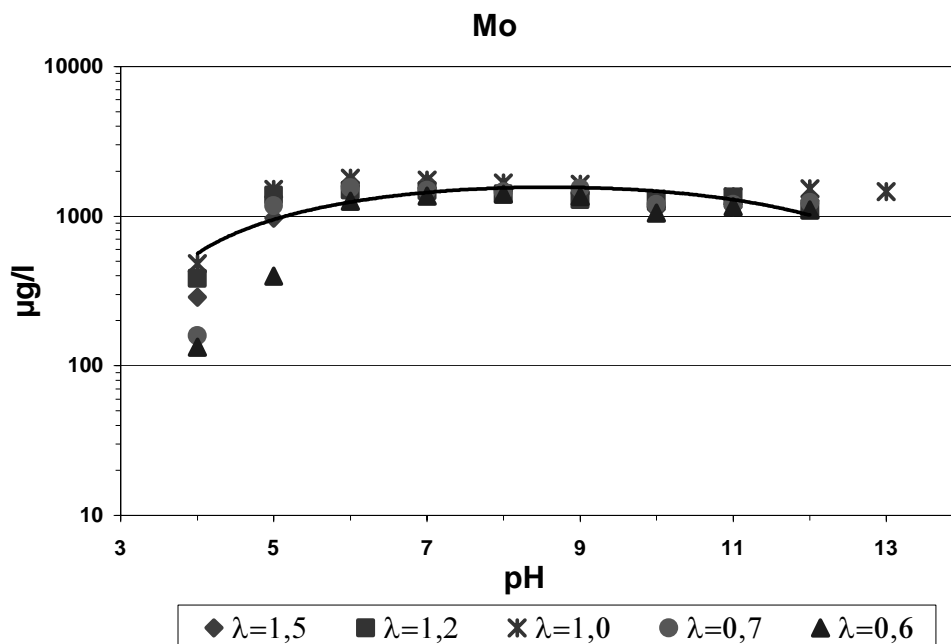


**Figure 6.7:** Leaching of Mo as a function of pH ( $\lambda$ : primary air ratio)

These two elements showed a much weaker dependence on pH than arsenic and antimony. The **chromium** release decreased for acid pH values. This would confirm the speciation of chromium as chromate ion in the leachates since the oxyanions could be sorbed to Fe/Al-hydroxide surfaces by a similar mechanism as for arsenic and antimony.

The strong effect of the air ratio ( $\lambda$  values 0,7 and 0,6) has been already discussed in *section 6.2* and gives evidence of the hexavalent speciation of chromium in the leachates. On the other hand, the moderate effect of the pH on chromium release for alkaline values could imply that the leaching behavior is solubility controlled by solid phases such as barium chromate  $\text{BaCrO}_4$ , as pointed out by Fällmann [Fällmann, 2000].

**Molybdenum** (figure 6.7) showed the weakest dependence on the pH. As has been pointed out by several other authors, the leaching mechanism of molybdenum is very likely to be controlled by the solubility of calcium molybdate  $\text{CaMoO}_4$  (powellite) [Coman et al., 1993; Johnson et al., 1996].

### 6.5 Time resolution of leaching

The column leaching test [NEN 7343, 1995] can be used to get information about the time resolution of the leaching process. The accumulated liquid-to-solid (L/S) ratio simulates the time range. The availability of the element is represented in the graphs as a horizontal line.

Figure 6.8 shows the results of the column leaching tests carried out on the TAMARA grate ashes. The time resolution of the leaching process was not significantly affected by air ratio variation.

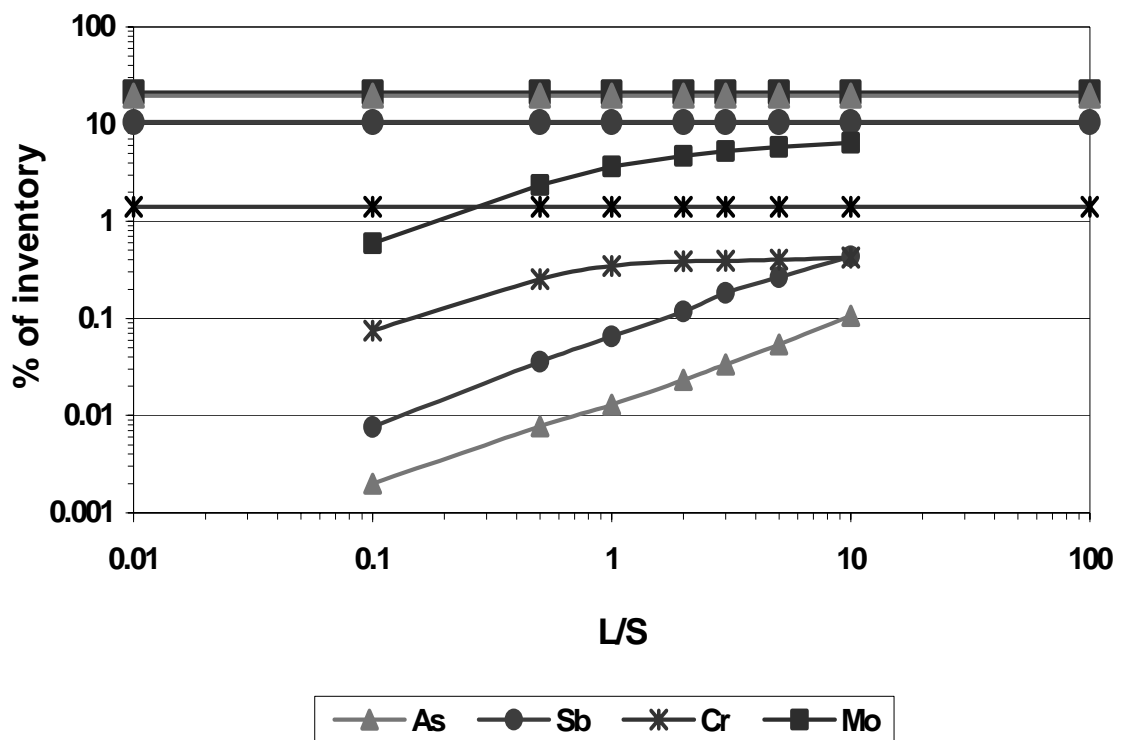


Figure 6.8: Column leaching test (averaged values)

**Arsenic** and **antimony** showed a release trend which is typical for most metals, i.e. a gradual release with time and a total release which is far below the element availability. The leaching of these elements from the grate ashes can thus be assumed to be controlled primarily by means of diffusion processes.

**Chromium** and **molybdenum**, on the other side, showed a very high release in the first leaching fractions, with concentrations in the leachates of up to 20-40 mg/l, followed by a transition to a slope of nearly zero.

This suggests that the elements might partly be adsorbed on the surface of the ash particles and are easily washed off as soon as the first leachant gets in contact with the material [IAWG, 1997]. Moreover, the released amount is relatively close to the total available amount.

## **Chapter 7**

### **Characterization of fly ashes**

#### **7.1 Characteristics of municipal solid waste incinerator fly ashes**

Generally, the term fly ashes is used to indicate all solid particles which are transported along with the flue gas out of the combustion chamber. In this sense the term will be used.

However, the cooling path of the flue gas is long and spreads over a wide range of temperatures, so that the residues will be very different in nature and composition depending on the location of their deposition. Thus, to avoid confusion it is better to follow the recommendation of the *International Ash Working Group [IAWG, 1997]* and refer to the various residue streams using the name of the unit they are collected in. Therefore, the first distinction to be made is between boiler ashes and filter ashes. The ashes sampled isokinetically downstream of the boiler will be in the following - to distinguish them from filter ashes - addressed as fly ashes, too.

The characterization of boiler ashes is a difficult task because the sampling of this kind of residue is strongly dependant on the geometry of the heat recovery unit. Sometimes a representative sampling might be impossible (for example if the boiler banks are located directly above the furnace and the ashes are discharged into the grate ash quench tank). The peculiar geometry of the TAMARA radiation boiler (*figure 4.1*) allows to collect samples at four different deposition temperatures, so that differences in the composition can be pointed out.

Typically ash from the heat recovery system of modern incinerators is a fine granular material, ranging from black-gray to reddish-beige in color. The particle size ranges from sub-micron to greater than 400  $\mu\text{m}$  in diameter. In some cases much larger chunks of boiler ash can be observed. These chunks are formed on the boiler walls or tubes by agglomerated particles and condensed flue gas constituents which form a hard, sometimes rock-like material [*IAWG, 1997*].

The chemical composition of the boiler ashes and especially their pH value are strongly influenced by the exposure time of the residues to the flue gas stream. Acid components of the raw gases like sulphates and chlorides might condense upon the surface of the ash particles forming an outer layer. Sorption of sulfur dioxide ( $\text{SO}_2$ ) in heat recovery ashes is a more important reaction than sorption of chlorides, since chlorides generally have a lower condensation temperature. If the exposure time before ash collection is long enough to allow sulphatation processes, then the residues can be neutral to mildly acidic in nature, even if generally boiler ashes are expected to be highly alkaline. The degree of sulphatation will also greatly influence the acid neutralization capacity of the ash [*IAWG, 1997*].

Filter ashes, on the other hand, appear as very fine, dusty materials with practically no water content. The color may vary from almost white through various shades of gray, depending on the combustion efficiency. Since the dedusting units usually have a well-defined operation temperature range (usually about 200°C), chemical and mineralogical characteristics of filter ashes can be better defined than those of boiler ashes and literature data can be more easily compared. Besides, great variations in residue nature can be expected depending on the conception of the whole air pollution control section (wet or dry gas cleaning, sorbent injection etc.).

The pH of filter ashes is normally alkaline to highly alkaline. However, the alkaline core of the filter ash is often coated by sorbed acidic condensation products (e.g. chlorides) the amount and nature of which depend on the temperature in the dedusting unit and on the exposure time, as previously seen for the boiler ashes. In some cases filter ashes generate an initially acidic pH when contacted with water, after which the pH gradually increases to an alkaline level. In other cases the amount of alkaline material is insufficient to neutralize the acidic condensation products and a neutral or slightly acidic pH is obtained [IAWG, 1997].

*Hundesrügge* conducted a mineralogical analysis on filter ashes of four different German municipal solid waste incinerators and found that the main mineralogical phases present were: amorphous phases, residual carbon (as graphite), quartz (SiO<sub>2</sub>), halite (NaCl), sylvine (KCl), anhydrite (CaSO<sub>4</sub>) and in one case portlandite (Ca(OH)<sub>2</sub>) and calcium chloride (CaCl<sub>2</sub>) [Hundesrügge, 1990] .

Table 7.1 lists the main chemical composition of boiler and filter ashes, as reported by *Angenend and Trondt* [Angenend and Trondt, 1990]. Compared to the grate ashes (see chapter 6), the iron and silicium content is lower while the content in deposited species from the raw gas (sulphur and chlorine) is markedly higher (in the grate ashes S and Cl content amounted to 0,3% and 0,1%, respectively).

**Table 7.1:** Chemical composition of boiler and filter ashes [Angenend and Trondt, 1990]

compound/element	boiler ash (%)	filter ash (%)
SiO <sub>2</sub>	39 - 58	35 - 42
CaO	11 - 13	12 - 15
Al <sub>2</sub> O <sub>3</sub>	9 - 12	11 - 16
Fe <sub>2</sub> O <sub>3</sub>	4 - 6	4 - 6
K <sub>2</sub> O	2 - 3	3 - 6
MgO	1,3 - 1,6	1,5 - 1,8
Na <sub>2</sub> O	1,2 - 1,9	1,5 - 4,1
S	2,1 - 2,5	1,8 - 3,0
Cl	1,5 - 1,7	2,6 - 5,0

Table 7.2 shows the concentrations of the four investigated elements as resulted from the chemical analysis of TAMARA boiler ashes (averaged unspiked data), compared with data taken from

literature [Schneider, 1986; Reimann, 1989; Angenend and Trondt, 1990; IAWG, 1997; Belevi, 1998] and with the concentration in the lithosphere [Ullmann, 1997]. For a better comparison with literature data, the column labeled as "present work" documents the concentration data in the entire boiler ash stream, that means they are a representative accumulation of the four separately sampled ashes. The slightly higher values analyzed in the TAMARA boiler ashes in respect to some literature data may be caused by deposits formed on the boiler walls during the spiked runs which might have fallen down in a later time thus causing a partial contamination of the unspiked samples ("memory effect"). Table 7.3 shows the analogous data for the filter ashes.

**Table 7.2:** Concentrations of the investigated elements in boiler ashes (mg/kg)

	<b>present work</b> (unspiked values)	<b>Angenend</b>	<b>Belevi</b>	<b>Schneider</b>	<b>IAWG</b>	<b>earth's crust</b>
As	35	23 - 41	17	30	20 - 60	6
Sb	227		510	190	150-350	0,3
Cr	379	200 - 250	1200	800	200-800	100
Mo	45		24			1

**Table 7.3:** Concentrations of the investigated elements in filter ashes (mg/kg)

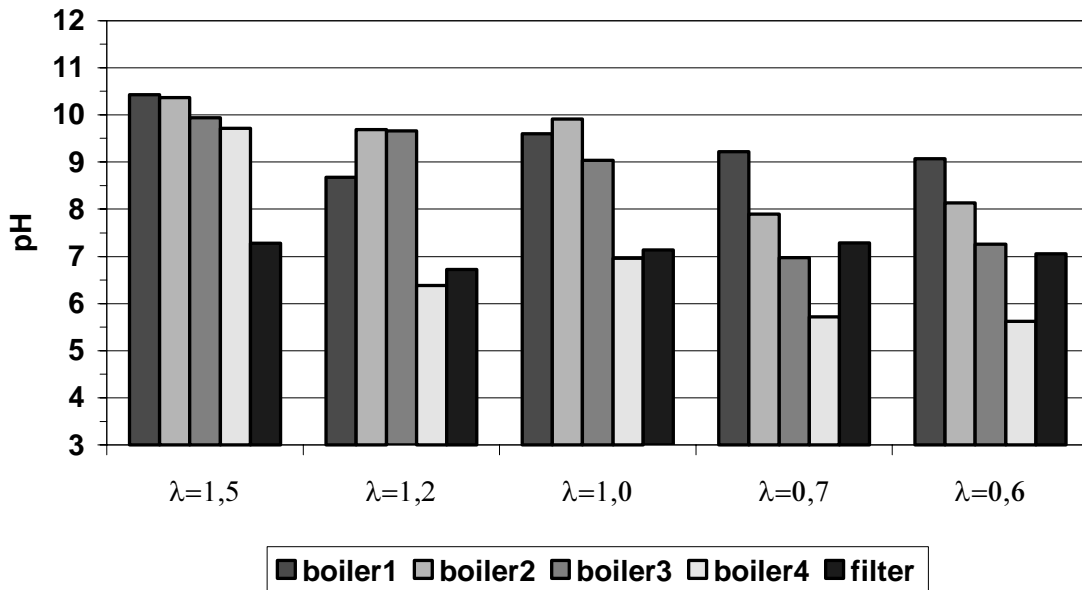
	<b>present work</b> (unspiked values)	<b>Angenend</b>	<b>Reimann</b>	<b>Belevi</b>	<b>Schneider</b>	<b>IAWG</b>	<b>earth's crust</b>
As	102	40 - 90	100	29	65	40-120	6
Sb	665			810	450	300-800	0,3
Cr	236	155 - 255	450	760	1000	100- 1000	100
Mo	60			25			1

Table 7.4 shows the values for the total carbon content (TC) of the TAMARA boiler and filter ashes, expressed as weight percent (daily averages). The low total carbon content, as discussed already in chapter 6, is an indicator for good combustion efficiency. TAMARA incineration residues generally show an excellent burnout with TC values always less than 0,05% [Merz et al., 1995].

**Table 7.4:** Total carbon content of boiler and filter ashes (%)

day	air ratio, $\lambda$ (daily average)	sample	TC (%)	sample	TC (%)
1	1,5	boiler 1	0,04	filter	0,03
		boiler 2	0,03		
		boiler 3	0,02		
		boiler 4	0,05		
2	1,3	boiler 1	0,03	filter	0,03
		boiler 2	0,02		
		boiler 3	0,02		
		boiler 4	0,02		
3	1,0	boiler 1	0,02	filter	0,04
		boiler 2	0,02		
		boiler 3	0,01		
		boiler 4	0,01		
4	0,7	boiler 1	0,02	filter	0,06
		boiler 2	0,02		
		boiler 3	0,01		
		boiler 4	0,01		
5	0,6	boiler 1	0,01	filter	0,05
		boiler 2	0,01		
		boiler 3	0,01		
		boiler 4	0,01		

Figure 7.1 shows the pH values of the fly ashes as measured from the agitated slurry in a L/S ratio 1:20 after 10 minutes. The terms "boiler1", "boiler2" etc. refer to the sampling location in TAMARA (see chapters 4 and 5).



**Figure 7.1:** pH values of the fly ashes (spiked runs)

The filter ashes exhibited a neutral pH value throughout the whole incineration campaign. This is very likely caused by the relatively long exposure time to the acid flue gases. The boiler ashes, on the contrary exhibited varying pH values, ranging from alkaline to neutral and in some cases weakly acidic. The pH values decreased with the deposition temperature, which confirms that the sulphatation process occurs in the last part of the radiation boiler. Furthermore, the pH values seem to follow a decreasing trend with decreasing air ratio.

## 7.2 Availability of the elements in the fly ashes

Figure 7.2 depicts the availability of **arsenic** from the TAMARA boiler and filter ashes (spiked runs). The procedure for the determination of the availability of the metals is described in *chapter 4*.

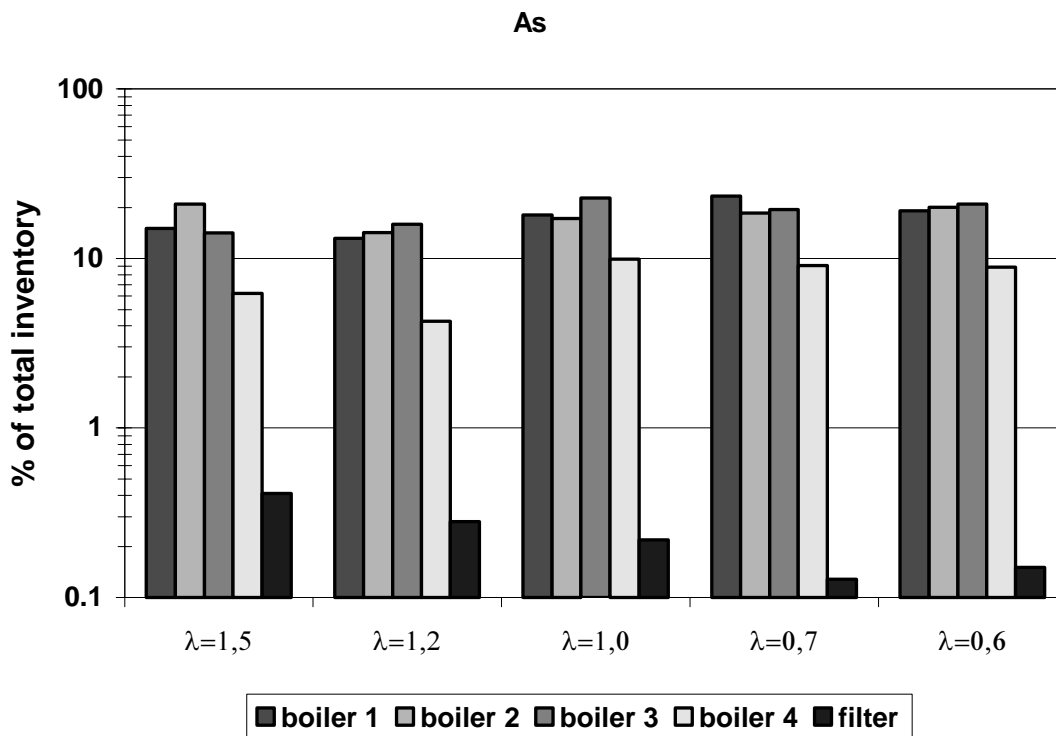


**Figure 7.2:** Availability of As from boiler and filter ashes ( $\lambda$ : air ratio)

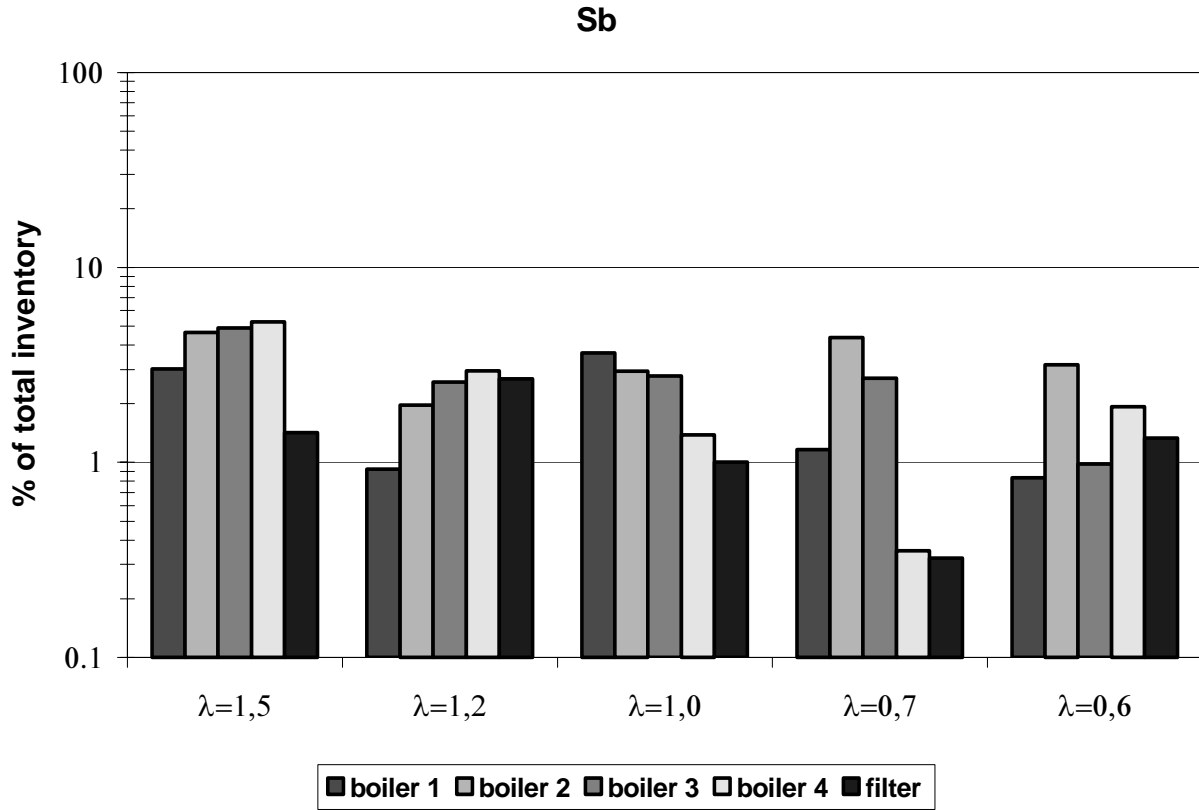


**Figure 7.3:** Availability of Sb from boiler and filter ashes ( $\lambda$ : air ratio)

The availability of arsenic from the first three boiler ash fractions (boiler 1, boiler 2, boiler 3) was in the same order of magnitude as that of the grate ashes (10-20%) and seemed to be rather independent from the air ratio variation.

Things started looking differently for the low temperature boiler ashes (boiler 4), where the availability decreased to values between 5-10% and dropped then dramatically to values below 1% for the filter ashes. Also in this case a decreasing trend with decreasing air ratio seemed to be recognizable. The low availability of arsenic in the filter ashes can be probably explained by the effect of the pH on the leaching trend for filter ashes, as will be discussed in the next section.

Figure 7.3 shows the availability of **antimony** from fly ashes. Antimony exhibits a lower availability than arsenic in the grate ashes as well as in the fly ashes. Furthermore, the behavior of the different fly ash fractions seemed to be more homogenous than in the case of arsenic. The availability from boiler ashes ranged between 5-10% while the availability from the filter ashes ranged in the order of few percent only. The air ratio did not seem to have any marked effect on the availability.

**Chromium** showed a remarkable availability from the first boiler ash fractions (figure 7.4) especially for high air ratio values (up to 20%). This fact was surprising considering the low

availability exhibited by this metal in the grate ashes (less than 2%). The low-temperature boiler ashes (boiler 4) and the filter ashes showed a moderate availability down to the detection limit for filter ashes at low air ratios. Except for boiler 1 ashes, the air ratio had - similarly to the availability from grate ashes - a very strong influence on the chromium availability.

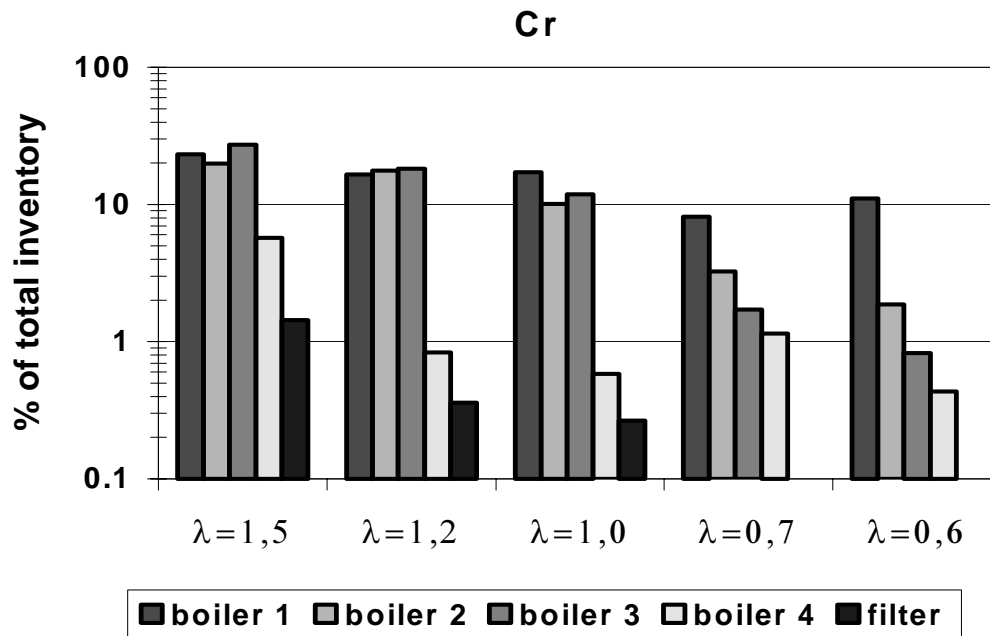


**Figure 7.4:** Availability of Cr from boiler and filter ashes ( $\lambda$ : air ratio)

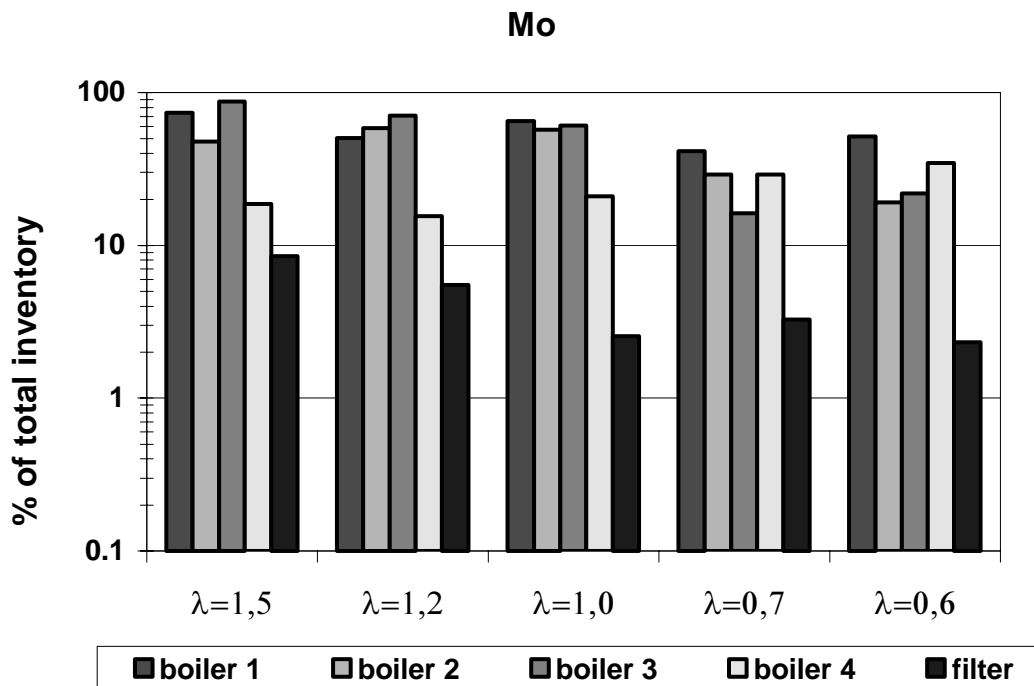


**Figure 7.5:** Availability of Mo from boiler and filter ashes ( $\lambda$ : air ratio)

**Molybdenum** showed tremendous availability values from boiler ashes, reaching 80% of the total residue content in a few cases (figure 7.5). Filter ashes exhibited a more moderate availability which decreased with decreasing air ratio.

### 7.3 Effect of leachate pH on the leaching behavior of the elements

Figures 7.6 to 7.9 show the leaching behavior of the investigated elements as a function of the leachate pH (pH-stat tests, see chapter 4). The diagrams depict the averaged values over the five spiked runs for each residue fraction.

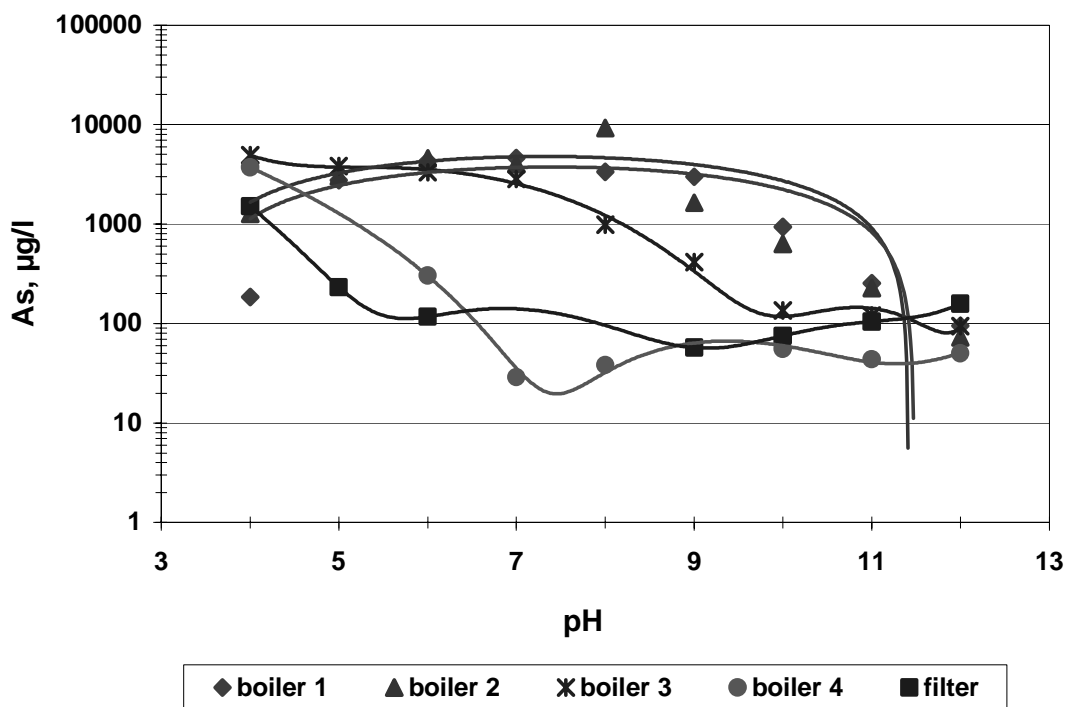


**Figure 7.6:** As leaching from boiler and filter ashes

**Arsenic** (figure 7.6) exhibited a great variation in its leaching pattern for the five residue fractions. While the first two boiler ashes (boiler 1 and boiler 2) followed the same pattern already seen for the grate ashes (figure 6.4) the boiler 3 residue marked a sort of a breakthrough in the leaching behavior. The last two residue fractions (boiler 4 and filter ashes) followed a completely different trend with a distinct minimum of the leachability for neutral to slightly alkaline pH values. This shape is more characteristic for cationic leaching. The change in the leaching behavior gives a hint to locate the condensation of cationic volatile species inside the boiler.

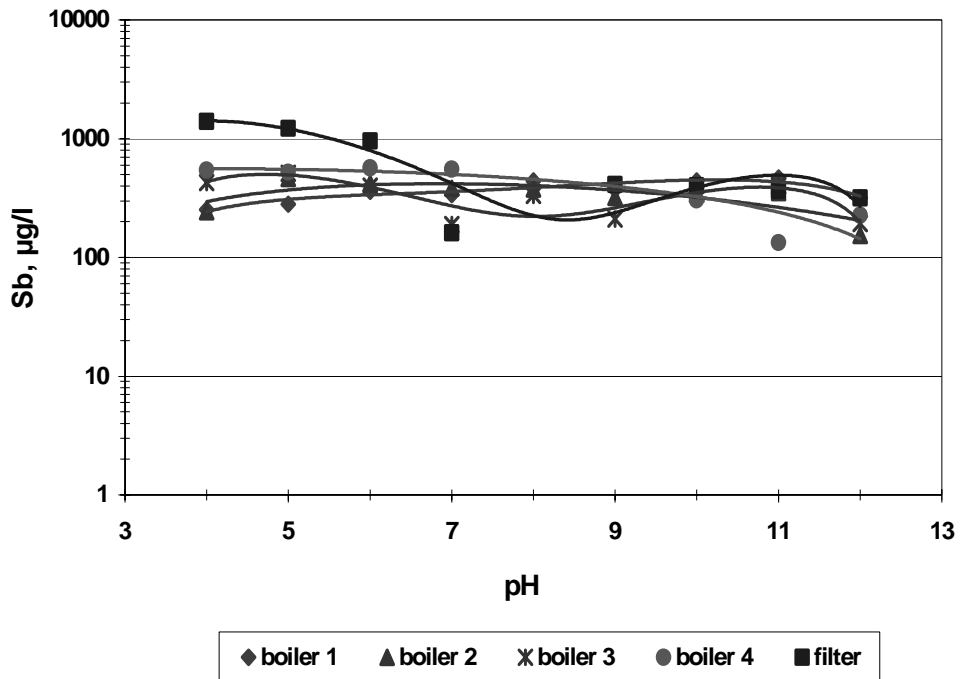


**Figure 7.7:** Sb leaching from boiler and filter ashes

The leachate concentrations of **antimony** (*figure 7.7*) exhibited a rather homogenous pattern for the various ash fractions. A shift in the trend may, however, be identified for the filter ashes, which show - similar to arsenic – a slight minimum in leachability for the pH range 7-8.

Investigations carried out by *van der Hoek et al.* on the speciation of arsenic and antimony in fly ash leachates pointed out that arsenic and antimony are found mainly in their pentavalent oxidation state [*van der Hoek et al., 1996*].

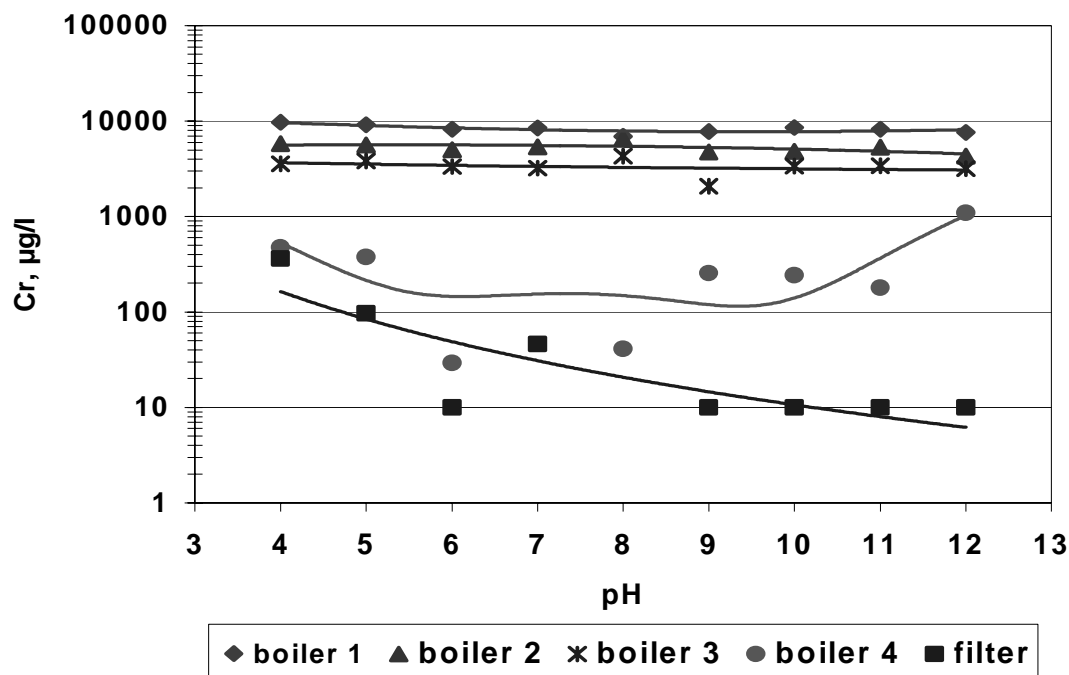


Figure 7.8: Cr leaching from boiler and filter ashes

**Chromium**, as well as arsenic, showed a distinct variation in the leaching pattern depending on the residue fraction (figure 7.8). Boiler ash fractions 1 to 3 showed chromium leachate concentrations which were virtually independent from the pH. Furthermore, these leachates exhibited a yellow coloration which varied in intensity from bright yellow (boiler 1) to pale yellow (boiler 3) regardless of the leachate pH. The leachates of the two remaining residue fractions (boiler 4 and filter ashes) were colorless at all pH.

The coloration of the leachates showed a strong correlation with the chromium concentration. Concentrations in the range of 4-6 mg/l were analyzed in the pale yellow leachates, 6-8 mg/l in the yellow ones, and 8-12 mg/l in the bright yellow ones. Since yellow color is a characteristic feature of hexavalent chromates the coloration of the leachates was interpreted as an evidence of hexavalent chromium.

On the other hand boiler 4 and filter ash leachates showed very low chromium concentrations which increased in the strongly acid and basic pH range. This fact, as well as the absence of any color, was taken as an indication of trivalent chromium speciation in these leachates. This would be consistent with former investigations carried out at the *Institute for Technical Chemistry - Division of Thermal Waste Treatment*. Lysimeter experiments on filter ashes and measurements of the redox potential of the leachates predicted chromium to be mainly present in the trivalent oxidation state as hydroxide ion  $\text{Cr}(\text{OH})_4^-$  [Volkman, 1990].

**Molybdenum**, similarly to antimony, did not show significant differences in the leaching pattern between the residue fractions (*figure 7.9*). A slight difference may be seen for the low temperature boiler ashes (boiler 4). On the other hand, the low concentrations in the leachates at weakly alkaline pH values (7-9) seemed to be characteristic of all of the four investigated elements, so that the explanation could possibly lie in some effect of the solid matrix (such as sorption processes). The weak dependence from the pH of molybdenum leaching behavior can be interpreted as an evidence of its oxyanionic speciation in the leachates. The lysimeter experiments predicted molybdenum to be present in the leachates in form of hexavalent molybdate ion  $\text{MoO}_4^{2-}$  [Volkman, 1990].

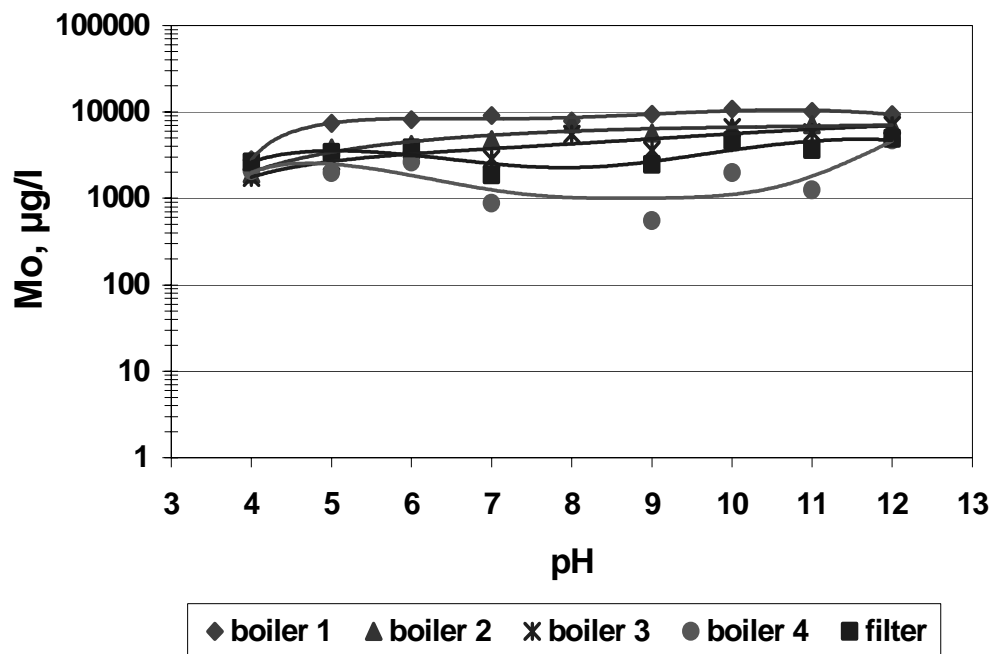


**Figure 7.9:** Mo leaching from boiler and filter ashes



## **Conclusions and outlook**

A number of metals respectively half-metals of high environmental concern have the capability to form oxyanionic compounds. The purpose of the present work was to investigate the behavior of selected elements out of this group, namely arsenic, antimony, chromium and molybdenum, during the waste combustion process and the environmental properties of the solid combustion residues. To a limited extent analogous conclusions can be drawn for other metals with similar chemical behavior, such as tungsten and vanadium.

The major objectives were:

- to get detailed information of the amount, the sources and the speciation of these elements in municipal solid waste,
- to understand the fundamental reaction mechanisms involving the selected half-metals inside the combustion chamber by theoretical considerations and specific thermoanalytical investigations in simple model systems,
- to measure the element partitioning in pilot plant tests, partly with spiking of selected compounds,
- to interpret the obtained partitioning data on the basis of the theoretical and laboratory work,
- to investigate the leaching properties of the elements out of the various solid residues and to draw further conclusions on their speciation in the respective compartments.

The final aims were to identify eventual risks associated with the elements in question and to point out the topics on which a further optimization of the combustion process is necessary and which need more detailed clarification on a full-scale basis.

Formation of oxyanionic species is a consequence of the weak metallic character of the selected elements and takes place in alkaline aquatic environment or in a high-temperature solid-phase environment, if alkaline reaction partners are available.

The first step in the investigation of the fate of the metals was the analysis of their concentration and chemical speciation (inventory) in municipal solid waste so that the input species entering the incineration plant can be defined. Theoretical calculations based on the chemical equilibrium assumption provided a basis for estimation of those reactions which are most likely to take place during combustion.

Thermogravimetric and calorimetric measurements in a thermobalance as well as X-ray diffractometric analysis of mixtures of metal salts and calcium oxide provided evidence that oxyanionic salts are formed in the temperature range around 500-900°C.

Spiking incineration test runs on TAMARA pilot plant for waste incineration pointed out that the primary air ratio has a distinct effect on the transfer of the elements out of the fuel bed on the grate and on their partitioning among the solid residues. Sampling and analysis of fly ash samples at different locations along the flue gas path allowed the characterization of the ashes as a function of the deposition temperature. A high enrichment of the metals in the low-temperature fly ashes is an indicator for volatile species formation during combustion: these species exit the furnace in gaseous form and condense upon the fly ashes during the cooling path of the flue gas.

The last part of this work is concerned with the characterization of the TAMARA grate and fly ashes and with the assessment of the leaching potential of the selected metals from the residues. Different regulatory tests were performed, the results were compared and interpreted in view of the speciation of the elements in question in these residues. The leachate pH appeared to be the dominant factor controlling the mobilization of the metals.

From theoretical considerations, arsenic and antimony should be expected highly volatile in waste combustion, but the experimental evidence contradicted these theoretical predictions, as over 70% of the total inventory was found in the grate ashes.

Thermogravimetric analysis, coupled with calorimetric measurements and diffractometric analysis of the residues, provided a reliable method of investigation and showed that arsenate and antimonate formation reduce the volatility of these metals in combustion processes. However, further detailed knowledge about the mechanisms leading to the formation of oxyanionic compounds during combustion is necessary. In particular, the kinetic aspects, the effect of oxygen partial pressure, and the different reaction partners need to be investigated more in detail on a laboratory scale. Ideally, thermodynamic data such as reaction enthalpies can be measured and used as an input for theoretical thermodynamic modeling of the thermal behavior of the elements.

In the spiking incineration tests, antimony showed the most volatile behavior (with 24% of the inventory transferred into the fly ashes), followed by arsenic (19%). The lower transfer factor for arsenic than for antimony is consistent with the theoretical prediction that chlorination plays a minor role in arsenic partitioning. This is a consequence of the weaker metallic character of arsenic, resulting in a lower affinity for chlorine.

Variation of the primary air ratio between the incineration tests proved to have a strong effect on the transfer of these two volatile metals. The results showed that an increased metal transfer is a

consequence not only of high fuel bed temperatures, but rather of the residence time of the fuel bed at high temperatures. Thus, the maximum mobilization for these two elements was achieved for primary air ratio values of slightly less than 1. The temperature profiles show that under these conditions the oxidation of the fixed carbon needed more time and therefore the high temperature zone was broadened. However, for low air ratio values the carbon oxidation might not be completed during the fuel bed residence time on the grate and high amounts of unburnt materials (total organic carbon) remained in the grate ashes. Such conditions need to be avoided by optimized air supply and air distribution control.

The determination of combustion conditions and mechanisms leading to the oxidation of chromium to its highly toxic hexavalent state is a very important issue. From theoretical considerations, at normal municipal incinerator temperatures, oxidation of trivalent species can be considered to be very unlikely. This is confirmed by the results of the incineration tests. Chromium exhibited a strong lithophilic behavior, which showed almost no effect of air ratio variations. However, local high temperature zones in the fuel bed and a high oxygen partial pressure might lead to the formation of highly volatile hexavalent chromium compounds and hence the possibility of increased transfer of this metal out of the fuel bed for high process temperatures must not be underestimated.

The leaching characteristics of the residues, on the other hand, showed that at least part of the chromium inventory is present in the hexavalent form, very likely as a consequence of chromate formation in the fuel bed.

Molybdenum, similarly to chromium, showed a lithophilic behavior during combustion. However, the transfer factor for this metal was comparatively high (campaign average value: 10%). Furthermore, molybdenum showed a considerable enrichment in low-temperature fly ashes. This semi-volatile behavior can be explained by the formation of volatile halogenated compounds, which seem thermodynamically to be more favored than respective chromium species. Formation of highly soluble molybdates in the grate ashes can be considered to be quite likely on the basis of theoretical calculations and this prediction was confirmed by the experiments in the thermobalance and by diffractometric analysis.

The leaching behavior of all the four investigated elements gave strong evidence of their oxyanionic speciation in the grate ashes. This implies a different leaching trend from most other metals, for

which a cationic speciation is generally assumed. Hence there is a risk to underestimate the potential for leaching of these elements .

Arsenic and antimony showed a strong dependence on the pH, with a maximum of solubility in the neutral range and then decreasing quickly to the detection limit for the strongly acid and basic pH values. The time resolution of the leaching process pointed out that the release of these elements from the ash matrix is very likely controlled by diffusion processes and hence is expected to take place rather slowly.

Chromium and molybdenum, on the contrary, showed a much weaker dependence of their leaching behavior from the pH value and exhibited high solubility over the entire pH range. The leaching of these two elements is very likely controlled by the solubility of chromates and molybdates, respectively. Moreover, the release of these two elements from the ash matrix seemed to take place by means of wash-off processes during the early stages of the contact between the aqueous leachant and the solid residues.

The change in the leaching trend for the investigated metals from anionic to cationic in the low-temperature boiler ashes and in the filter ashes, especially for arsenic and antimony, gives a hint to locate the condensation of cationic volatile species in the low-temperature section of the boiler.

The detailed speciation of oxyanionic forming metals in leachates, however, needs further investigation. Chemical species of the metals can theoretically be assessed by means of measurements of the redox potential, evaluation of the pH-Eh diagrams (Pourbaix's diagrams) and use of geochemical models. The availability of analytical methods which are sensitive to the different oxidation states of the elements should also be considered.

The interpretation of the laboratory results and of the pilot-scale experiments allows to draw following conclusions which are relevant on a full-scale basis:

- the volatile half-metals arsenic and antimony are highly enriched in the filter ashes due to their high transfer out of the fuel bed. However, the majority of the input inventory is retained in the grate ashes as a consequence of the formation of oxyanionic compounds (arsenates and antimonates). No gaseous compounds could be analyzed at temperatures below 200°C and hence no environmental risks through stack emissions are expected, provided that an efficient dust removal system is installed.
- chromium shows a strong lithophilic behavior and no volatilization from the fuel bed. Nevertheless, high process temperatures (above 1200°C) are not recommended, as above this temperature dissociation reactions might begin, leading to the formation of gaseous, highly toxic pentavalent and hexavalent compounds.

- chromium revealed a leaching behavior which is strongly dependant on the combustion parameters. For low air ratio values (0,6), the amounts released by means of leaching processes from the grate ashes are nearly two orders of magnitude lower than for the reference air ratio value (1,5). An optimization between complete burnout of the residues and reduced chromium leaching as a consequence of primary air ratio reduction is necessary. The distribution, as well as the total amount, of primary air below the grate might play a crucial role in this optimization process.
- highly soluble molybdates and chromates are released from the grate ashes into the quench water as a result of rapid wash-off processes. This could be a beneficial effect if the residence time of the grate ashes in the quench tank is high enough to allow a certain washing effect. The quench water could be then recirculated and reutilized in the flue gas scrubbers and subsequently treated by means of metal precipitation. Further possible treatment options could be the addition of sorbents as well as aging and washing of the residues.



**References**

- Alvin, M.A., O' Neill, E.P., Keairns, D.L. (1977): Thermodynamic projections of trace element release in fluidized-bed combustion systems, Proceedings of the 5<sup>th</sup> international conference on fluidized-bed combustion, Dec. 12-14<sup>th</sup>, 1977, 526-542.
- Angenend, F.J. and Trondt, L. (1990): Schadstoffinput-Schadstoffoutput - Bilanzierung bei der Müllverbrennung am Beispiel des Müllheizkraftwerkes Essen-Karnap, VGB-Kraftwerkstechnik, 1, 36-42.
- Anger, G., Halstenberg, J., Hochgeschwender, K., Uecker, G., Korallus, U., Knopf, H., Schmidt, P., Ohlinger, M. (1997): Chromium compounds, in: Ullmann's encyclopedia of industrial chemistry, 5<sup>th</sup> edition on CD-ROM, Wiley, VCH, Weinheim.
- Bale, C.W. and Eriksson, G. (1990): Metallurgical thermochemical databases - A review, Canadian Metallurgical Quarterly, 29, 2, 105-132.
- Barin, I. (1989): Thermochemical data of pure substances, VCH, Weinheim.
- Barin, I., Igelbüscher, A., Zenz, F.R. (1996): Thermodynamische Modelle zur Analyse der Verfahren für die thermische Entsorgung von Müll, Schriftenreihe GMDB 77- Simulation von metallurgischen Prozessen, 77, 2, 59-73.
- Barton, R.G., Clark, W.D., Seeker, W.R. (1990): Fate of metals in waste combustion systems, Combust. Sci. Tech., 74, 327-342.
- Belevi, H. (1998): Environmental engineering of municipal solid waste incineration, EAWAG - Swiss Federal Institute for Environmental Science and Technology.
- Bidlingmaier, W. (1990): Schwermetalle im Hausmüll - Herkunft, Schadwirkung, Analyse, Stuttgarter Berichte zur Abfallwirtschaft - Band 42, Erich Schmidt Verlag.
- Binnewies, M. and Milke, E. (1999): Thermochemical data of elements and compounds, Wiley-VCH, Weinheim.
- Bittner, M. and Broekaert, J.A.C. (1998): Speciation of chromium by solid-phase extraction coupled to reversed-phase liquid chromatography with UV detection, Analytica Chimica Acta, 364, 31-40.
- Bool, L.E. III and Helble, J.J. (1995): Laboratory study of the partitioning of trace elements during pulverized coal combustion, Energy and Fuels, 9, 5, 880-887.
- Brunner, P. H. and Ernst, W. R. (1986): Alternative methods for the analysis of municipal solid waste, Waste Management and Research, 4, 147-160.
- Brunner, P.H. and Mönch, H. (1986): The flux of metals through municipal solid waste incinerators, Waste Management and Research, 4, 105-119.

- Bulewicz, E.M. and Padley, P.J. (1971): Photometric investigations of the behavior of chromium additives in premixed  $H_2+O_2+N_2$  flames, Proc. Roy. Soc. Lond., A 323, 377-400.
- Bundesamt für Umweltschutz (1991): Entwurf zur Vernehmlassung einer technischen Verordnung über Abfälle (TVA), Bern, Switzerland, August, 1988, Revision 1991.
- Bundesministerium für Umwelt, Naturschutz und Reaktorsicherheit (1990): 17. Verordnung zur Durchführung des Bundesimmissionsschutzgesetzes (Verordnung über Verbrennungsanlagen für Abfälle und ähnliche brennbare Stoffe) - 17. BImSchV., Bundesgesetzblatt, Teil 1, 2 545, corr. 2832.
- Bundesministerium für Umwelt, Naturschutz und Reaktorsicherheit (1993): Dritte Allgemeine Verwaltungsvorschrift zum Abfallgesetz (TA Siedlungsabfall), Technische Anleitung zur Verwertung, Behandlung und sonstigen Entsorgung von Siedlungsabfällen vom 14. Mai 1993, Bundesanzeiger, Jahrgang 45, Nr. 99a, Erich Schmidt Verlag, Berlin, Kennzahl 0675, Lfg. 4/93.
- Carbonell-Barrachina, A.A., Jugsujinda, A., Burlo, F., Delaune, R.D., Patrick, W.H., Jr. (1999): Arsenic chemistry in municipal sewage sludge as affected by redox potential and pH, Wat. Res., 34, 1, 216-224.
- Chandler, A.J., Sawell, S.E., Rigo, H.G. (1993): The Waste Analysis, Sampling, Testing and Evaluation (WASTE) Program – Report, A.J. Chandler & Associates Ltd., Compas Environmental Inc., Rigo & Rigo Associates Inc., The Environmental Research Group-University of New Hampshire, Waste Waster Technology Centre.
- Clapp, T.J., Magee, J.F. II, Ahlert, R.C., Kosson, D.S. (1988): Municipal solid waste composition and the behavior of metals in incinerator ashes, Environmental Progress, Vol. 7, no. 1, 22-30.
- Clemens, A.H., Damiano, L.F., Gong, D., Matheson, T.W. (1999): Partitioning behavior of some toxic volatile elements during stoker and fluidised bed combustion of alkaline sub-bituminous coal, Fuel, 78, 1379-1385.
- Comans, R.N.J., van der Sloot, H.A., Bonouvie, P. (1993): Geochemical reactions controlling the solubility of major and trace elements during leaching of municipal solid waste incinerator residues, Proceedings of the 1993 international conference on municipal waste combustion, Williamsburgh, VA, U.S.A., 30.3-2.4.1993, The Air and Waste Management Association, 667-675.
- Cosic, B. and Fontijn, A. (2000): Transitions in order and molecularity with temperature in gaseous metal oxidation reactions. The Sb- $O_2$  system, Z. Phys. Chem., 214, 11, 1521-1531.
- Davis, R.D. (1982) Uptake of molybdenum and copper by forage crops growing on sludge-treated soils and its implications for the health of grazing animals, Proc. of the international conference on heavy metals in the environment, Amsterdam, 15-18 September, 1981, 194-197.

- DIN (Deutsches Institut für Normung) 38405 (1987), Teil 24: Deutsche Einheitsverfahren zur Wasser-, Abwasser-, und Schlammuntersuchung: Anionen (gruppe D)-Photometrische Bestimmung von Chrom (VI) mittels 1,5-Diphenylcarbazid (D24).
- DIN (Deutsches Institut für Normung) 38414 (1984), Teil 1: Deutsche Einheitsverfahren zur Wasser-, Abwasser- und Schlammuntersuchung; Schlamm und Sedimente (Gruppe S), Bestimmung der Eluierbarkeit mit Wasser (DEV-S4).
- DIN (Deutsches Institut für Normung) 51007 (1994): Thermische Analyse (TA) - Differenzthermoanalyse (DTA) - Grundlagen.
- DIN (Deutsches Institut für Normung) 51718 (1995): Prüfung fester Brennstoffe - Bestimmung des Wassergehaltes und der Analysenfeuchtigkeit.
- Djona, M., Allain, E., Gaballah, I. (1995) :Kinetics of chlorination and carbochlorination of molybdenum trioxide, Metallurgical and materials transactions, 26B, 703-710.
- Downing, J.H., Deeley, P.D., Fichte, R. (2001): Chromium and chromium alloys, in: Ullmann's encyclopedia of industrial chemistry, 2001 electronic release, Wiley, VCH, Weinheim.
- Ebbinghaus, B.B. (1992): Analysis of chromium volatility in the DWTF incinerator and in the molten salt processor, Proc. of the 1992 incineration conference, Albuquerque NM, USA, May 1992, 599-604.
- Ebbinghaus, B.B. (1993a): Thermodynamics of gas phase chromium species: the chromium oxides, the chromium oxyhydroxides, and volatility calculations in waste incineration processes, Combustion and Flame, 93, 119-137.
- Ebbinghaus, B.B. (1993b): Thermodynamics of gas phase chromium species: the chromium chlorides, oxychlorides, fluorides, oxyfluorides, hydroxides, oxyhydroxides, mixed oxyfluorochlorohydroxides and volatility calculations in waste incineration processes, Combustion and Flame, 101, 311-338.
- Enders, R., Vater, C., Jekel, M. (1990): Antimon im Abwasser von Abfallverbrennungsanlagen, Müll und Abfall, 12, 784-787.
- Endriss, H. (1997): Aktuelle anorganische Bunt-Pigmente, ed. by Dr. Ulrich Zorll, Vincentz Verlag, Hannover.
- Eriksson, G. and Hack, K. (1990): ChemSage - A computer program for the calculation of complex chemical equilibria, Metallurgical Transactions, 21B, 1013-1023.
- Eusden Dykstra, J., Taylor Eighmy, T., Hockert, K., Holland, E., Marsella, K. (1999): Petrogenesis of municipal solid waste combustion ash, Applied Geochemistry, 14, 1073-1091.

- Fällmann, A.M. (1990): International seminar on leach tests, Swedish Environmental Protection Agency, Solna, Sweden, 19.9.1990, Report 317, Statens Geotekniska Institute, Linköping, Sweden.
- Fällmann, A.M. (2000): Leaching of chromium and barium from steel slag in laboratory and field tests - A solubility controlled process?, *Waste Management*, 20, 149-154.
- Frandsen, F., Dam-Johansen, K., Rasmussen, P. (1994): Trace elements from combustion and gasification of coal - an equilibrium approach, *Prog. Energy Combust. Sci.*, 20, 115-138, 1994.
- Frandsen, F., Erickson, T.A., Kühnel, V., Helble, J.J., Linak, W.P. (1996): Equilibrium speciation of As, Cd, Cr, Hg, Ni, Pb, and Se in oxidative thermal conversion of coal - A comparison of thermodynamic packages, in: *Proceedings of the 3<sup>rd</sup> international symposium on high-temperature gas cleaning*, University of Karlsruhe, edited by E. Schmidt, Institut für Mechanische Verfahrenstechnik und Mechanik, University of Karlsruhe, 462-473.
- Glemser, O. and Müller, A. (1964): Über ein gasförmiges Hydroxid des Chroms, *Z. Anorg. Allgem. Chem.*, 334, 151-154.
- Gordy, W. and Orville Thomas, W.J. (1956): Electronegativities of the elements, *J. Chem. Phys.*, 21, 2, 439-444.
- Gougar, M.L.D., Scheetz, B.E., Roy, D.M. (1996): Ettringite and C-S-H Portland cement phases for waste ion immobilisation: a review, *Waste Management*, 16, 4, 295-303.
- Gullett, B.K. and Ragnunathan, K. (1994): Reduction of coal-based emissions by furnace sorbent injection, *Energy and fuels*, 8, 5, 1068-1076.
- Hardt, H.-D. (1987): *Die periodischen Eigenschaften der chemischen Elemente*, 2<sup>nd</sup> ed., Georg Thieme Verlag, Stuttgart.
- Haynes, B.S., Neville, M., Quann, R.J., Sarofim, A.F. (1982): Factors governing the surface enrichment of fly ash in volatile trace species, *Journal of Colloid and Interface Science*, 87, 1, 266-278.
- Herbst, K.A., Rose, G., Hanusch, K., Schumann, H., Wolf, H.U. (1997): Antimony and antimony compounds, in: *Ullmann's encyclopedia of industrial chemistry*, 5<sup>th</sup> edition on CD-ROM, Wiley, VCH, Weinheim.
- Hirsch, M.E., Sterling, R.O., Huggins, F.E., Helble, J.J. (2000): Speciation of combustion-derived particulate phase arsenic, *Environmental Engineering Science*, 17, 6, 315-327.
- Honig, R. (1962): *Vapor pressure data for the solid and liquid elements*, RCA Laboratories, Princeton, N.J.
- Hundesrügge, T. (1990): Phasenanalytische Untersuchungen an Filteraschen aus Müllverbrennungsanlagen, *Aufschluss*, 41, 281-285.

- Hunsinger, H. (1999): personal communication, Institute for Technical Chemistry-Division Thermal Waste Treatment.
- IAWG (The International Ash Working Group) (1997): A.J. Chandler, T.T. Eighmy, J. Hartlén, D.S. Kosson, S.E. Sawell, H. van der Sloot and J. Vehlow: Municipal solid waste incineration residues, Elsevier studies in environmental science, Amsterdam, Lausanne, New York, Oxford, Shannon, Tokyo.
- Jensen, W.B. (1980): The Lewis acid-base concept, J. Wiley and Sons, New York - Chichester - Brisbane- Toronto.
- Johnson, C.A., Kersten, M., Ziegler, F., Moor, H.C. (1996): Leaching behavior and solubility-controlling solid phases of heavy metals in municipal solid waste incinerator ash, Waste Management, 16, 1-3, 129-134.
- Kahanek, P., Merz, A. & Schuy, K. (1988) An isokinetic sampling system for continuous long-term monitoring of hazardous flue gas emissions. In: Andersen, L., Møller, J. (ed.) (1988): Proceedings of the 5<sup>th</sup> international solid waste conference, Academic Press Ltd., London, San Diego, New York, Berkeley, Boston, Sydney, Tokyo, Toronto.
- Kashireninov, O. and Fontijn, A. (1998): Modeling of chromium combustion in incineration: thermochemistry of Cr-C-H-Cl combustion in air and selection of key reactions, Combustion and Flame, 113, 498-506.
- Kim, Y.W. and Belton. G.R. (1974): The thermodynamics of volatilization of chromic oxide: Part I. The species  $\text{CrO}_3$  and  $\text{CrO}_2\text{OH}$ , Metallurgical Transactions, 5, 1811-1816.
- Klein, D.H., Andren, A.W., Carter, J.A., Emery, J.F., Feldman, C., Fulkerson, W., Lyon, W.S., Ogle, J.C., Talmi, Y., van Hook, R.I., Bolton, N. (1975): Pathways of 37 trace elements through coal-fired power plant, Environmental Science and Technology, 9, 10, 973-979.
- Knoth, J. and Schwenke, H. (1978): An X-ray fluorescence spectrometer with totally reflecting sample support for trace analysis at the ppb level, Fresenius Z. Anal. Chemie, 291, 200-214.
- Kumarathasan, P., McCarthy, G., Hassett, D.J., Pflughoeft-Hassett, D.F. (1990): Oxyanion substituted ettringites: synthesis and characterization and their potential role in immobilization of As, B, Cr, Se, V, Mat. Res. Soc. Symp. Proc., The Materials Research Society, 178, 83-104.
- Landolt H. and Börnstein, R. (1960): Zahlenwerte und Funktionen aus Physik, Chemie, Astronomie, Geophysik und Technik, Vol. II, Part 2, 6<sup>th</sup> ed., Springer Verlag, Berlin, 1960.
- Lee, C.C. (1988): A model analysis of metal partitioning in a hazardous waste incineration system, Journal of the Air Pollution Control Association, 38, 7, 941-945.
- Lide, D.R. (ed.) (1994): CRC Handbook of chemistry and physics, 75<sup>th</sup> edition, CRC Press, Boca Raton-Ann Arbor-London-Tokyo.

- Lorber, K.E. (1983): Die Zusammensetzung des Mülls und die durch Müllverbrennungsanlagen emittierten Schadstoffe, in: Thomé-Kozmiensky K.J. (ed.), Müllverbrennung und Rauchgasreinigung, EF-Verlag, Berlin, Vol. 7, 559-594.
- Mark, F.E. (1996): Municipal waste combustion: the effects of mixed plastics waste addition on solid residues and chlorinated organic compounds, in: Recycling and Recovery of Plastics, ed. by J. Brandrup, M. Bittner, W. Michaeli, G. Menges, pp. 831-848, Hanser Publishers.
- Mast, P.G., Süßkraut, G., van den Elsen, H., Stekete, J., Duzijn, R. (1996): Einfluss der Abfallzusammensetzung auf Schadstoffgehalt und -Menge der Verbrennungsrückstände - Phase 1, Ufoplan Nr. 10310903, TAUW Umwelt GmbH.
- Matschullat, J. (2000): Arsenic in the geosphere - A review, The Science of the Total Environment, 249, 297-312.
- McCarthy, G., Hassett, D.J., Bender, J.A. (1992): Synthesis, crystal chemistry and stability of ettringite, a material with potential applications in hazardous waste immobilization, Mat. Res. Soc. Symp. Proc., Materials Research Society, 245, 129-140.
- Meima, J.A. and Comans, R.N.J. (1997): Geochemical modeling of weathering reactions in municipal solid waste incinerator bottom ash, Environmental Science and Technology, 31, 1269-1276.
- Meima, J.A., and Comans, R.N.J. (1998): Reducing Sb-leaching from municipal solid waste incinerator bottom ash by addition of sorbent minerals, Journal of Geochemical Exploration, 62, 299-304.
- Meima, J.A. and Comans, R.N.J. (1999): The leaching of trace elements from municipal solid waste incinerator bottom ash at different stages of weathering, Applied Geochemistry 14, 159-170.
- Merz, A., Hunsinger, H., Vogg, H., Heinz, G. (1995): TAMARA-A pilot-scale research plant for municipal waste incineration, Proc. of the Chinese and German Environmental Protection Technology Symposium, Taipei, Taiwan, Oct., 3-6, 1995, 1, 159-172.
- Merz, A. and Seifert, H. (1999): Abschlussbericht zum Forschungsprojekt "Prozesskontrolle bei Abfallverbrennungsanlagen" (VGB-Projekt Nr. 173), Institute for Technical Chemistry - Division Thermal Waste Treatment.
- Merz, A. and Seifert, H. (2000): Abschlussbericht zum Forschungsprojekt "Verweilzeit von Verbrennungsgasen" (VGB-Projekt Nr. 174), Institute for Technical Chemistry - Division Thermal Waste Treatment.
- Morf, L.S. and Brunner, P.H. (1998): The municipal solid waste incinerator as a monitoring tool for waste management, Environmental Science and Technology, 32, 1825-1831.

- Nakamura, K., Kinoshita, S., Takatsuki, H. (1996): The origin and behavior of lead, cadmium and antimony in municipal solid waste incinerators, *Waste Management*, 16, 5/6, 509-517.
- Neville, M. and Sarofim, A.F. (1982): The stratified composition of inorganic submicron particles produced during coal combustion, *Proc. of the Combustion Institute*, Vol. 19, 1441-1449.
- NIST (The National Institute of Standards and Technology) (1988): NIST-JANAF Thermochemical Tables, 4<sup>th</sup> ed., ed. by The American Chemical Society (ACS), The American Institute of Physics (AIP), The National Institute of Standards and Technology (NIST).
- NEN (The Netherlands Normalization Institute) 7341 (1995): Leaching characteristics of solid (earthy and stony) building and waste materials- Leaching tests - Determination of the availability of inorganic components for leaching, 1<sup>st</sup> ed.
- NEN (The Netherlands Normalization Institute) 7343 (1995): Leaching characteristics of solid (earthy and stony) building and waste materials- Leaching tests - Determination of the leaching of inorganic components from granular materials with the column test, 1<sup>st</sup> ed.
- Paoletti, F., Sirini, P., Seifert, H., Vehlow, J. (2001): Fate of antimony in municipal solid waste incineration, *Proceedings of the 6<sup>th</sup> international conference on toxic combustion byproducts*, Karlsruhe, 27-30.06.1999, in: *Chemosphere*, 42, 5-7, 533-543.
- Paoletti, F., Seifert, H., Vehlow, J., Sirini, P. (2000): Oxyanions forming elements in waste combustion - Partitioning of antimony, *Waste Management and Research*, 18, 141-150.
- Paracelsus, alias Theophrastus Bombastus von Hohenheim (1589): *Volumen Medicinae Paramirum Theophrasti, de Medica Industria*, edited by Johannes Huser, available in the internet under: <http://www.mhiz.unizh.ch/Paracelsus.html>, The Zurich Paracelsus Project, University of Zurich, Institute and Museum for the History of Medicine.
- Patent Document DE 3422062 C2 (1988): Verfahren zur Langzeitbestimmung und Dauerüberwachung des Schadstoffgehaltes von feststoffbeladenen Abgasströmen, Kernforschungszentrum Karlsruhe.
- Patent Document DE 3520380 C2 (1994): Verfahren zur Langzeitbestimmung und Dauerüberwachung des Schadstoffgehaltes von Abgasen aus Großfeuerungen und Müllverbrennungsanlagen, Kernforschungszentrum Karlsruhe.
- Pauling, L. (1932): *The nature of the chemical bond and the structure of molecules and crystals*, Cornell University Press, Ithaca, N.Y., 1<sup>st</sup> ed.
- Paulus, E.F. and Gieren, A. (1999): Structure analysis by diffraction, in: *Ullmann Encyclopedia of Industrial Chemistry*, 6th edition, electronic release, Wiley-VCH.

- Pfrang-Stotz, G. and Schneider, J. (1995): Comparative studies of waste incineration bottom ashes from various grate and firing systems, conducted with respect to mineralogical and geochemical methods of examination, *Waste Management and Research*, 13, 273-292.
- Prange, A. (1987): Totalreflexions-röntgenfluoreszenzanalyse, *GIT Fachzeitschrift für das Laboratorium*, 31, 513-526.
- Quann, R.J. and Sarofim, A.F. (1982): Vaporization of refractory oxides during pulverized coal combustion, *Proc. of the Combustion Institute*, Vol. 19, 1429-1440.
- Querol, X., Fernandez-Turiel, J.L., López-Soler, A. (1995): Trace elements in coal and their behavior during combustion in a large power station, *Fuel*, 74, 3, 331-343.
- Reimann, D.O. (1989): Heavy metals in domestic refuse and their distribution in incineration residues, *Waste Management and Research*, 7, 57-62.
- Remy, H. (1960): *Lehrbuch der anorganischen Chemie*, 2<sup>nd</sup> ed., Akademische Verlagsgesellschaft Geest & Portig K.-G., Leipzig, Band 1, 786.
- Rizeq, R.G., Clark, W., Seeker, W.R. (1992): Analysis of toxic metals emissions from waste combustion devices, *Proceedings of the 1992 international incineration conference*, Albuquerque NM, USA, May 1992, 625-630.
- Schneider, J. (1986): Bestimmung der elementaren Müllzusammensetzung durch Analytik der Müllverbrennungsrückstände, in: Thomé-Kozmiensky, K.J. (ed.), *Recycling International*, EF-Verlag, Berlin, Vol. 1.1, 318, 283-290.
- Sebenik, R.F., Burkin, A.B., Dorfler, R.R., Laferty, J.M., Leichtfried, G., Meyer-Grünow, H., Mitchell, P.C. H., Vukasovich, M.S., Chruch, D.A., Van Riper, G.G., Gilliland, J.C., Thielke, S.A. (1997): Molybdenum and molybdenum compounds, in: *Ullmann's encyclopedia of industrial chemistry*, 5<sup>th</sup> edition on CD-ROM, Wiley, VCH, Weinheim.
- Seames, W.S. and Wendt, J.O.L. (2000): The partitioning of arsenic during pulverized coal combustion, *Proc. of the Combustion Institute*, Vol. 28, pp. 2305-2312.
- Senior C.L. and Flagan, R.C. (1982): Ash vaporization and condensation during combustion of a suspended coal particle, *Aerosol Science and Technology*, 1, 371-383.
- Senior, C.L., Bool, L.E. III, Srinivasachar, S., Pease, B.R., Porle, K. (2000): Pilot-scale study of trace element vaporization and condensation during combustion of a pulverized sub-bituminous coal, *Fuel Processing Technology*, 63, 2-3, 149-165.
- Shiryayev, A. (1994): Thermodynamics of SHS processes: an advanced approach, *International Journal of Self-propagating High-temperature Synthesis*, 4, 4, 351-362.

- Starnes, W.H. Jr., Wescott, L.D. Jr., Reents, W.D. Jr., Cais, R.E., Villacorta, G.M., Plitz, I.M., Anthony, L.J. (1984): Mechanism of poly(vinyl chloride) fire retardance by molybdenum(VI)oxide. Further evidence in favor of the Lewis acid theory, *Polym. Sci. Technology*, 26, 237-248.
- Strafford, K.N., Forster, G., Datta, P.K. (1991): Estimation and calculation of the values of thermodynamic functions for certain group V and group VI metal chlorides, *Proceedings of the extractive metallurgy conference, Perth, Australia, 2-4-October, 1991*, 311-322.
- Ullmann's encyclopaedia of industrial chemistry (1997), 5<sup>th</sup> edition on CD-ROM, Wiley, VCH, Weinheim.
- USEPA (United States of America Environmental Protection Agency) Method 1310 (1984): Extraction procedure toxicity method (EpTox). Test method for evaluation of solid waste, SW 846.
- Valkovic, V. (1983): Trace elements in coal, CRC Press, Inc., Boca Raton, Florida.
- Van der Hoek, E.E., Van Elteren, J.T., Comans, R.N.J. (1996): Determination of As, Sb and Se speciation in fly ash leachates, *Intern. J. Environm. Anal. Chem.*, 63, 67-79.
- Van Velzen, D., Langenkamp, H., Herb, G. (1998): Antimony, its sources and flow paths into urban and industrial waste: a review, *Waste Management and Research*, 16, 1, 32-40.
- Vehlow, J. (1993): Heavy metals in waste incineration, *Proc. of the DAKOTA Conference: Affalsforbraending Under Nye Betingelser*, Copenhagen, Denmark, Sep.1993.
- Vehlow, J., Wanke, T. & Mark, F.E. (1996) Co-Verbrennung von Kunststoffabfällen und Hausmüll (Co-combustion of plastics and municipal solid waste), *VDI Berichte 1288*, VDI-Verlag, Düsseldorf, Germany.
- Vehlow, J., Birnbaum, L., Köppel, W. (1997): Arsen und Antimon in der Abfallverbrennung, *Abfallwirtschaftsjournal*, 3, 9-19.
- Vehlow, J. and Mark, F.E. (1997): Electrical and electronic plastic waste co-combustion with municipal solid waste for energy recovery, *Technical paper from APME- Association of plastics manufacturers in Europe*.
- Vehlow, J. and Mark, F.E. (2000): Influence of bromine on metal volatilization in waste combustion, *J. Mater. Cycles Waste Manag.*, 2, 89-99.
- Vehlow, J., Bergfeldt, B., Jay, K., Seifert, H., Wanke, T. (2000): Thermal treatment of electrical and electronic waste plastics, *Waste Management and Research*, 18, 131-140.

- Verein Deutscher Ingenieure (VDI) (1994): Richtlinie N. 3868. Determination of total emission of metals, metalloids, and their compounds – Manual measurement in flowing, emitted gases – Sampling system for particulate and filter-passing matter, Part 1, VDI-Handbuch Reinhaltung der Luft, Band 4, Beuth Verlag, Berlin.
- Verhulst, D., Buekens, A., Spencer, P.J. & Eriksson, G. (1996) Thermodynamic behaviour of metal chlorides and sulfates under the conditions of incineration furnaces. *Environment, Science and Technology*, 30, 50-56, 1996.
- Volkman, Y. (1990): unpublished results, Institute for Technical Chemistry - Division of Thermal Waste Treatment.
- Warrington, S.B. and Höhne, G.W.H. (1994): Thermal analysis and calorimetry, in: Ullmann's encyclopedia of industrial chemistry, VCH Publishers, Inc., B6, 1-22.
- Watanabe, N., Inoue, S., Ito, H. (1999): Mass balance of arsenic and antimony in municipal waste incinerators, *J. Mater. Cycles Waste Manag.*, 1, 38, 47, 1999.
- Watanabe, N., Inoue, S., Ito, H. (2000): Chlorine promotes antimony volatilization in municipal waste incineration, *J. Mater. Cycles Waste Manag.*, 2, 10-15.
- Weast, R.C., ed. (1975) *Handbook of chemistry and physics*, 56<sup>th</sup> ed., CRC Press, Cleveland, Ohio.
- Weiss, J. (1984): Einführung in die Ionenchromatographie - Grundlagen, Instrumentation und Anwendungsmöglichkeiten, *CLB - Chemie für Labor und Betrieb*, 35, 2, 59-66.
- Wiese, K. (1996): unpublished results, Institute for Technical Chemistry - Division of Thermal Waste Treatment.
- Wilde, K.A. and Halbrook, M.E. (1977): Thermodynamic distribution of trace elements by minimization of free energy, *Ind. Eng. Chem., Fundam.*, 16, 4, 489-492.
- Williams, A., Ross, A., Chaiklangmuang, S., Jones, J.M., Pourkashanian, M. (2000): Super-equilibrium concentrations of carbon monoxide and hydrocarbon in fuel gases and their relationship with VOC and metal emissions, *Symp.-Am.Chem.Soc., Div. Fuel Chem*, 45, 1, 11-14.
- Wu, C.Y. and Biswas, P. (1993): An equilibrium analysis to determine the speciation of metals in an incinerator, *Combustion and flame*, 93, 31-40.